The Force Method

9

Abstract

Up to this point, we have focused on the analysis of statically determinate structures because the analysis process is fairly straightforward; only the force equilibrium equations are required to determine the member forces. However, there is another category of structures, called statically indeterminate structures, which are also employed in practice. Indeterminate structures require another set of equations, in addition to the force equilibrium equations, in order to solve for the member forces. There are two general methods for analyzing indeterminate structures, the force (flexibility) method and the displacement (stiffness) method. The force method is more suited to hand computation whereas the displacement method is more procedural and easily automated using a digital computer.

In this chapter, we present the underlying theory of the force method and illustrate its applications to a range of statically indeterminate structures including trusses, multi-span beams, arches, and frames. We revisit the analysis of these structures in the next chapter using the displacement method, and also in Chap. 12, "Finite Element Displacement Method for Framed Structures," which deals with computer-based analysis.

9.1 Introduction

The force method is a procedure for analyzing statically indeterminate structures that works with force quantities as the primary variables. It is applicable for linear elastic structures. The method is based on superimposing structural displacement profiles to satisfy a set of displacement constraints. *From a historical perspective*, the force method was the "classical" analysis tool prior to the introduction of digital-based methods. The method is qualitative in the sense that one reasons about deflected shapes and visualizes how they can be combined to satisfy the displacement constraints. We find the method very convenient for deriving analytical solutions that allow one to identify key behavior properties and to assess their influence on the structural response. The key step

J.J. Connor, S. Faraji, *Fundamentals of Structural Engineering*,
DOI 10.1007/978-3-319-24331-3_9

is establishing the displacement constraints which are referred to as the geometric compatibility equations.

Consider the structure shown in Fig. 9.1. Since there are four displacement restraints, the structure is indeterminate to the first degree, i.e., one of the restraints is not needed for stability, and the corresponding reaction force cannot be determined using only the force equilibrium equations.

The steps involved in applying the force method to this structure are as follows:

1. We select one of the force redundants and remove it. The resulting structure, shown in Fig. 9.2, is called the primary structure. Note that one cannot arbitrarily remove a restraint. One needs to ensure that the resulting structure is stable.
2. We apply the external loading to the primary structure and determinate the displacement at C in the direction of the restraint at C. This quantity is designated as $\Delta_{C,\,0}$. Figure 9.3 illustrates this notation.
3. Next, we apply a unit value of the reaction force at C to the primary structure and determine the corresponding displacement. We designate this quantity as δ_{CC} (see Fig. 9.4).
4. We obtain the total displacement at C of the primary structure by superimposing the displacement profiles generated by the external loading and the reaction force at C.

$$\Delta_C\big|_{\text{primary structure}} = \Delta_{C,\,0} + \delta_{CC} R_C \tag{9.1}$$

5. The key step is to require the displacement at C of the primary structure to be equal to the displacement at C of the actual structure.

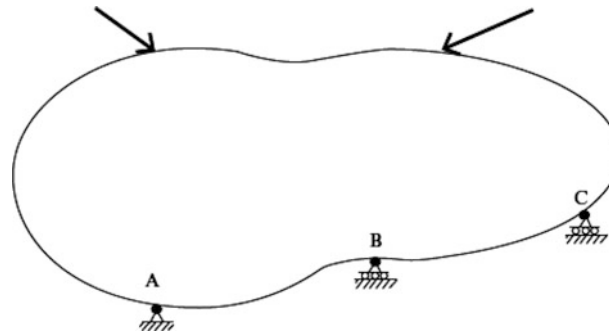

Fig. 9.1 Actual structure

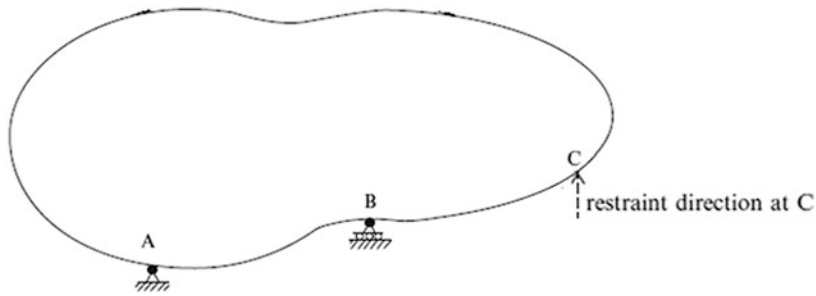

Fig. 9.2 Primary structure

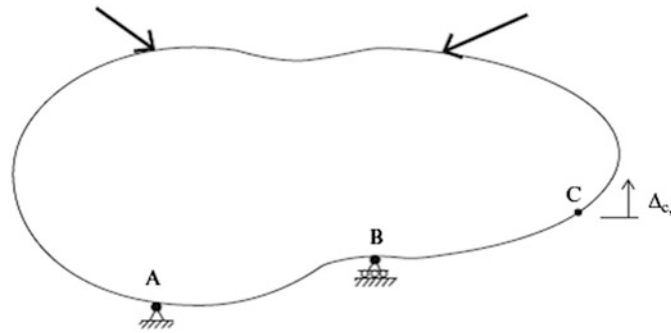

Fig. 9.3 Displacements due to the external loading

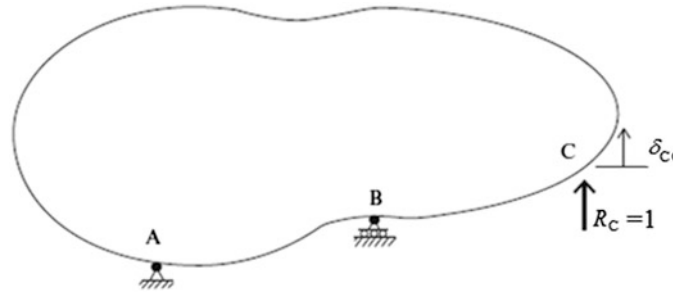

Fig. 9.4 Displacement due to unit value of R_C

$$\Delta_C\big|_{\text{actual}} = \Delta_C\big|_{\text{primary}} = \Delta_{C,0} + \delta_{CC}R_C \tag{9.2}$$

Equation (9.2) is referred to as the "geometric compatibility equation." When this equation is satisfied, the final displacement profiles for the actual and the primary structure will be identical. It follows that the forces in the primary structure and the actual structure will also be identical.

6. We solve the compatibility equation for the reaction force, R_C.

$$R_C = \frac{1}{\delta_{CC}}\left(\Delta_C\big|_{\text{actual}} - \Delta_{C,0}\right) \tag{9.3}$$

Note that $\Delta_C\big|_{\text{actual}} = 0$ when the support is unyielding. When R_C is negative, the sense assumed in Fig. 9.4 needs to be reversed.

7. The last step involves computing the member forces in the actual structure. We superimpose the member forces computed using the primary structure according to the following algorithm:

$$\text{Force} = \text{Force}\big|_{\text{external load}} + R_C\left(\text{Force}\big|_{R_C=1}\right) \tag{9.4}$$

Since the primary structure is statically determinate, all the material presented in Chaps. 2, 3, 4, 5, and 6 is applicable. The force method involves scaling and superimposing displacement profiles. The method is particularly appealing for those who have a solid understanding of structural behavior. For simple structures, one can establish the sense of the redundant force through qualitative reasoning.

Fig. 9.5 Actual structure

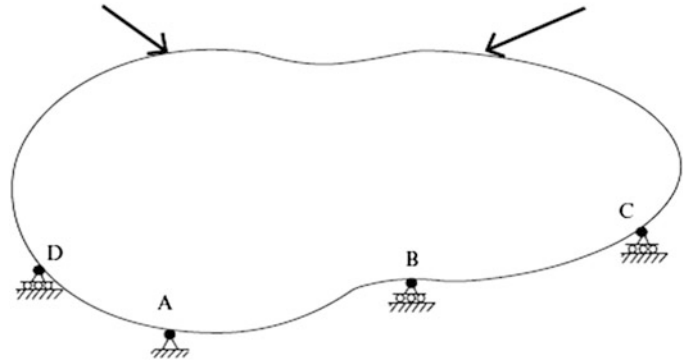

Essentially, the same approach is followed for structures having more than one degree of indeterminacy. For example, consider the structure shown in Fig. 9.5. There are two excess vertical restraints.

We obtain a primary structure by removing two of the vertical restraints. Note that there are multiple options for choosing the restraints to be removed. The only constraint is that the primary structure must be "stable." Figure 9.6 shows the different choices.

Suppose we select the restraints at C and D as the redundants. We apply the external loading to the primary structure (Fig. 9.7) and determine the vertical displacements at C and D shown in Fig. 9.8.

The next step involves applying unit forces corresponding to $R_C = 1$ and $R_D = 1$ and computing the corresponding displacements at C and D. Two separate displacement analysis are required since there are two redundant reactions (Fig. 9.9).

Combining the three displacement profiles leads to the total displacement of the primary structure.

$$\begin{aligned} \Delta_C\big|_{\text{primary structure}} &= \Delta_{C,0} + \delta_{CC}R_C + \delta_{CD}R_D \\ \Delta_D\big|_{\text{primary structure}} &= \Delta_{D,0} + \delta_{DC}R_C + \delta_{DD}R_D \end{aligned} \tag{9.5}$$

The coefficients of R_C and R_D are called flexibility coefficients. It is convenient to shift over to matrix notation at this point. We define

$$\begin{aligned} \underline{\mathbf{\Delta_0}} &= \begin{Bmatrix} \Delta_{C,0} \\ \Delta_{D,0} \end{Bmatrix} \quad \underline{\mathbf{X}} = \begin{Bmatrix} R_C \\ R_D \end{Bmatrix} \\ \text{flexibility matrix} &= \underline{\boldsymbol{\delta}} = \begin{bmatrix} \delta_{CC} & \delta_{CD} \\ \delta_{DC} & \delta_{DD} \end{bmatrix} \end{aligned} \tag{9.6}$$

Using this notation; the geometric compatibility equation takes the form

$$\underline{\mathbf{\Delta}}\big|_{\text{actual structure}} = \underline{\mathbf{\Delta_0}} + \underline{\boldsymbol{\delta}}\,\underline{\mathbf{X}} \tag{9.7}$$

Note that $\underline{\mathbf{\Delta}}\big|_{\text{actual structure}} = \underline{0}$ when the supports are unyielding. Given the choice of primary structure, the flexibility coefficients are properties of the primary structure whereas $\underline{\mathbf{\Delta_0}}$ depends on the both the external loading and the primary structure. We solve (9.7) for $\underline{\mathbf{X}}$,

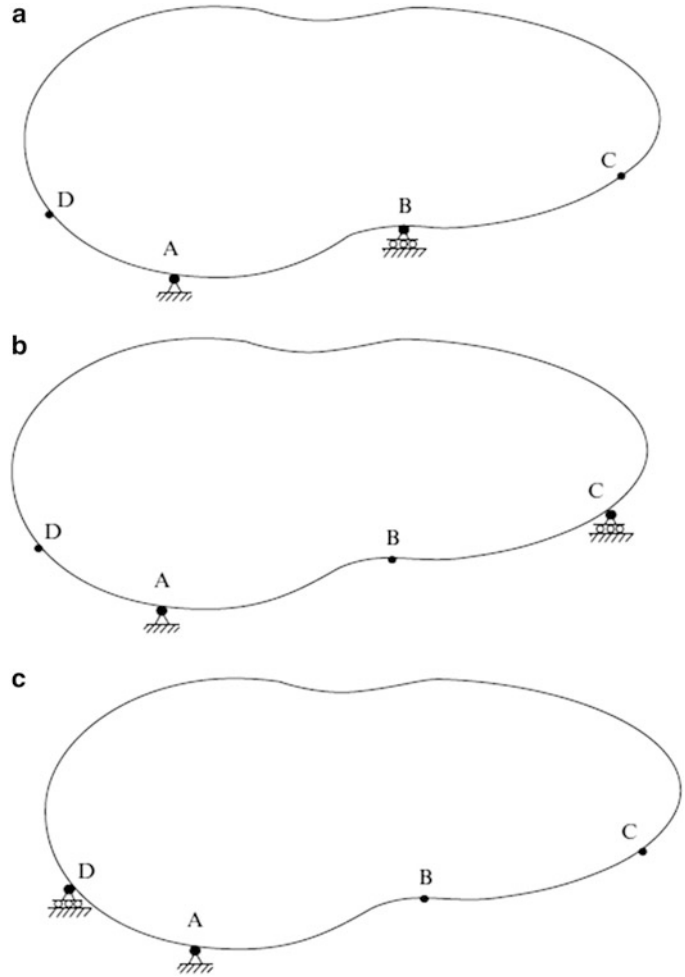

Fig. 9.6 Choices for primary structure. (**a**) Option 1. (**b**) Option 2. (**c**) Option 3

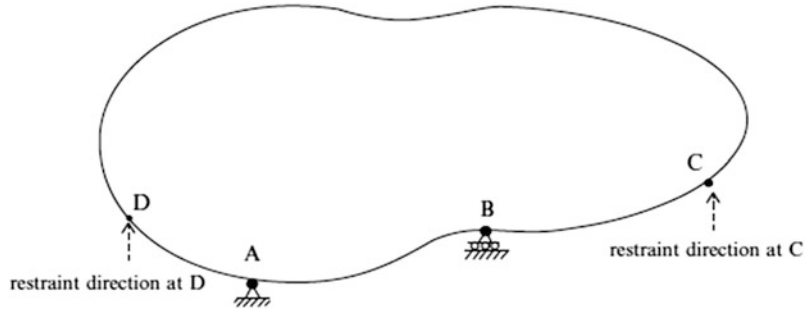

Fig. 9.7 Primary structure

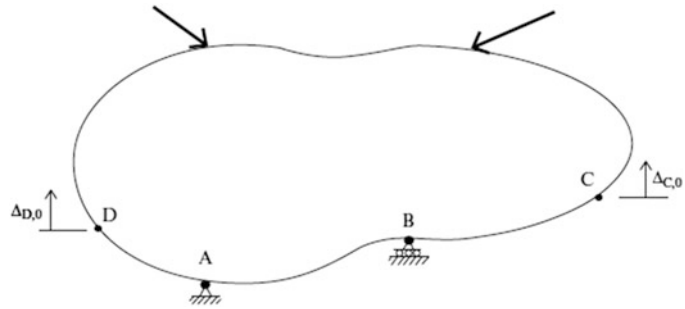

Fig. 9.8 Displacements due to external loading

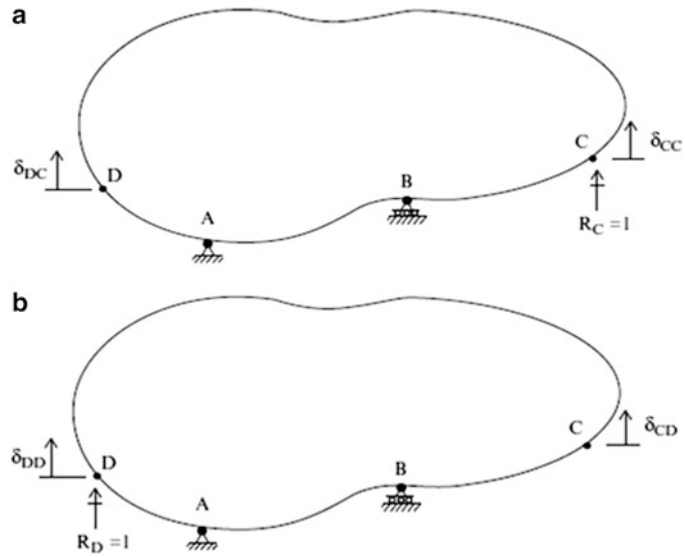

Fig. 9.9 Displacement due to unit values of the redundant. (**a**) $R_C = 1$. (**b**) $R_D = 1$

$$\underline{\mathbf{X}} = \underline{\boldsymbol{\delta}}^{-1}\left(\underline{\boldsymbol{\Delta}}\big|_{\text{actual structure}} - \underline{\boldsymbol{\Delta}}_{\mathbf{0}}\right) \tag{9.8}$$

and then determine the member forces by superimposing the individual force states as follows:

$$\underline{\mathbf{F}} = \underline{\mathbf{F}}\big|_{\text{external load}} + \left(\underline{\mathbf{F}}\big|_{R_C=1}\right)R_C + \left(\underline{\mathbf{F}}\big|_{R_D=1}\right)R_D \tag{9.9}$$

The extension of this approach to an nth degree statically indeterminate structure just involves more computation since the individual matrices are now of order n. Since there are more redundant force quantities, we need to introduce a more systematic notation for the force and displacement quantities.

Consider the frame structure shown in Fig. 9.10a. It is indeterminate to the third degree. One choice of primary structure is shown in Fig. 9.10b. We remove the support at D, take the reactions as the force redundants, and denote the jth redundant force as X_j and the corresponding measure as Δ_j.

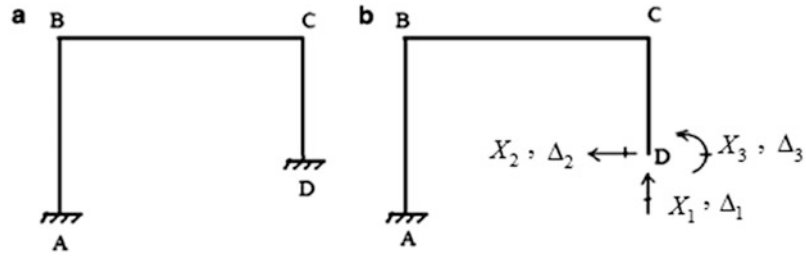

Fig. 9.10 (**a**) Actual structure. (**b**) Primary structure—redundant reactions

The resulting displacements of the primary structure due to the external loading and the three force redundants are expressed as

$$\begin{aligned}
\Delta_1\big|_{\text{primary structure}} &= \Delta_{1,0} + \delta_{11}X_1 + \delta_{12}X_2 + \delta_{13}X_3 \\
\Delta_2\big|_{\text{primary structure}} &= \Delta_{2,0} + \delta_{21}X_1 + \delta_{22}X_2 + \delta_{23}X_3 \\
\Delta_3\big|_{\text{primary structure}} &= \Delta_{3,0} + \delta_{31}X_1 + \delta_{32}X_2 + \delta_{33}X_3
\end{aligned} \tag{9.10}$$

The matrix form of (9.10) is

$$\underline{\boldsymbol{\Delta}}\big|_{\text{primary structure}} = \underline{\boldsymbol{\Delta}}_0 + \underline{\boldsymbol{\delta}}\,\underline{\mathbf{X}} \tag{9.11}$$

where

$$\underline{\boldsymbol{\delta}} = \begin{bmatrix} \delta_{11} & \delta_{12} & \delta_{13} \\ \delta_{21} & \delta_{22} & \delta_{23} \\ \delta_{31} & \delta_{32} & \delta_{33} \end{bmatrix} \quad \underline{\boldsymbol{\Delta}}_0 = \begin{Bmatrix} \Delta_{1,0} \\ \Delta_{2,0} \\ \Delta_{3,0} \end{Bmatrix} \quad \underline{\mathbf{X}} = \begin{Bmatrix} X_1 \\ X_2 \\ X_3 \end{Bmatrix}$$

Note that the displacement measures may be either a translation or a rotation. A major portion of the computational effort is involved with computing the flexibility coefficients using the Principle of Virtual Forces. The matrix form of the geometric compatibility equation (9.7) is generic, i.e., it is applicable for all structures. One just has to establish the appropriate form for $\underline{\boldsymbol{\Delta}}_0$ and $\underline{\boldsymbol{\delta}}$.

Other possible choices of primary structures are shown in Fig. 9.11. We can retain the two fixed supports, but cut the structure at an arbitrary interior point (Fig. 9.11a). The redundants are taken as the internal forces (axial, shear, and moment) at the point. The flexibility coefficients are now interpreted as the relative displacements of the adjacent cross sections (e.g., spreading, sliding, relative rotation). Another choice involves removing excess reactions as in Fig. 9.11b.

For multi-bay multistory frames, one needs to work with internal force redundants since removing fixed supports is not sufficient to reduce the structure to a statically determinate structure. Figure 9.12 illustrates this case.

Multi-span beam-type structures are handled in a similar way when choosing a primary structure. Consider Fig. 9.13. One can either select certain excess reactions or work with bending moments at interior points. We prefer the latter choice since the computation of the corresponding flexibility coefficients is simpler due to the fact that the deflection profiles associated with the redundant moments are confined to adjacent spans.

For truss-type structures, various cases arise. The truss may have more supports than needed, such as shown in Fig. 9.14a. One choice would be to remove sufficient supports such that the resulting structure is statically determinate (Fig. 9.14b).

We can also keep the original restraints, and remove some members, as indicated in Fig. 9.14c.

Another example is shown in Fig. 9.15a. The truss has too many members and therefore the only option is to remove some of the diagonals. Figure 9.15b illustrates one choice of redundants.

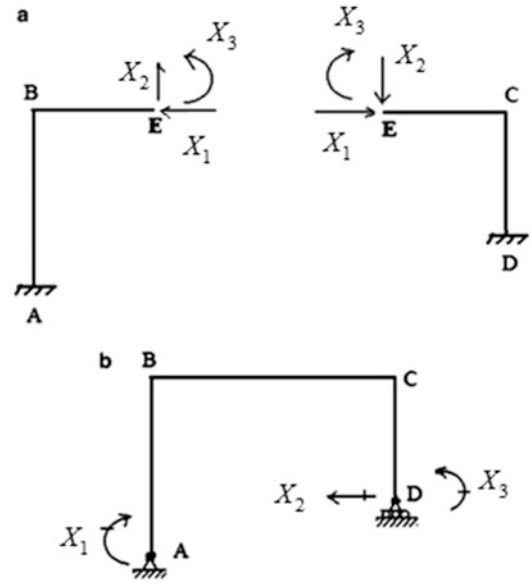

Fig. 9.11 (**a**) Primary structure—redundant internal forces. (**b**) Primary structure—redundant reactions

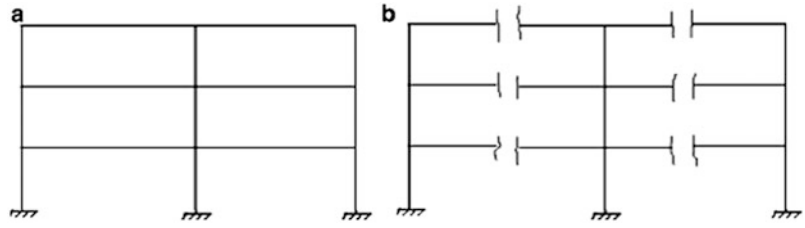

Fig. 9.12 (**a**) Actual structure. (**b**) Primary structure

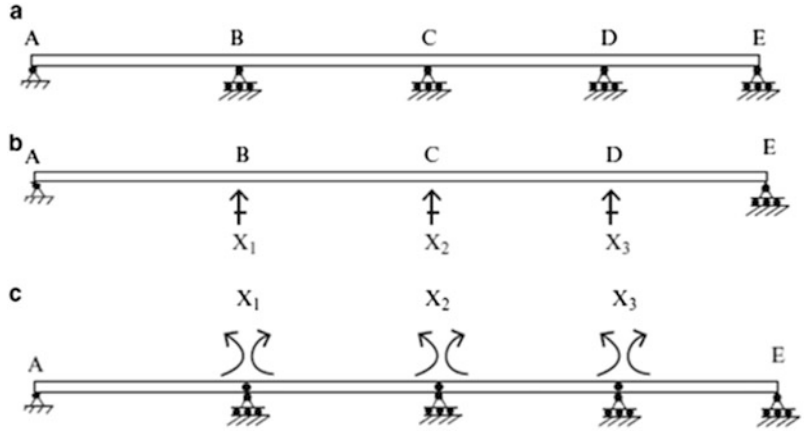

Fig. 9.13 Multi-span beam. (**a**) Actual structure. (**b**) Primary structure—redundant reactions. (**c**) Primary structure—redundant moments

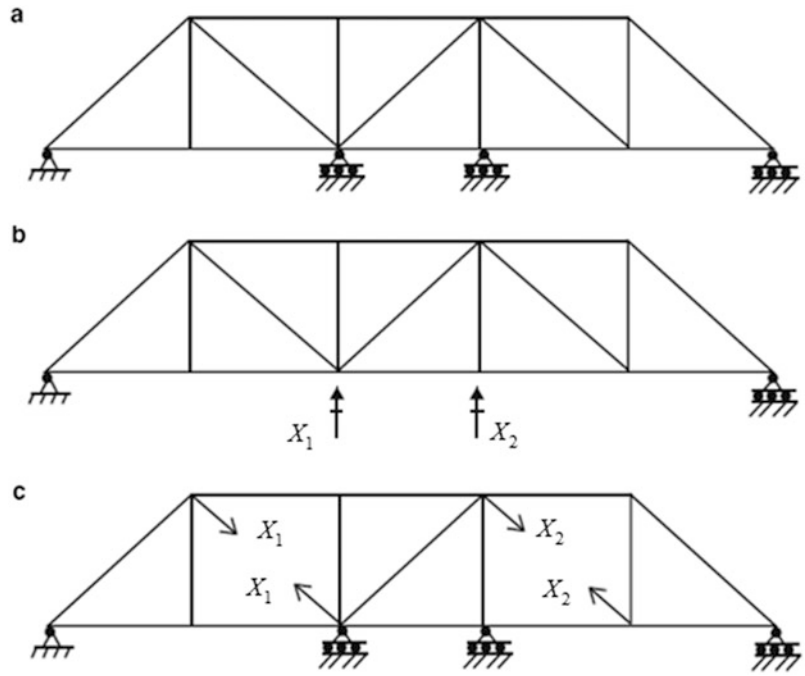

Fig. 9.14 (**a**) Actual structure. (**b**) Primary structure—redundant reactions. (**c**) Primary structure—redundant internal forces

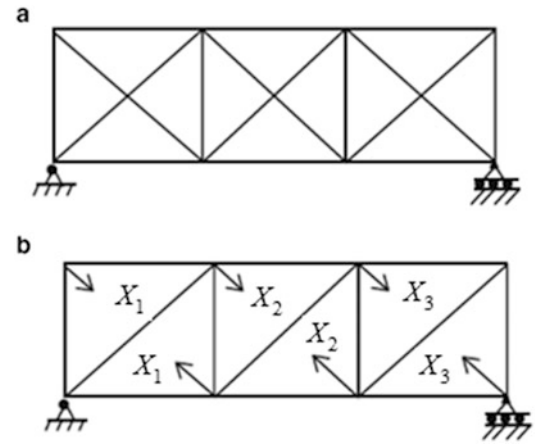

Fig. 9.15 (**a**) Actual structure. (**b**) Primary structure—redundant internal forces

9.2 Maxwell's Law of Reciprocal Displacements

The geometric compatibility equations involve the flexibility matrix, $\underline{\boldsymbol{\delta}}$. One computes the elements of $\underline{\boldsymbol{\delta}}$ using one of the methods described in Part I, such as the Principal of Virtual Forces. Assuming there are n force redundants, $\underline{\boldsymbol{\delta}}$ has n^2 elements. For large n, this computation task becomes too difficult to deal with manually. However, there is a very useful relationship between the elements of $\underline{\boldsymbol{\delta}}$, called "Maxwell's Law," which reduces the computational effort by approximately 50 %. In what follows, we introduce Maxwell's Law specialized for member systems.

We consider first a simply supported beam on unyielding supports subjected to a single concentrated unit force. Figure 9.16a defines the geometry and notation. The deflected shape due to

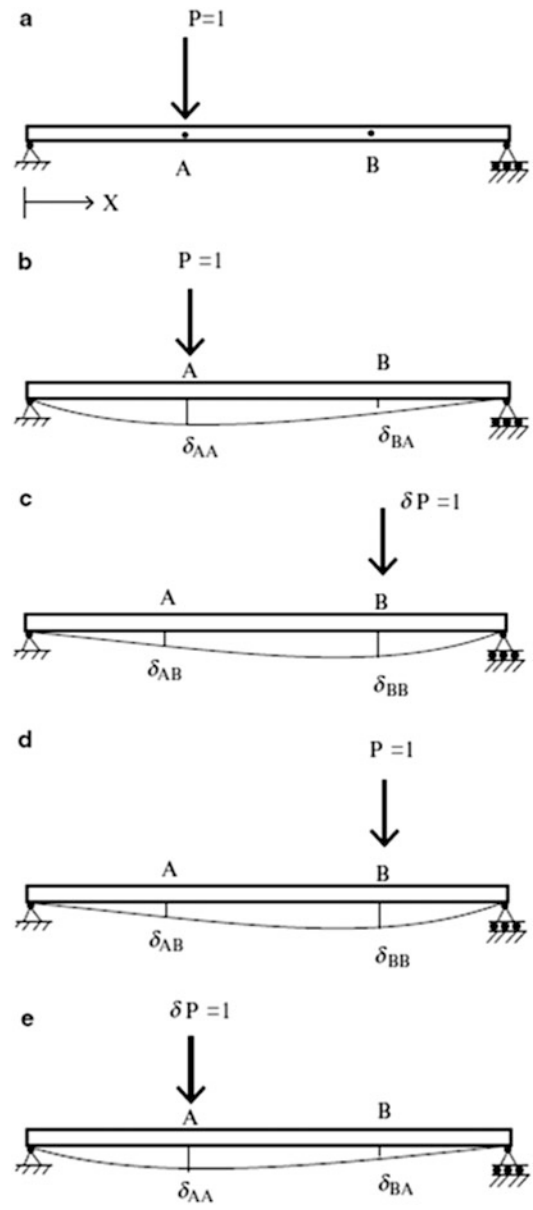

Fig. 9.16 Reciprocal loading conditions. (**a**) Actual structure. (**b**) Actual loading (M_A). (**c**) Virtual loading (δM_B). (**d**) Actual loading (M_B). (**e**) Virtual loading (δM_A)

the unit force applied at A is plotted in Fig. 9.16b. Suppose we want to determine the deflection at B due to this load applied at A. We define this quantity as δ_{BA}. Using the Principle of Virtual Forces specialized for beam bending; we apply a unit virtual force at B (see Fig. 9.16c) and evaluate the following integral:

$$\delta_{BA} = \int M_A \delta M_B \frac{dx}{EI} \tag{9.12}$$

where M_A is the moment due to the unit load applied at A, and δM_B is the moment due to the virtual unit load applied at B.

Now, suppose we want the deflection at A due to a unit load at B. The corresponding virtual force expression is

$$\delta_{AB} = \int M_B \delta M_A \frac{dx}{EI} \tag{9.13}$$

where δM_A is the virtual moment due to a unit force applied at A and M_B is the moment due to the load at B. Since we are applying unit loads, it follows that

$$\begin{aligned} M_A &= \delta M_A \\ M_B &= \delta M_B \end{aligned} \tag{9.14}$$

and we find that the expressions for δ_{AB} and δ_{BA} are identical.

$$\delta_{AB} \equiv \delta_{BA} \tag{9.15}$$

This identity is called *Maxwell's Law*. It is applicable for linear elastic structures [1]. Returning back to the compatibility equations, defined by (9.7), we note that the coupling terms, δ_{ij} and δ_{ji}, are equal. We say the coefficients are symmetrical with respect to their subscripts and it follows that δ is symmetrical. Maxwell's Law leads to another result called Müller–Breslau Principle which is used to establish influence lines for indeterminate beams and frames. This topic is discussed in Chaps. 13 and 15.

9.3 Application of the Force Method to Beam-Type Structures

We apply the theory presented in the previous section to a set of beam-type structures. For completeness, we also include a discussion of some approximate techniques for analyzing partially restrained single-span beams that are also useful for analyzing frames.

Example 9.1

Given: The beam defined in Fig. E9.1a. Assume $I = 120(10)^6$ mm^4, $L = 6$ m, $w = 30$ kN/m, $v_B = 40$ mm, and $E = 200$ GPa

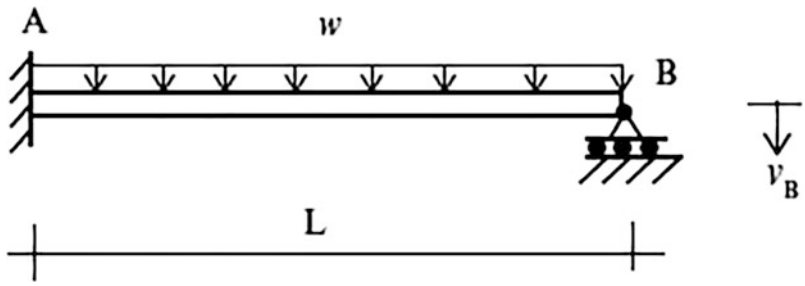

Fig. E9.1a

Determine: The reactions for the following cases:

(i) $w = 30$ kN/m, $v_B = 0$
(ii) $w = 0$, $v_B = 40$ mm
(iii) $w = 30$ kN/m, $v_B = 40$ mm

Solution: The beam is indeterminate to the first degree. We work with the primary structure shown below (Fig. E9.1b).

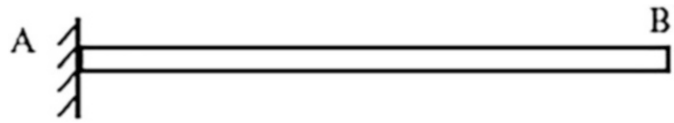

Fig. E9.1b Primary structure

Applying the external loading and the unit load results in the following deflected shapes (Figs. E9.1c and E9.1d):

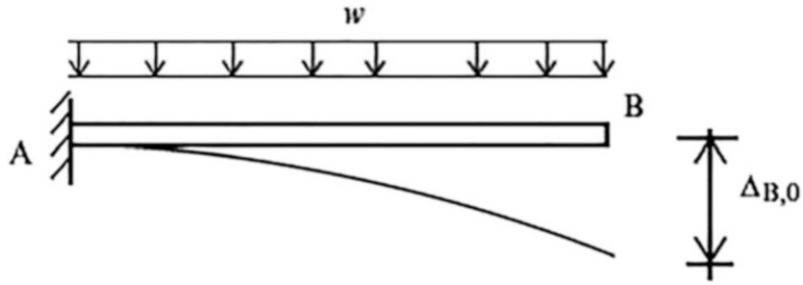

Fig. E9.1c Displacement due to external loading

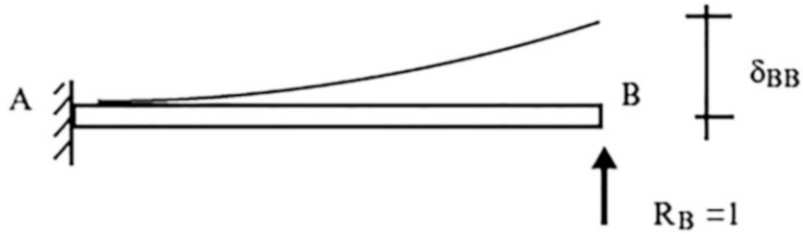

Fig. E9.1d Displacement due to the unit values of R_B The deflection terms are given in Table 3.1.

$$\Delta_{B,0} = \frac{wL^4}{8EI} \downarrow$$

$$\delta_{BB} = \frac{L^3}{3EI} \uparrow$$

Then

$$+\uparrow \quad \Delta_B\big|_{actual} = \Delta_{B,0} + \delta_{BB} R_B$$

$$\Downarrow$$

$$\Delta_B\big|_{actual} = -\frac{wL^4}{8EI} + \frac{L^3}{3EI} R_B \quad \therefore \; R_B = \frac{\Delta_B\big|_{actual} + \left(wL^4/8EI\right)}{\left(L^3/3EI\right)}$$

Case (i): For $\Delta_B\big|_{actual} = 0$

$$R_B = \left(\left(wL^4/8EI\right)/\left(L^3/3EI\right)\right) = \frac{3}{8}wL = \frac{3}{8}(30)(6) = 67.5\,\text{kN}\uparrow$$

Knowing the value of R_B, we determine the remaining reactions by using the static equilibrium equations.

$$\sum F_y = 0 \quad R_A = \frac{5}{8}wL = \frac{5}{8}(30)(6) = 112.5\,\text{kN}\uparrow$$

$$\sum M_{@A} = 0 \quad M_A = \frac{wL^2}{8} = 135\,\text{kN m} \quad \text{counterclockwise}$$

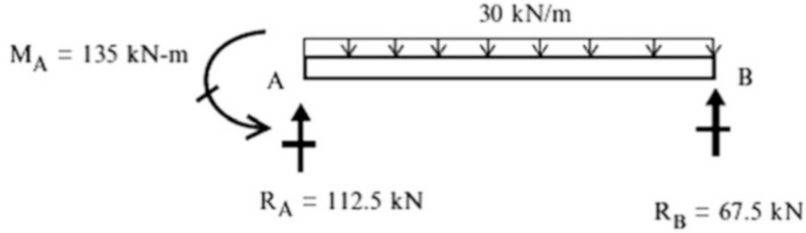

Case (ii): For $w = 0$, $\Delta_B|_{actual} = -v_B$

$$R_B = \frac{(-v_B)}{\left(L^3/3EI\right)} = -\frac{3EI}{L^3}v_B = -\frac{3(200)(10)^6 120(10)^{-6}}{(6)^3}(0.040) = -13.33\,\text{kN} \;\therefore\; R_B = 13.33\,\text{kN}\downarrow$$

The reactions are

$$\sum F_y = 0 \quad R_A = \frac{3EI}{L^3}v_B = 13.3\,\text{kN}\uparrow$$

$$\sum M_{@A} = 0 \quad M_A = \frac{3EI}{L^2}v_B = 80\,\text{kN m} \quad \text{counterclockwise}$$

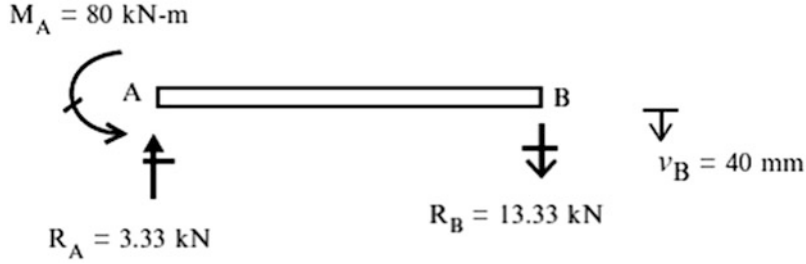

Case (iii): For $w \neq 0$ and $\Delta_B\big|_{actual} = -v_B$

$$R_B = \frac{-v_B + \left(wL^4/8EI\right)}{\left(L^3/3EI\right)} = +\frac{3}{8}wL - \frac{3EI}{L^3}v_B = 67.5 - 13.33 = 54.2\,\text{kN}\uparrow$$

The reactions are as follows:

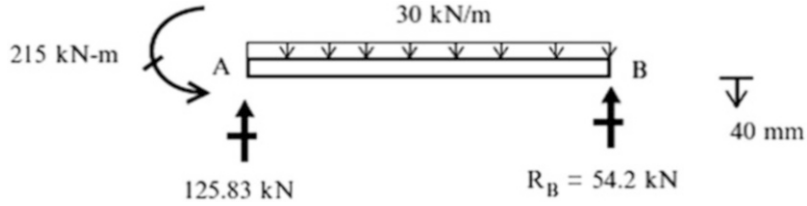

Note that since the structure is linear, one can superimpose the solutions for **cases** (**i**) and (**ii**).

Example 9.2

Given: The beam and loading defined in Fig. E9.2a. Assume $I = 400$ in.^{4}, $L = 54$ ft, $w = 2.1$ kip/ft, $\delta_A = 2.4$ in., and $E = 29{,}000$ ksi.

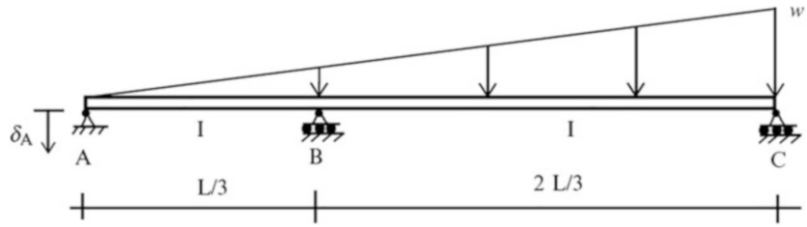

Fig. E9.2a

Determine: The reactions due to
(i) The distributed load shown
(ii) The support settlement at A

Solution: The beam is indeterminate to the first degree. We take the vertical reaction at B as the force unknown and compute the deflected shapes due to w and $R_B = 1$ applied to the primary structure (Figs. E9.2b and E9.2c).

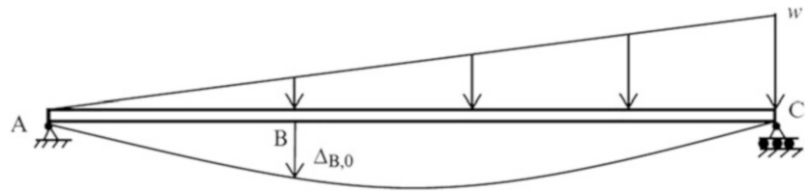

Fig. E9.2b Deflected shape due to w

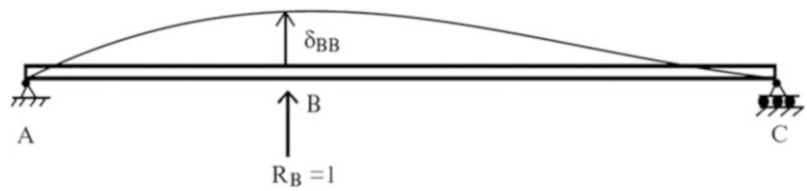

Fig. E9.2c Deflected shape due to unit value of R_B

Case (**i**): The distributed load shown

$$+\uparrow \quad \Delta_B\big|_{\text{actual}} = \Delta_{B,0} + \delta_{BB} R_B$$
$$\Downarrow$$
$$\Delta_{B,0} + \delta_{BB} R_B = 0 \ \therefore \ R_B = -\frac{\Delta_{B,0}}{\delta_{BB}}$$

The deflection terms can be determined using (3.34).

$$\Delta_{B,0} = -\frac{4wL^4}{729EI}$$
$$\delta_{BB} = \frac{4L^3}{243EI}$$

Then

$$R_B = -\frac{\Delta_{B,0}}{\delta_{BB}} = \frac{\left(4wL^4/729EI\right)}{\left(4L^3/243EI\right)} = \frac{wL}{3} = 37.8\,\text{kip} \uparrow$$

Knowing the value of R_B, we determine the remaining reactions by using the static equilibrium equations.

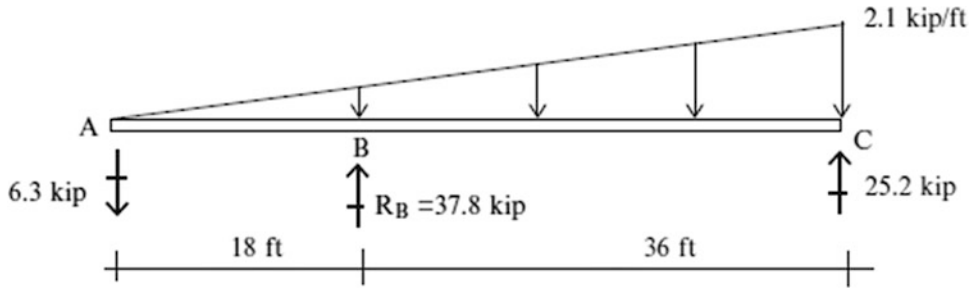

Case (**ii**): The support settlement at A (Fig. E9.2d)

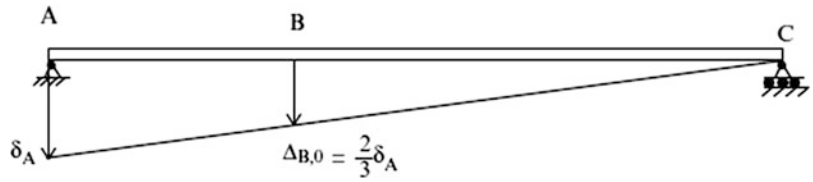

Fig. E9.2d Displacement due to support settlement at A

$$+\uparrow \quad \Delta_B\big|_{\text{actual}} = \Delta_{B,0} + \delta_{BB} R_B$$

where

$$\delta_{BB} = \frac{4L^3}{243EI} = \frac{4(54)^3(12)^3}{243(29,000)(400)} = 0.386\,\text{in.}$$
$$\Delta_{B,0} = \frac{2}{3}\delta_A = -1.6\,\text{in.}$$

Therefore

$$R_B = -\frac{\Delta_{B,0}}{\delta_{BB}} = -\frac{(-1.6)}{0.386} = 4.14\,\text{kip} \uparrow$$

We determine the remaining reactions using the static equilibrium equations.

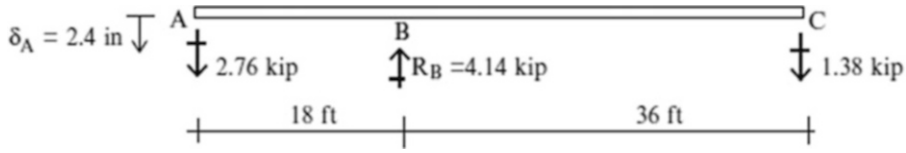

Example 9.3

Given:
The three-span beam defined in Fig. E9.3a. Assume EI is constant, $L = 9$ m, and $w = 20$ kN.

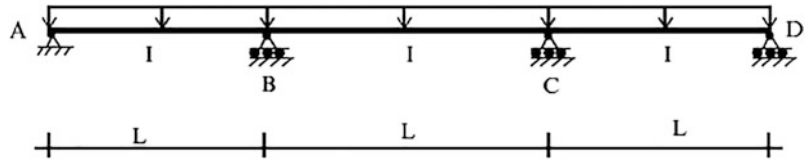

Fig. E9.3a

Determine: The reactions

Solution: The beam is indeterminate to the second degree. We remove the supports at B and C, take the vertical reactions at B and C as the force redundants, and compute the deflected shapes due to w, $X_1 = 1$, and $X_2 = 1$ applied to the primary structure (Figs. E9.3b, E9.3c, E9.3d).

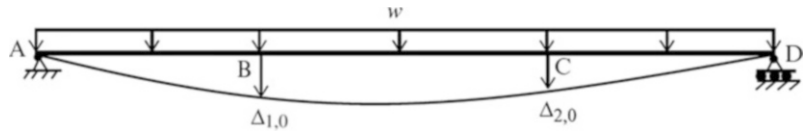

Fig. E9.3b Deflected shape due to external loading

Fig. E9.3c Deflected shape due to $X_1 = 1$

Fig. E9.3d Deflected shape due to $X_2 = 1$

The displacements of the primary structure due to the external loading and the two force redundants are expressed as:

$$\Delta_{1,0} + \delta_{11}X_1 + \delta_{12}X_2 = 0$$
$$\Delta_{2,0} + \delta_{21}X_1 + \delta_{22}X_2 = 0$$

Noting symmetry and the deflection results listed in Table 3.1, it follows that:

$$X_1 = X_2$$
$$\Delta_{1,0} = \Delta_{2,0} = -\frac{11wL^4}{12EI}$$
$$\delta_{11} = \delta_{22} = \frac{4L^3}{9EI}$$
$$\delta_{21} = \delta_{12} = \frac{7L^3}{18EI}$$

Then

$$X_1 = X_2 = \frac{-\Delta_{1,0}}{\delta_{11} + \delta_{12}} = \frac{\left(11wL^4/12EI\right)}{\left(4L^3/9EI\right) + \left(7L^3/18EI\right)} = 1.1\,wL = 1.1(20)(9) = 198\,\text{kN}$$

Lastly, we determine the remaining reactions

$$\sum F_Y = 0 \quad R_A = R_D = 0.4wL = 72\,\text{kN} \uparrow$$

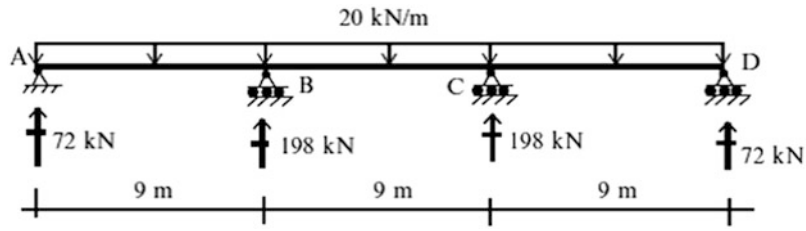

9.3.1 Beam with Yielding Supports

We consider next the case where a beam is supported by another member, such as another beam or a cable. Examples are shown in Fig. 9.17. When the beam is loaded, reactions are developed, and the supporting members deform. Assuming linear elastic behavior, the supporting members

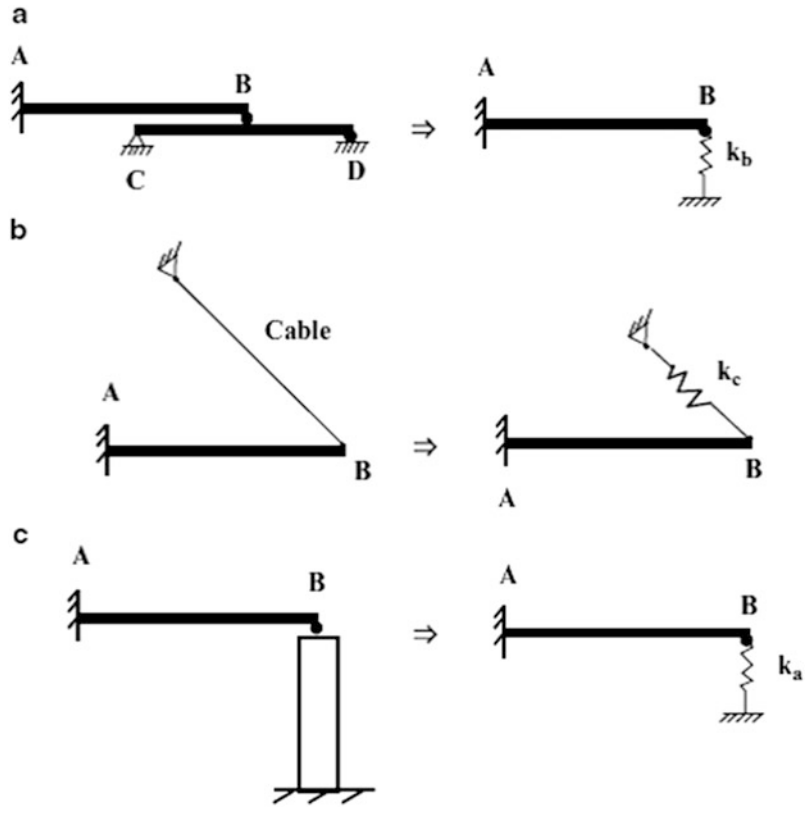

Fig. 9.17 Beam on flexible supports. (**a**) Beam. (**b**) Cable. (**c**) Column

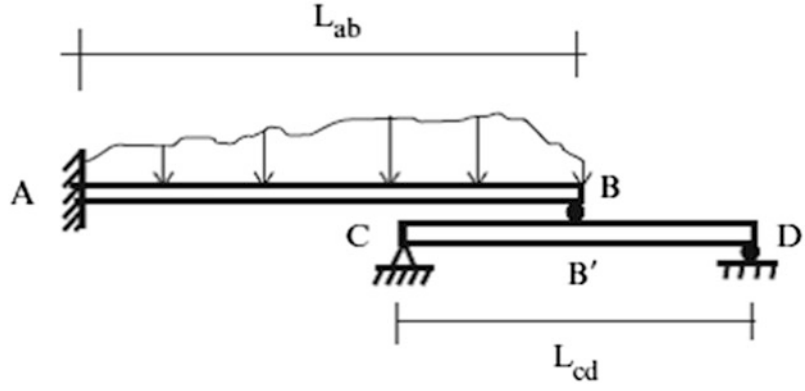

Fig. 9.18 Beam supported by another beam

behave as linear elastic restraints, and can be modeled as equivalent spring elements, as indicated in Fig. 9.17.

We consider here the case where a vertical restraint is provided by another beam. Figure 9.18 illustrates this case. Point B is supported by beam CD which is parallel to beam AB. In this case, point B deflects when the load is applied to beam AB. One strategy is to work with a primary structure that includes both beams such as shown in Fig. 9.19. The force redundant is now a pair of self-equilibrating forces acting at B, and the corresponding displacement measure is the relative displacement apart between the upper and lower contact points, designated as B and B′.

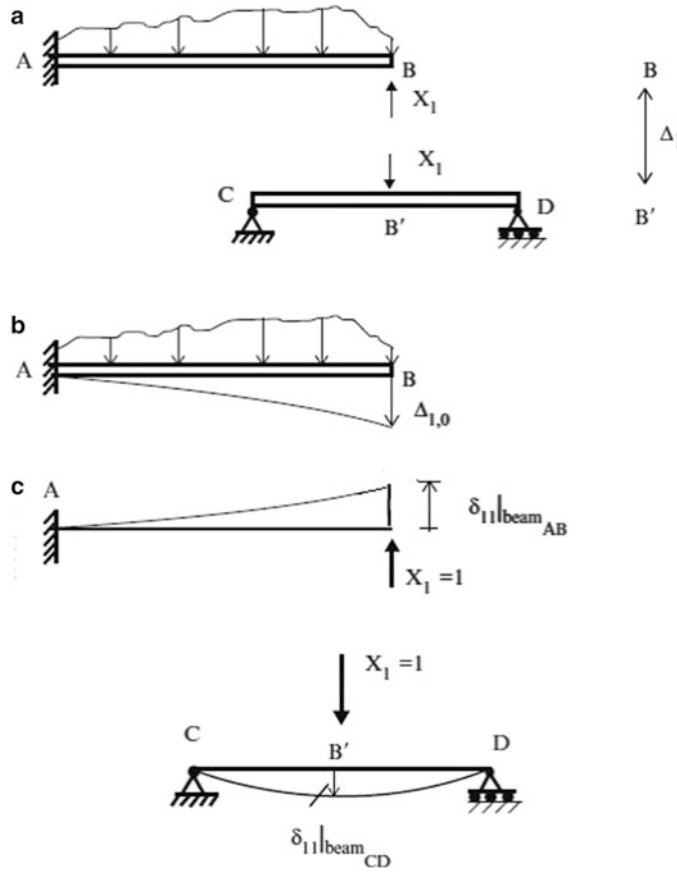

Fig. 9.19 Choice of force redundant and displacement profiles. (**a**) Primary structure—force redundant system. (**b**) Deflection due to external loading. (**c**) Deflection due to redundant force at B

The total displacement corresponding to $X_1 = 1$ is the sum of two terms,

$$\begin{aligned}\delta_{11} &= \delta_{11}\big|_{\text{AB}} + \delta_{11}\big|_{\text{CD}} \\ &= \frac{L^3}{3EI} + \delta_{11}\big|_{\text{CD}}\end{aligned}$$

Beam CD functions as a restraint on the movement of beam AB. The downward movement of B′ is resisted by the bending action of beam CD. Assuming linear elastic behavior, this restraint can be modeled as a linear spring of stiffness k. One chooses the magnitude of k such that the spring deflection due to the load P is the same as the beam deflection.

Then, it follows from Fig. 9.20 that

$$\delta_{11}\big|_{\text{CD}} = \frac{1}{k_{\text{CD}}} \tag{9.16}$$

Assuming the two beams are rigidly connected at B, the net relative displacement must be zero.

$$\Delta_1 = \Delta_{1,0} + X_1\left(\frac{1}{k_{\text{CD}}} + \frac{L^3}{3EI}\right) = 0 \tag{9.17}$$

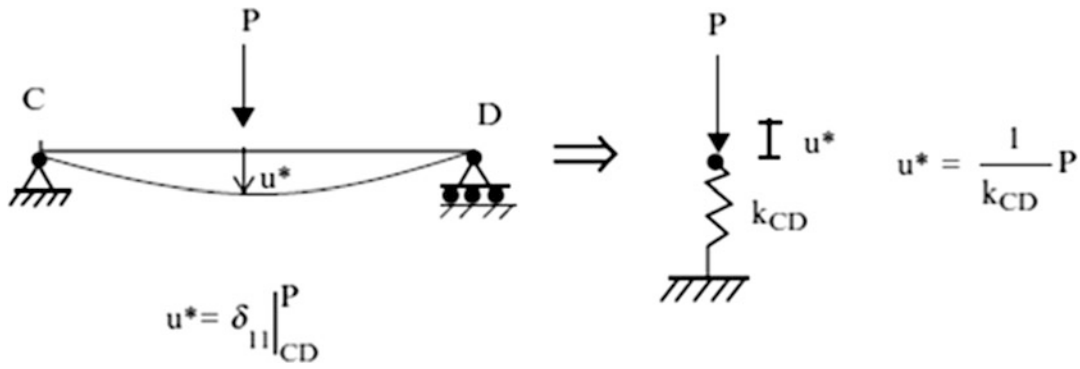

Fig. 9.20 Equivalent spring

Solving (9.17) for X_1 leads to

$$X_1 = \left\{ \frac{-1}{(L^3/3EI) + (1/k_{CD})} \right\} \Delta_{1,0} \tag{9.18}$$

Note that the value of X_1 depends on the stiffness of beam CD. Taking $k_{CD} = \infty$ corresponds to assuming a rigid support, i.e., a roller support. When $k_{CD} = 0$, $X_1 = 0$. It follows that the bounds on X_1 are

$$\mathbf{0} < X_1 < \left(\frac{3EI}{L^3} \right) \Delta_{1,0} \tag{9.19}$$

When the loading is uniform,

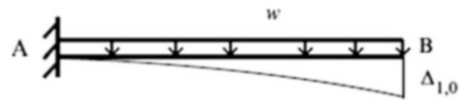

$$\Delta_{1,0} = \frac{wL^4}{8EI} \downarrow$$

Another type of elastic restraint is produced by a cable. Figure 9.21 illustrates this case. We replace the cable with its equivalent stiffness, $k_C = \frac{A_c E_c}{h}$ and work with the primary structure shown in Fig. 9.21b.

Using the results derived above, and noting that $\Delta_1 = 0$, the geometric compatibility equation is

$$\Delta_1 = \Delta_{1,0} + \left(\delta_{11}\big|_{AB} + \delta_{11}\big|_{BC} \right) X_1 = 0$$

For the external concentrated loading,

$$\Delta_{1,0} = \frac{P}{EI} \left(\frac{a^2 L}{2} - \frac{a^3}{3} \right)$$

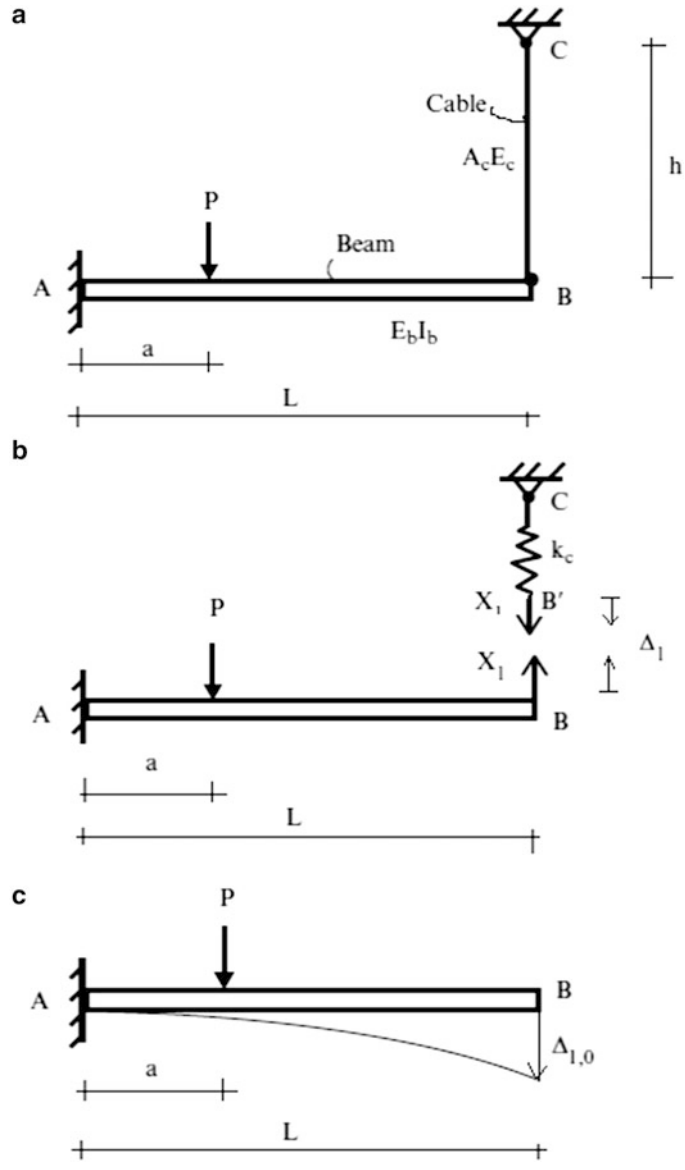

Fig. 9.21 (**a**) Actual structure. (**b**) Primary structure—force redundant system. (**c**) Deflection due to applied load

Substituting for the various flexibility terms leads to

$$X_1 = \left[\frac{-1}{\left(L^3/3E_bI_b\right) + \left(1/k_c\right)}\right]\Delta_{1,0} \tag{9.20}$$

If $\frac{1}{k_c}$ is small with respect to $\frac{L^3}{3E_bI_b}$, the cable acts like a rigid support, i.e., X_1 approaches the value for a rigid support. When $\frac{1}{k_c}$ is large with respect to $\frac{L^3}{3E_bI_b}$, the cable is flexible and provides essentially no resistance, i.e., $X_1 \Rightarrow 0$. The ratio of cable to beam flexibilities is a key parameter for the behavior of this system.

Cable-stayed schemes are composed of beams supported with inclined cables. Figure 9.22a shows the case where there is just one cable. We follow essentially the same approach as described earlier

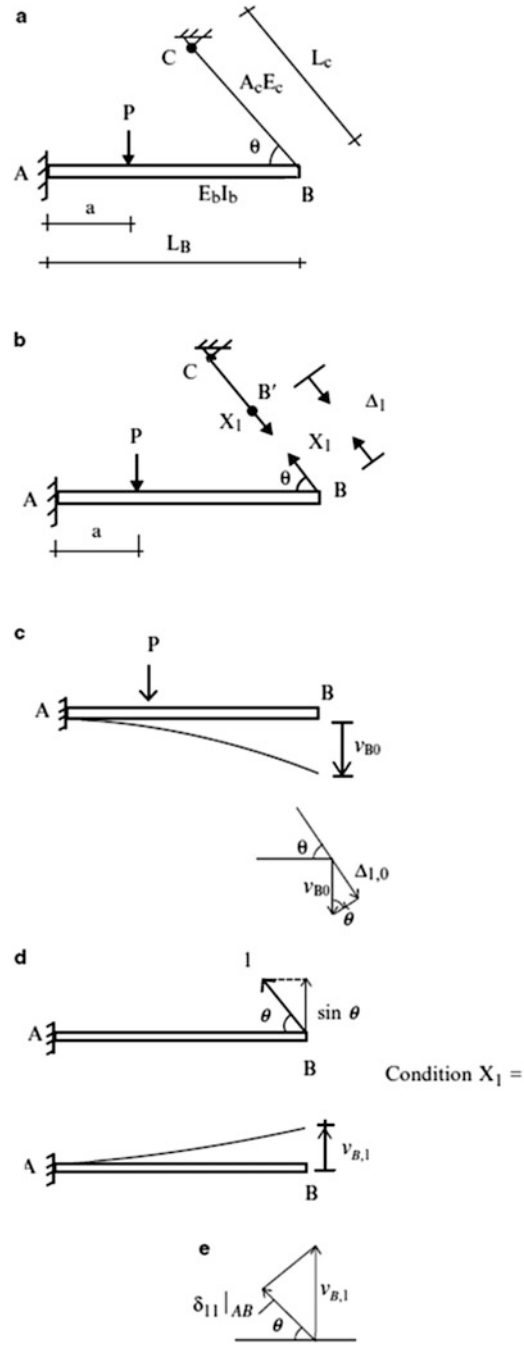

Fig. 9.22 (**a**) Cable-stayed scheme. (**b**) Force redundant. (**c**) Deflection due to applied load. (**d**) Deflection due to $X_1 = 1$. (**e**) Displacement components

except that now the cable is inclined. We take the cable force as the redundant and work with the structure defined in Fig. 9.22b.

Note that Δ_1 is the relative movement together of points B and B′ along the inclined direction. Up to this point, we have been working with vertical displacements. Now we need to project these movements on an inclined direction.

We start with the displacement profile shown in Fig. 9.22c. The vertical deflection is v_{B0}. Projecting on the direction of the cable leads to

$$\Delta_{1,0} = -\sin\theta v_{B0} = -\sin\theta\left\{\frac{P}{E_B I_B}\left(\frac{a^2 L_B}{2} - \frac{a^3}{6}\right)\right\} \tag{9.21}$$

Next, we treat the case where $X_1 = 1$ shown in Fig. 9.22d. The total movement consists of the elongation of the cable and the displacement of the beam.

$$\delta_{11} = \delta_{11}\big|_{BC} + \delta_{11}\big|_{AB}$$

The elongation of the cable is

$$\delta_{11}\big|_{BC} = \frac{L_c}{A_C E_C} = \frac{1}{k_C}$$

The beam displacement follows from Fig. 9.22e.

$$\delta_{11}\big|_{AB} = v_{B,1}\sin\theta = \sin\theta\left\{\frac{\sin\theta L_B^3}{3E_B I_B}\right\} = (\sin\theta)^2\left(\frac{L_B^3}{3E_B I_B}\right)$$

Requiring $\Delta_1 = 0$ leads to

$$X_1 = \frac{1}{(\sin\theta)^2\left(L_B^3/3E_B I_B\right) + (1/k_C)}\left[\frac{P\sin\theta}{E_B I_B}\left(\frac{a^2 L_B}{2} - \frac{a^3}{6}\right)\right] \tag{9.22}$$

Finally, we express X_1 in terms of the value of the vertical reaction corresponding to a rigid support at B.

$$X_1 = \frac{\sin\theta}{(\sin\theta)^2 + 3\left(E_B I_B/L_B^3\right)\left(L_C/E_C A_C\right)} R\big|_{\text{rigid support at B}} \tag{9.23}$$

There are two geometric parameters, θ, and the ratio of $I_B/{L_B}^3$ to A_C/L_C. Note that X_1 varies with the angle θ. When cables are used to stiffen beams, such as for cable-stayed bridges, the optimum cable angle is approximately 45°. The effective stiffness provided by the cable degrades rapidly with decreasing θ.

Example 9.4

Given: The structure defined in Fig. E9.4a.

Assume $I = 400$ in.^{4}, $L = 54$ ft, $w = 2.1$ kip/ft, $k_v = 25$ kip/in., and $E = 29{,}000$ ksi.

Determine: The reactions, the axial force in the spring, and the displacement at B.

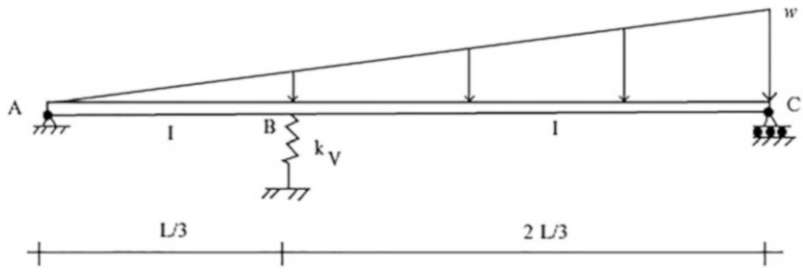

Fig. E9.4a

Solution: The structure is indeterminate to the first degree. We take the axial force in the spring at B as the force unknown.

The geometric compatibility equation is

$$\Delta_{1,0} + \left(\delta_{11}|_{\text{ABC}} + \frac{1}{k_v}\right) X_1 = 0$$

The deflection terms can be determined using (3.34).

$$\Delta_{1,0} = -\frac{4wL^4}{729EI} = 14.6\,\text{in.}$$

$$\delta_{11}\big|_{\text{ABC}} = \frac{4L^3}{243EI} = 0.386\,\text{in.}$$

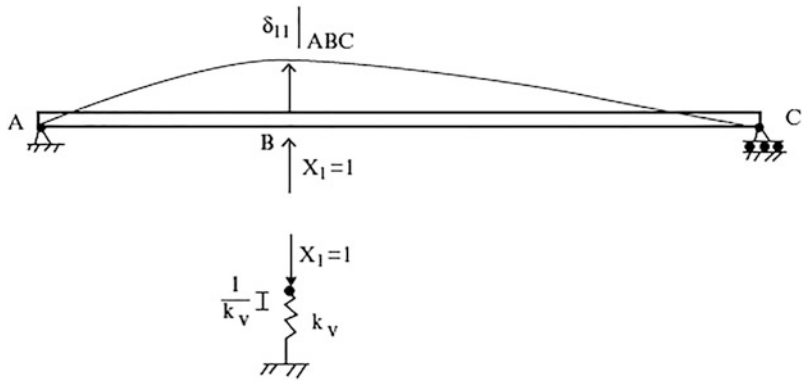

Fig. E9.4b Deflected shape due to $X_1 = 1$

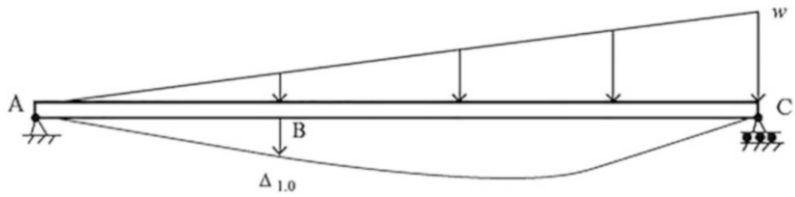

Fig. E9.4c Deflected shape due to external loading

Solving for X_1, leads to:

$$X_1 = \frac{\Delta_{1,0}}{\delta_{11}\big|_{ABC} + (1/k_v)} = \frac{14.6}{0.386 + (1/25)} = 34.26\,\text{kip} \uparrow$$

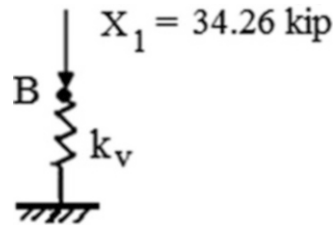

The displacement at B is

$$v_B = \frac{X_1}{k_v} = \frac{34.26}{25} = 1.37\,\text{in.} \downarrow$$

Next, we determine the remaining reactions by using the static equilibrium equations.

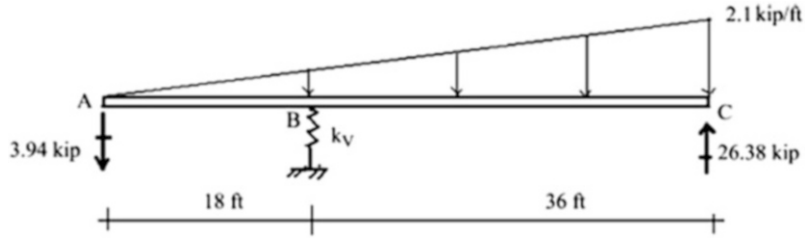

Example 9.5

Given: The structure defined in Fig. E9.5a. Assume $I = 200(10)^6$ mm^4, $L = 18$ m, $P = 45$ kN, $A_C = 1300$ mm^2, and $E = 200$ GPa.

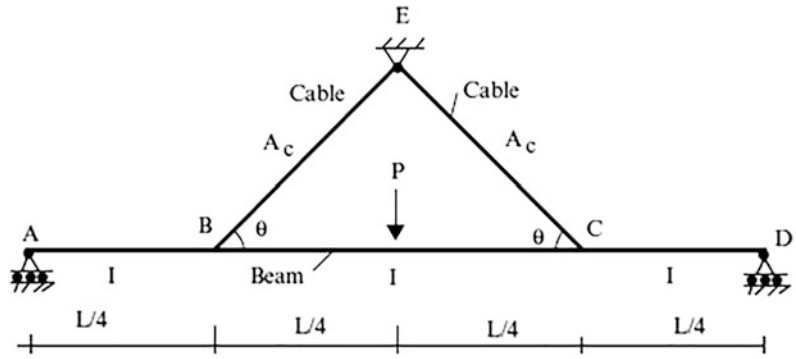

Fig. E9.5a

Determine: The forces in the cables, the reactions, and the vertical displacement at the intersection of the cable and the beam.

(a) $\theta = 45^\circ$
(b) $\theta = 15^\circ$

Solution: The structure is indeterminate to the second degree. We take the cable forces as the force redundants and work with the structure defined below (Fig. E9.5b).

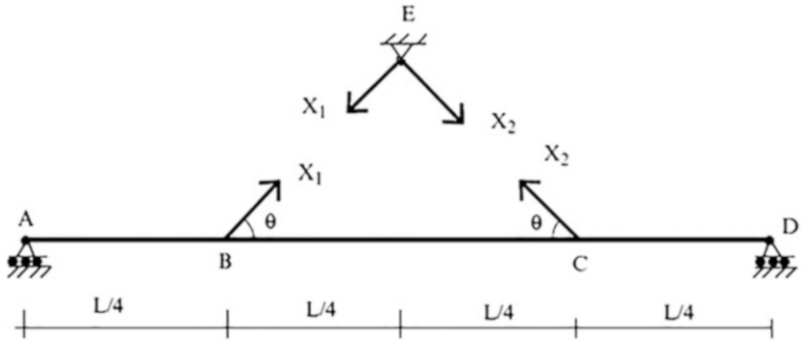

Fig. E9.5b Primary structure

Next, we compute the deflected shapes due to external loading P, $X_1 = 1$, and $X_2 = 1$ applied to the primary structure (Figs. E9.5c, E9.5d, E9.5e).

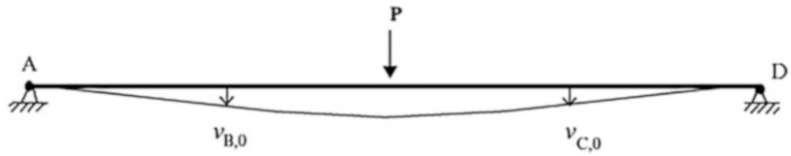

Fig. E9.5c External loading P

Fig. E9.5d $X_1 = 1$

Fig. E9.5e $X_2 = 1$

The displacements of the primary structure due to the external loading and the two force redundants are expressed as

$$\Delta_{1,0} + \delta_{11}X_1 + \delta_{12}X_2 = 0$$
$$\Delta_{2,0} + \delta_{21}X_1 + \delta_{22}X_2 = 0$$

where

$$\delta_{11} = \delta_{11}|_{\text{Beam}} + \delta_{11}|_{\text{cable}}$$
$$\delta_{22} = \delta_{22}|_{\text{Beam}} + \delta_{22}|_{\text{cable}}$$
$$\delta_{12} = \delta_{12}|_{\text{Beam}}$$
$$\delta_{21} = \delta_{21}|_{\text{Beam}}$$

also

$$\Delta_{1,0} = v_{\text{B},0}\sin\theta$$
$$\Delta_{2,0} = v_{\text{C},0}\sin\theta$$
$$\delta_{11}|_{\text{Beam}} = v_{\text{B},1}\sin\theta$$
$$\delta_{21}|_{\text{Beam}} = v_{\text{C},1}\sin\theta$$
$$\delta_{21}|_{\text{Beam}} = v_{\text{B},2}\sin\theta$$
$$\delta_{22}|_{\text{Beam}} = v_{\text{C},2}\sin\theta$$

Because of symmetry:

$$\delta_{11}|_{\text{Beam}} = \delta_{22}|_{\text{Beam}} = v_{\text{B},1}\sin\theta = \frac{3\sin\theta^2 L^3}{256EI}$$
$$\delta_{12}|_{\text{Beam}} = \delta_{21}|_{\text{Beam}} = v_{\text{B},2}\sin\theta = \frac{7\sin\theta^2 L^3}{768EI}$$
$$\Delta_{1,0} = \Delta_{2,0} = v_{\text{B},0}\sin\theta = \frac{11\sin\theta PL^3}{768EI}$$
$$\delta_{11}|_{\text{Cable}} = \delta_{22}|_{\text{Cable}} = \frac{L_{\text{C}}}{A_{\text{C}}E} = \frac{L}{4\cos\theta A_{\text{C}}E}$$
$$X_1 = X_2$$

Lastly, the redundant forces are

$$X_1 = X_2 = \frac{\Delta_{1,0}}{\left(\delta_{11}|_{\text{Beam}} + \delta_{11}|_{\text{Cable}}\right) + \delta_{12}|_{\text{Beam}}}$$

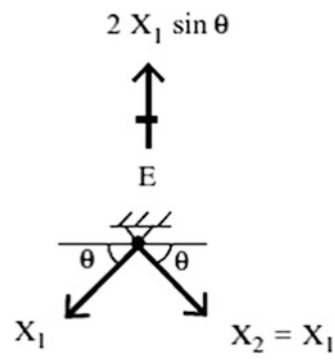

(a) For $\theta = 45^\circ$

$$X_1 = X_2 = \frac{\Delta_{1,0}}{\left(\delta_{11}\big|_{\text{Beam}} + \delta_{11}\big|_{\text{Cable}}\right) + \delta_{12}\big|_{\text{Beam}}} = 43\,\text{kN}$$

$$\therefore\ 2X_1 \sin\theta = 2(43)\sin 45 = 60.8\,\text{kN}$$

The remaining reactions are determined using the static equilibrium equations.

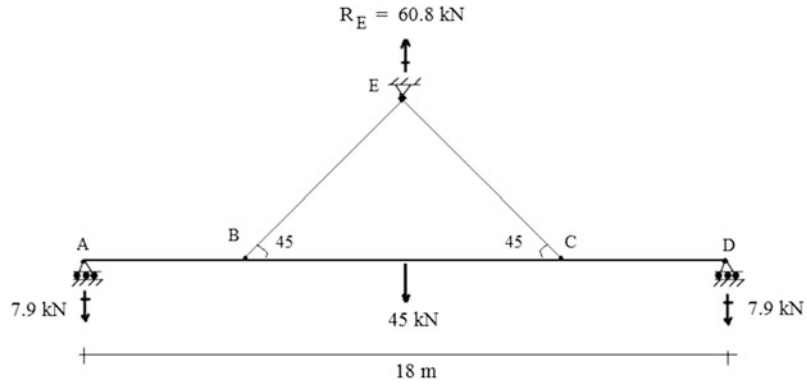

(b) For $\theta = 15^\circ$

$$X_1 = X_2 = \frac{\Delta_{1,0}}{\left(\delta_{11}\big|_{\text{Beam}} + \delta_{11}\big|_{\text{Cable}}\right) + \delta_{12}\big|_{\text{Beam}}} = 109.8\,\text{kN}$$

$$\therefore\ 2X_1 \sin\theta = 2(109.8)\sin 15 = 56.9\,\text{kN}$$

The remaining reactions are determined using the static equilibrium equations.

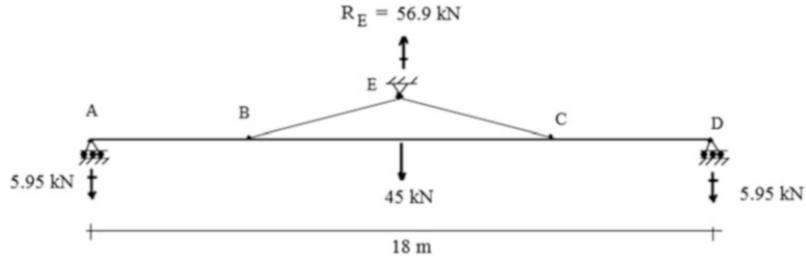

9.3.2 Fixed-Ended Beams

We treat next the beam shown in Fig. 9.23a. The structure is fully restrained at each end and therefore is indeterminate to the second degree. We take as force redundants the counterclockwise end moments at each end. The corresponding displacement measures are the counterclockwise end rotations, θ_A and θ_B.

We write the general form of the compatibility equations as (we use θ instead of Δ to denote the displacement measures and M instead of X for the force measures):

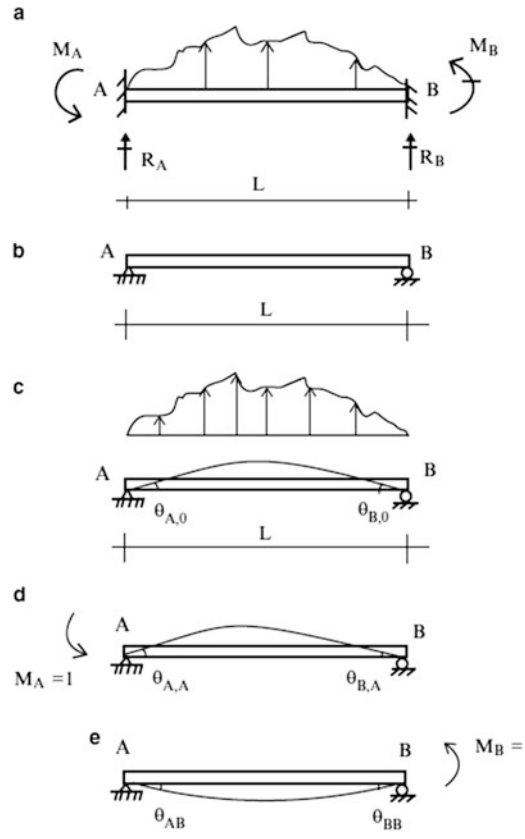

Fig. 9.23 (**a**) Beam with full end restraint. (**b**) Primary structure. (**c**) External loading—displacement profile. (**d**) Displacement profile for $M_A = 1$. (**e**) Displacement profile for $M_B = 1$

$$\begin{aligned}\theta_A &= \theta_{A,0} + M_A\theta_{AA} + M_B\theta_{AB}\\ \theta_B &= \theta_{B,0} + M_A\theta_{BA} + M_B\theta_{BB}\end{aligned} \tag{9.24}$$

where $\theta_{A,0}$ and $\theta_{B,0}$ depend on the nature of the applied loading, and the other flexibility coefficients are

$$\begin{aligned}\theta_{AA} &= \frac{L}{3EI}\\ \theta_{BB} &= \frac{L}{3EI}\\ \theta_{AB} &= \theta_{BA} = -\frac{L}{6EI}\end{aligned}$$

We solve (9.24) for M_A and M_B

$$\begin{aligned}M_A &= \frac{2EI}{L}\{2(\theta_A - \theta_{A,0}) + (\theta_B - \theta_{B,0})\}\\ M_B &= \frac{2EI}{L}\{2(\theta_B - \theta_{B,0}) + (\theta_A - \theta_{A,0})\}\end{aligned} \tag{9.25}$$

When the ends are fixed, $\theta_A = \theta_B = 0$, and the corresponding values of M_A and M_B are called the fixed end moments. They are usually denoted as $M_A{}^F$ and $M_B{}^F$

$$M_{\mathrm{A}}^{\mathrm{F}} = -\frac{2EI}{L}\{2\theta_{\mathrm{A},0} + \theta_{\mathrm{B},0}\}$$
$$M_{\mathrm{B}}^{\mathrm{F}} = -\frac{2EI}{L}\{2\theta_{\mathrm{B},0} + \theta_{\mathrm{A},0}\} \tag{9.26}$$

Introducing this notation in (9.25), the expressions for the end moments reduce to

$$M_{\mathrm{A}} = \frac{2EI}{L}\{2\theta_{\mathrm{A}} + \theta_{\mathrm{B}}\} + M_{\mathrm{A}}^{\mathrm{F}}$$
$$M_{\mathrm{B}} = \frac{2EI}{L}\{2\theta_{\mathrm{B}} + \theta_{\mathrm{A}}\} + M_{\mathrm{B}}^{\mathrm{F}} \tag{9.27}$$

We will utilize these equations in Chap. 10.

Example 9.6 Fixed End Moments for Uniformly Distributed Loading

Given: The uniform distributed loading applied to a fixed end beam (Fig. E9.6a).

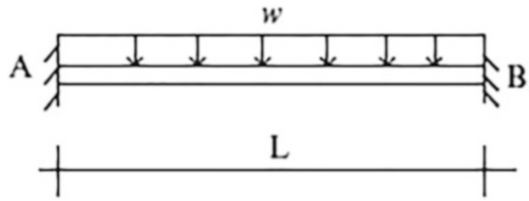

Fig. E9.6a

Determine: The fixed end moments.

Solution: We take the end moments at A and B as force redundant (Fig. E9.6b).

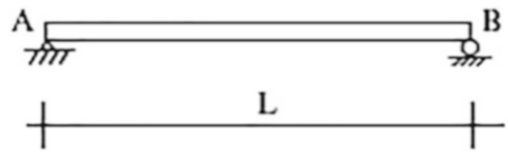

Fig. E9.6b Primary structure

Noting Table 3.1, the rotations due to the applied load are (Fig. E9.6c)

$$EI\theta_{\mathrm{A},0} = -\frac{wL^3}{24} \quad EI\theta_{\mathrm{B},0} = \frac{wL^3}{24}$$

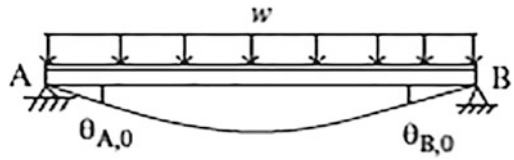

Fig. E9.6c Deformation of primary structure due to applied load

Substituting their values in (9.26) leads to

$$M_{\mathrm{A}}^{\mathrm{F}} = -\frac{2EI}{L}\{2\theta_{\mathrm{A},0} + \theta_{\mathrm{B},0}\} = \frac{wL^2}{6} - \frac{wL^2}{12} = \frac{wL^2}{12}$$
$$M_{\mathrm{B}}^{\mathrm{F}} = -\frac{2EI}{L}\{2\theta_{\mathrm{B},0} + \theta_{\mathrm{A},0}\} = -\frac{wL^2}{6} + \frac{wL^2}{12} = -\frac{wL^2}{12}$$

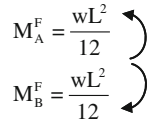

The shear and moment diagrams are plotted in Fig. E9.6d.

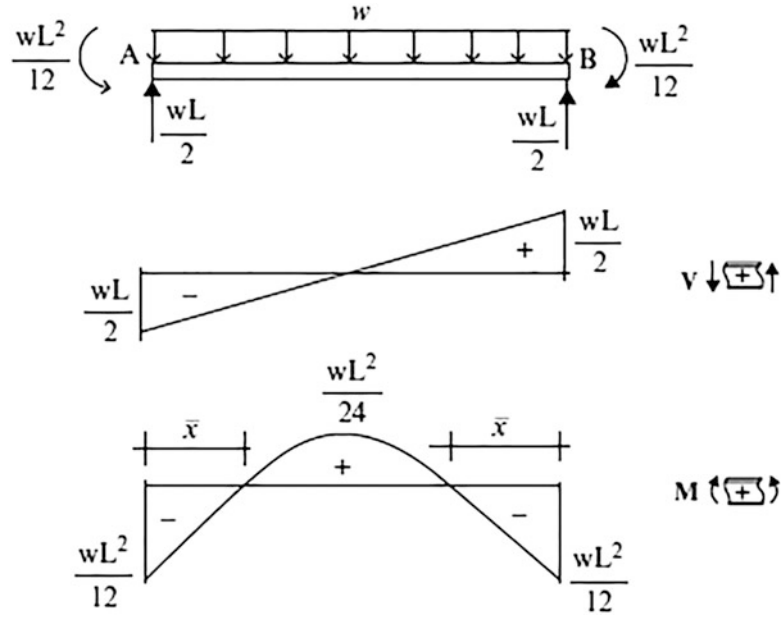

Fig. E9.6d

Note that the peak positive moment for the simply supported case is $+(wL^2/8)$. Points of inflection are located symmetrically at

$$\overline{x} = \frac{L}{2}\left(1 - \frac{1}{\sqrt{3}}\right) \approx 0.21L$$

This solution applies for full fixity. When the member is part of a frame, the restraint is provided by the adjacent members, and the end moments will generally be less than the fully fixed value.

Example 9.7 Fixed End Moment—Single Concentrated Force

Given: A single concentrated force applied at an arbitrary point $x = a$ on the fixed end beam shown in Fig. E9.7a.

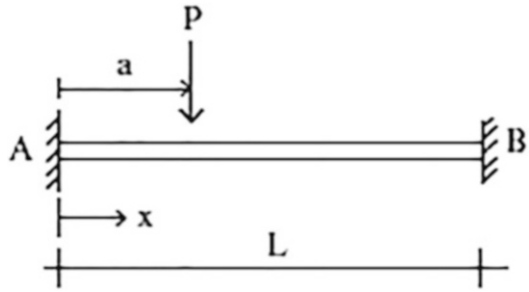

Fig. E9.7a

Determine: The fixed end moments.

Solution: We work with the primary structure defined in Fig. E9.7b.

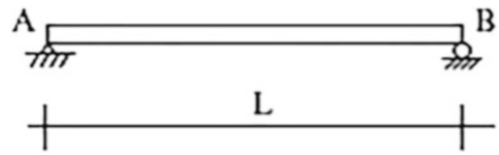

Fig. E9.7b Primary structure

Using the results listed in Table 3.1, the rotations are given by (Fig. E9.7c)

$$EI\theta_{\mathrm{A},0} = -\frac{Pa(L-a)(2L-a)}{6\mathrm{L}}$$

$$EI\theta_{\mathrm{B},0} = \frac{Pa(L-a)(L+a)}{6L}$$

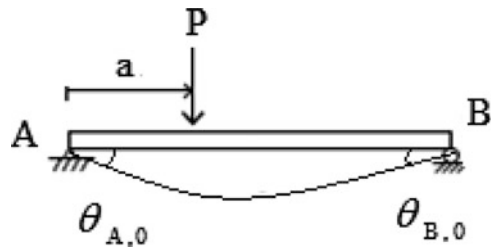

Fig. E9.7c Deformation of primary structure due to external loading

Substituting into (9.26) leads to

$$M_{\mathrm{A}}^{\mathrm{F}} = \frac{Pa(L-a)^2}{L^2}$$

$$M_{\mathrm{B}}^{\mathrm{F}} = -\frac{P(L-a)a^2}{L^2}$$

The critical location for maximum fixed end moment is $a = L/2$; the corresponding maximum values are $M_{\mathrm{A}}^{\mathrm{F}} = -M_{\mathrm{B}}^{\mathrm{F}} = \frac{PL}{8}$. The shear and moment diagrams are plotted below.

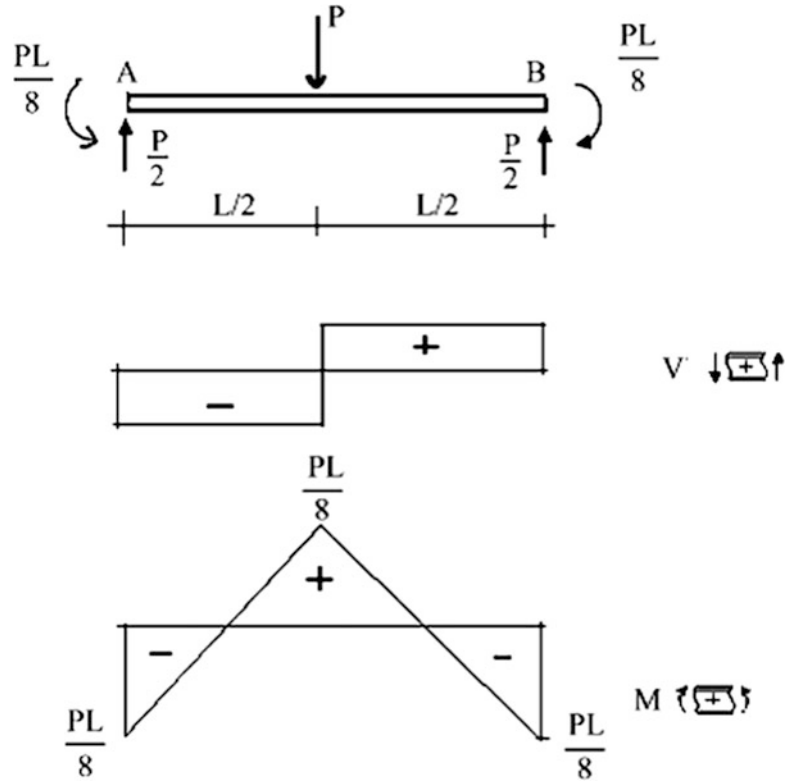

Note that there is a 50 % reduction in peak moment due to end fixity.
Results for various loadings and end conditions are summarized in Tables 9.1 and 9.2.

Table 9.1 Fixed end actions for fully fixed

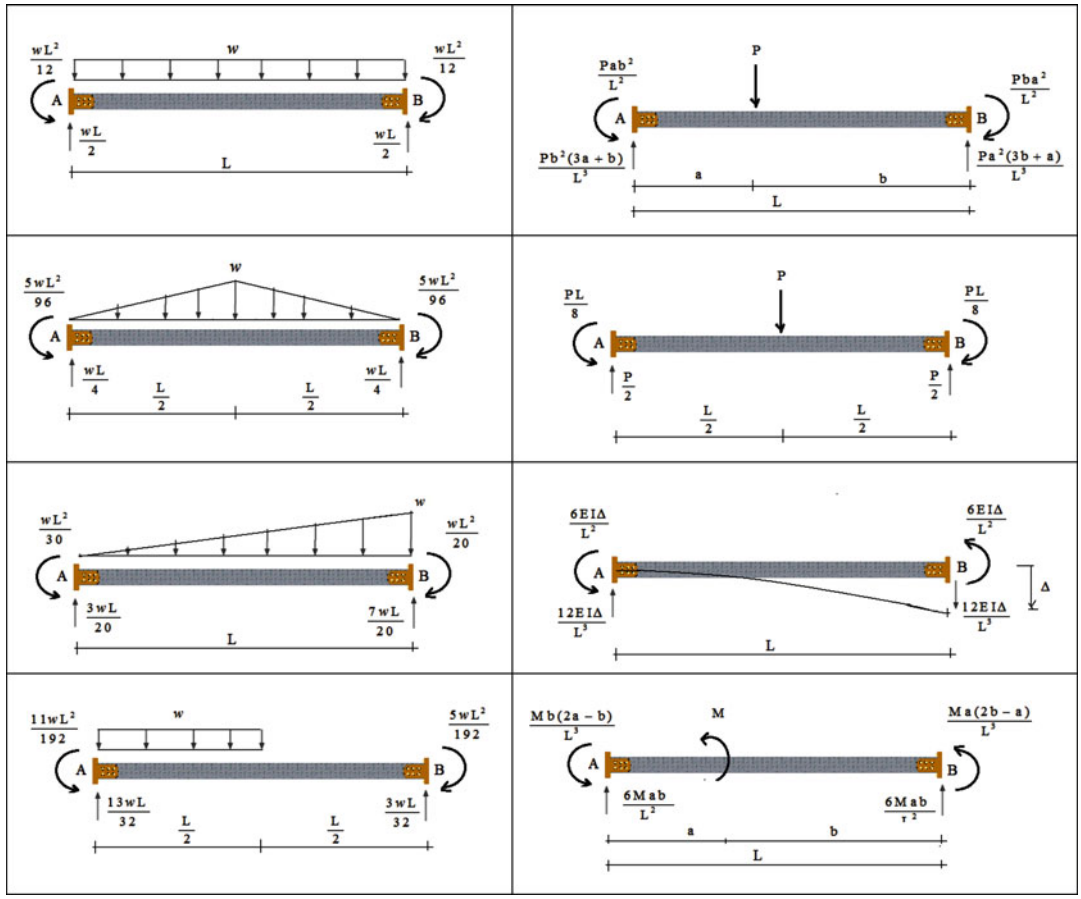

Table 9.2 Fixed end actions for partially fixed

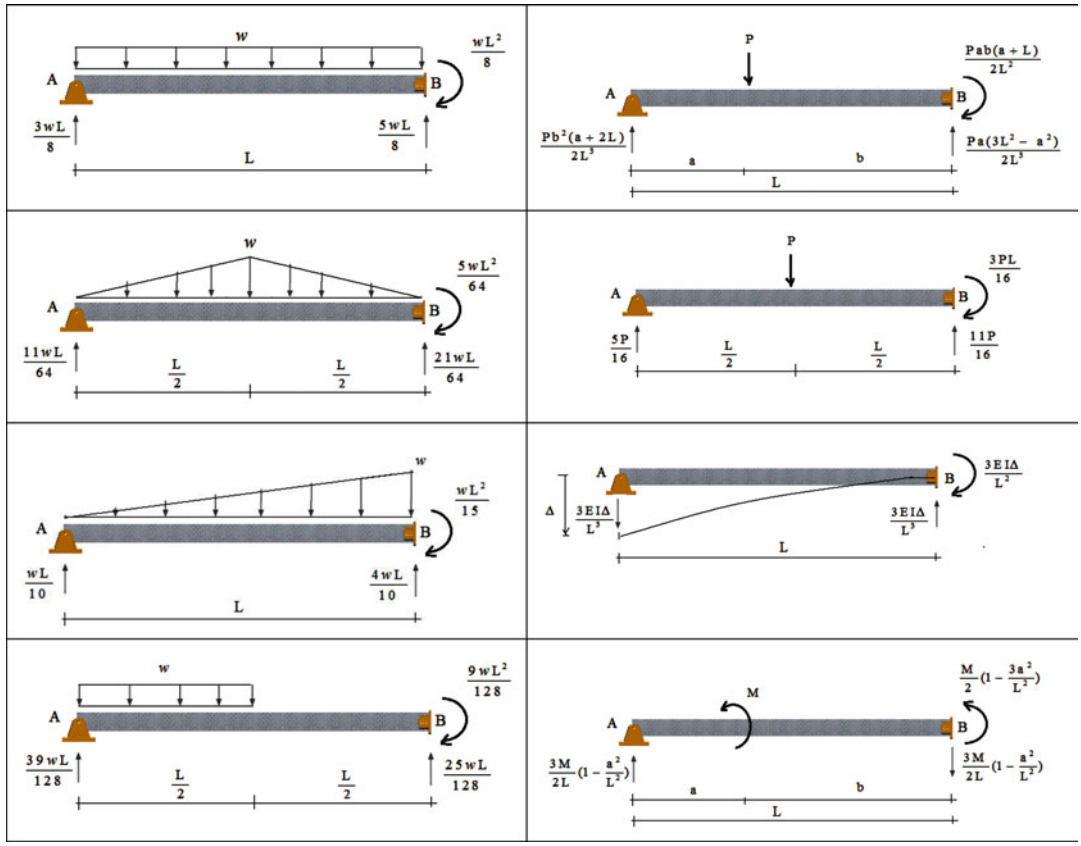

9.3.3 Analytical Solutions for Multi-Span Beams

Consider the two-span beam shown in Fig. 9.24a. We allow for different lengths and different moments of inertia for the spans. Our objective here is to determine analytically how the maximum positive and negative moments vary as the load moves across the total span. We choose the negative moment at B as the redundant. The corresponding primary structure is shown in Fig. 9.24b. Here, $\Delta\theta_B$ is the relative rotation together of adjacent cross sections at B.

The geometric compatibility equation involves the relative rotation at B.

$$\Delta\theta_B = \Delta\theta_{B,0} + \delta\theta_{BB} M_B = 0$$

The various rotation terms are given in Table 3.1. Note that the $\delta\theta_{BB}$ term is independent of the applied loading.

$$\delta\theta_{BB} = \frac{1}{3E}\left(\frac{L_1}{I_1} + \frac{L_2}{I_2}\right)$$

When the loading is on span AB (see Table 3.1),

$$\Delta\theta_{B,0} = -\frac{P}{6EI_1L_1}a\left(a^2 - L_1^2\right)$$

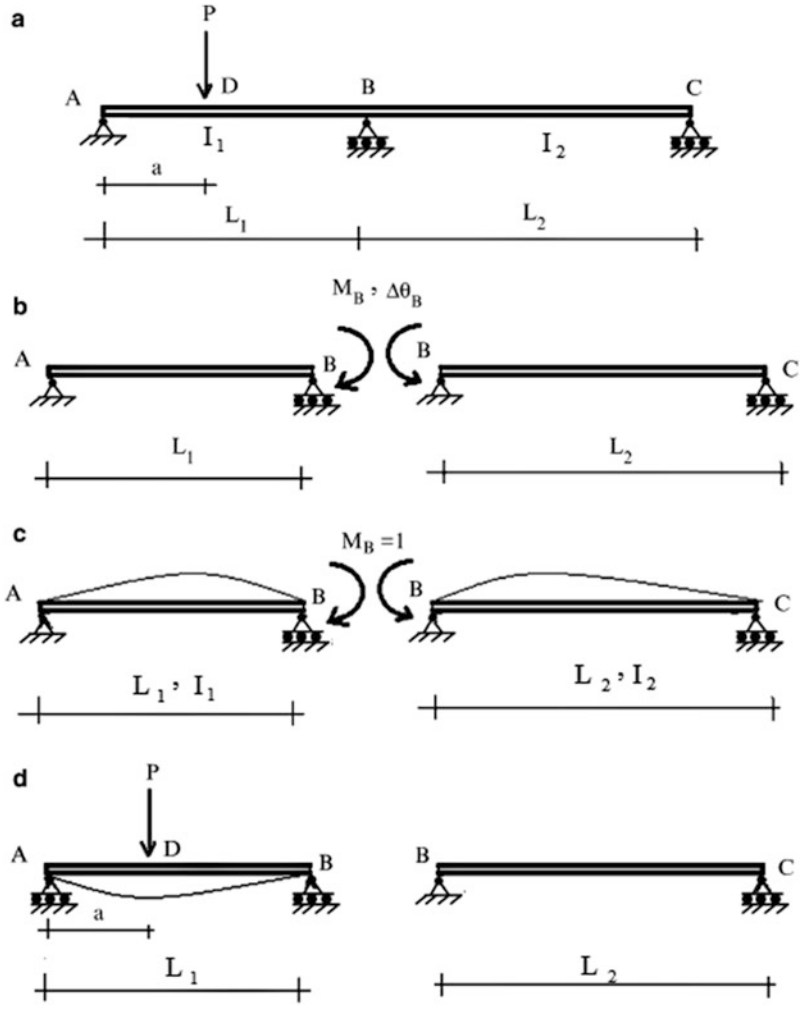

Fig. 9.24 (**a**) Actual structure—notation for a two-span beam. (**b**) Primary structure—redundant moment. (**c**) Displacement due to a unit value of the redundant moment. (**d**) Rotation due to external loading

Then

$$M_{\mathrm{B}} = \frac{-\Delta\theta_{\mathrm{B},0}}{\delta\theta_{\mathrm{BB}}} = \left\{\frac{(L_1/I_1)}{(L_1/I_1)+(L_2/I_2)}\right\}\frac{1}{2}Pa\left(1-\frac{a^2}{{L_1}^2}\right) \tag{9.28}$$

Given the value of M_{B}, we can determine the reactions by using the static equilibrium equations. Noting (9.28), the peak moments are given by:

$$\begin{aligned}\text{Negative moment } M_{\mathrm{B}} &= -\frac{PL_1}{2}f\frac{a}{L_1}\left(1-\frac{a^2}{{L_1}^2}\right)\\ \text{Positive moment } M_{\mathrm{D}} &= PL_1\left(\frac{a}{L_1}\right)\left\{\left(1-\frac{a}{L_1}\right)-\frac{f}{2}\frac{a^2}{L_1^2}\left(1-\frac{a^2}{L_1^2}\right)\right\}\end{aligned} \tag{9.29}$$

where

$$f = \frac{1}{1+(I_1/L_1)(L_2/I_2)}$$

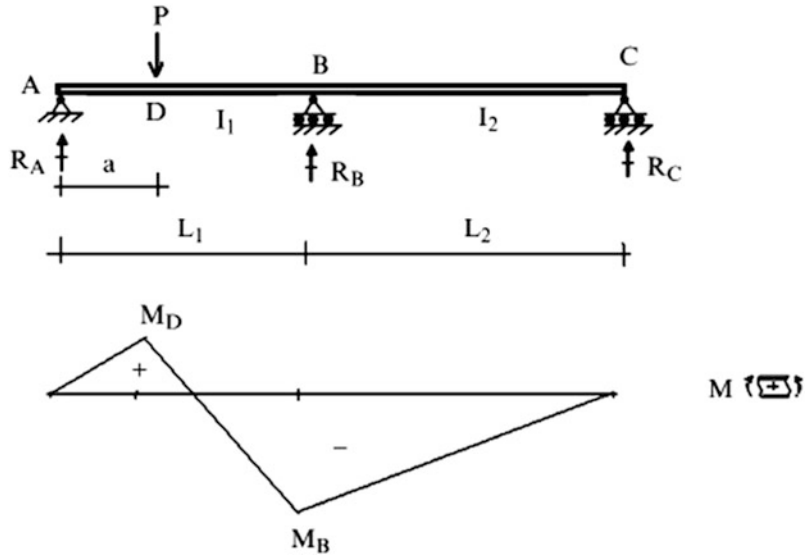

Fig. 9.25 Bending moment distribution for load on span AB

We define the ratio of I to L as the "relative stiffness" for a span and denote this parameter by r.

$$r_i = \left.\frac{I}{L}\right|_{\text{span } i} \tag{9.30}$$

With this notation, f takes the form

$$f = \frac{1}{1 + (r_1/r_2)}$$

The typical bending moment diagram is plotted in Fig. 9.25.

When the load is on span BC, one just has to use a different expression for $\Delta\theta_{B,0}$. Redefining the location of P as shown in Fig. 9.26a, the solution takes the following form:

$$\Delta\theta_{B,0} = -\frac{Pb\left(1 - \frac{b}{L_2}\right)\left(2 - \frac{b}{L_2}\right)}{6EI_2}$$

Then

$$M_B = \frac{-\Delta\theta_{B,0}}{\delta\theta_{BB}} = \frac{1}{(1 + (r_2/r_1))}\left(\frac{1}{2}PL_2\right)\frac{b}{L_2}\left(1 - \frac{b}{L_2}\right)\left(2 - \frac{b}{L_2}\right) \tag{9.31}$$

Given M_B, one can construct the moment diagram. It is similar to Fig. 9.25, but rotated 180°.

Example 9.8

Given: The two-span beam shown in Figs. E9.8a and E9.8ab.

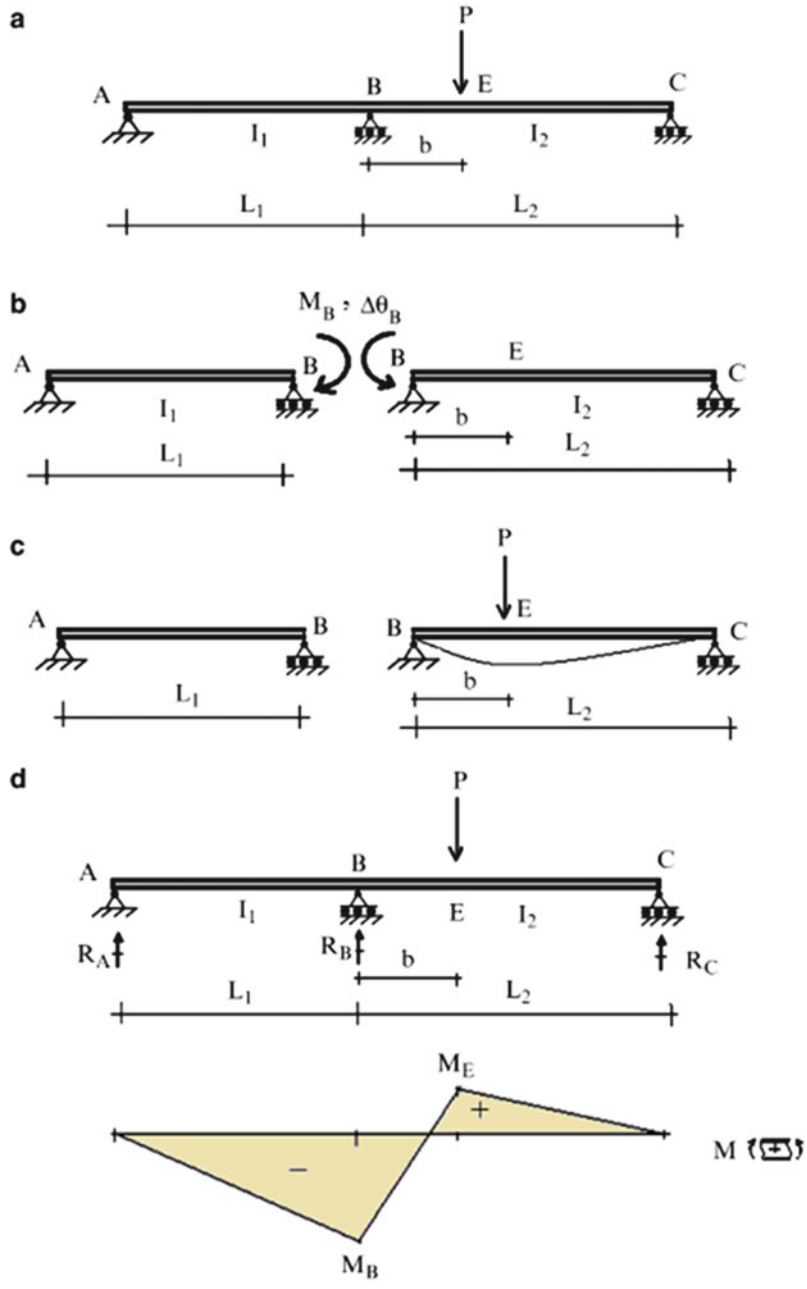

Fig. 9.26 (**a**) Actual structure—loading on span BC. (**b**) Primary structure—redundant moment. (**c**) Rotation due to external loading. (**d**) Bending moment distribution for load on span BC

Determine: The variation of the bending moment at B with relative stiffness of the adjacent spans ($r_1/r_2 = 0.1$, 1, and 10).

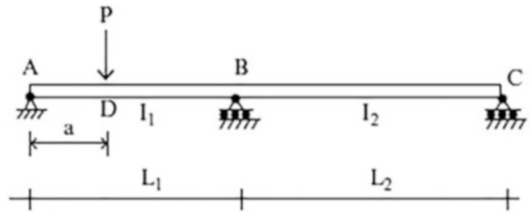

Fig. E9.8a

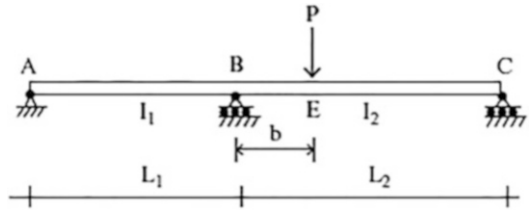

Fig. E9.8b

Solution: We determine the variation of the moment at B for a range of relative stiffness ratios covering the spectrum from one span being very flexible to one span being very rigid with respect to the other span using (9.29) and (9.31). Results for the individual spans are plotted in Figs. E9.8c and E9.8d.

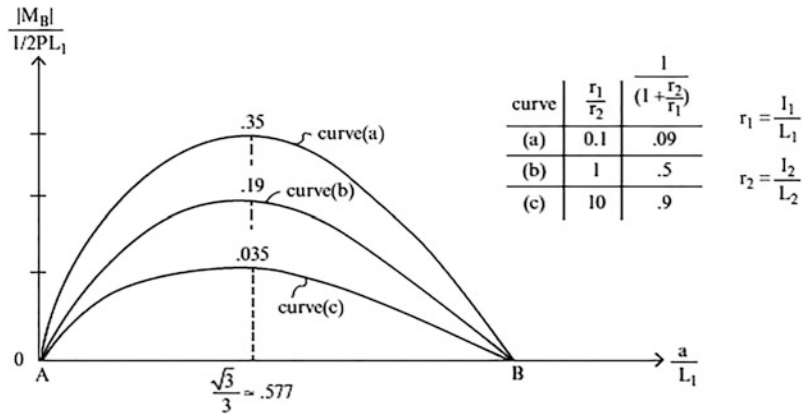

Fig. E9.8c Load on the left span (9.29)

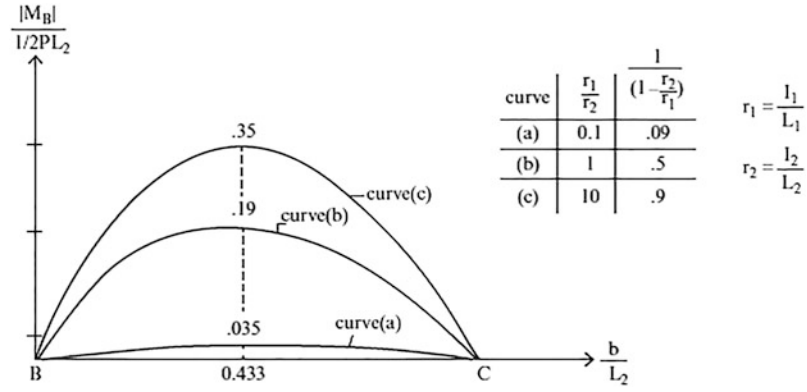

Fig. E9.8d Load on the right span (9.31)

Example 9.9 Two-Span Continuous Beam—Uniform Loading

Given: The two-span beam shown in Fig. E9.9a.

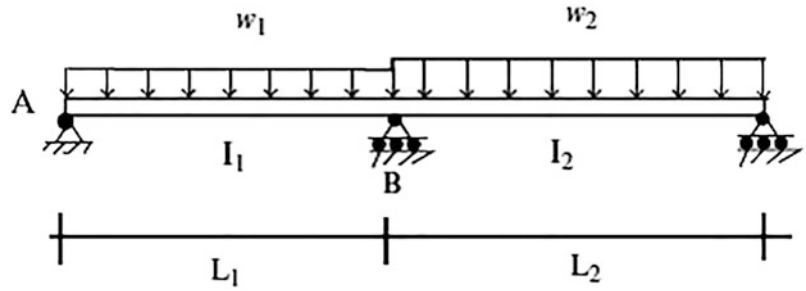

Fig. E9.9a

Determine: The bending moment at support B.

Solution: We take the negative moment at the interior support as the force redundant. The solution process is similar to that followed for the case of a concentrated load. One determines the relative rotations at B, and then enforces continuity at B (Fig. E9.9b).

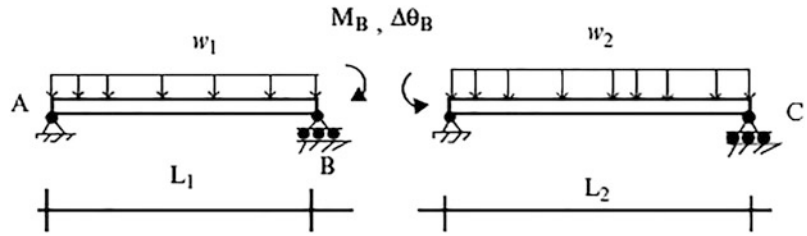

Fig. E9.9b

The various terms are (see Table 3.1)

$$\Delta\theta_{B,0} = -\frac{w_1 L_1^3}{24EI_1} - \frac{w_2 L_2^3}{24EI_2}$$

$$\delta\theta_{BB} = \frac{L_1}{3EI_1} + \frac{L_2}{3EI_2}$$

Requiring the relative rotation at B equal to zero leads to

$$M_B = \frac{-\Delta\theta_{B,0}}{\delta\theta_{BB}} = \left(\frac{w_1 L_1^2}{8}\right)\frac{1 + (w_2/w_1)(L_2/L_1)^2(r_1/r_2)}{1 + (r_1/r_2)}$$

where

$$r_1 = \frac{I_1}{L_1}, \quad r_2 = \frac{I_2}{L_2}$$

Suppose the loading and span lengths are equal. In this case,

$$M_B = \frac{wL^2}{8}$$

for all combinations of I_1 and I_2. The moment diagram is plotted below (Fig. E9.9c).

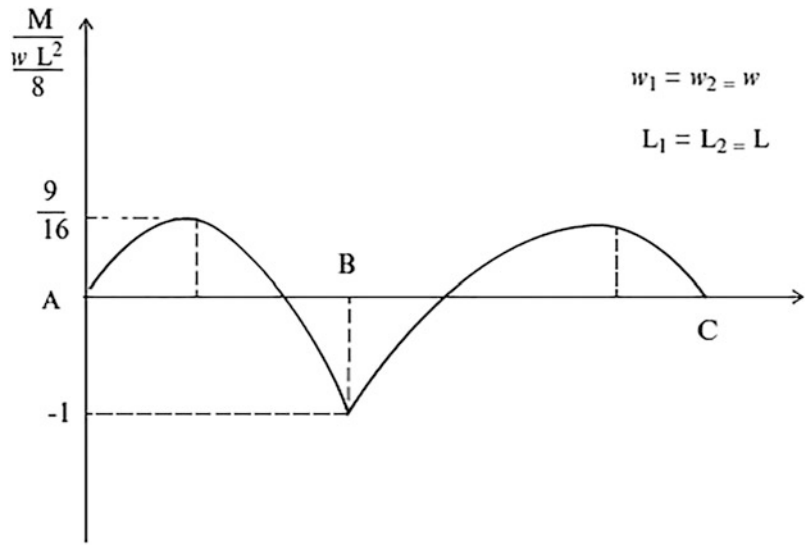

Fig. E9.9c

Another interesting case is where $w_2 = 0$ and $I_1 = I_2$. The solution depends on the ratio of span lengths.

$$M_B = \frac{w_1 L_1^2}{8}\frac{1}{1 + (L_2/L_1)}$$

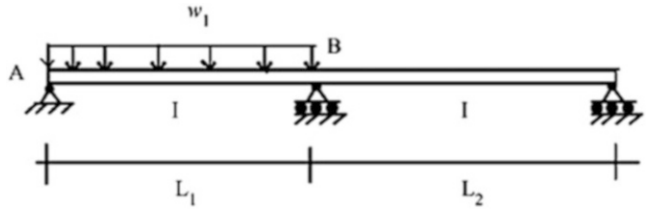

Suppose $L_2 = L_1$ and $I_1 = I_2$, then

$$M_B = \frac{1}{2}\left(\frac{w_1 {L_1}^2}{8}\right)$$

Example 9.10 Two-Span Continuous Beam with Support Settlement

Given: The two-span beam shown in Fig. E9.10a. The supports at B or A experience a vertical displacement downward due to settlement of the soil under the support.

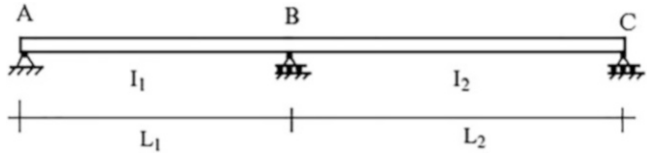

Fig. E9.10a

Determine: The bending moment at B.

Solution: We work with the primary structure shown in Fig. E9.10b.

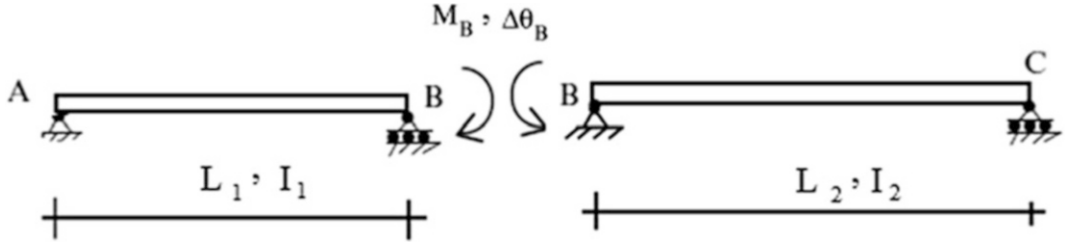

Fig. E9.10b Primary structure—redundant moment

If the support at B moves downward an amount v_B, the relative rotation of the section at B is

$$\Delta\theta_{B,0} = \frac{v_B}{L_1} + \frac{v_B}{L_2}$$

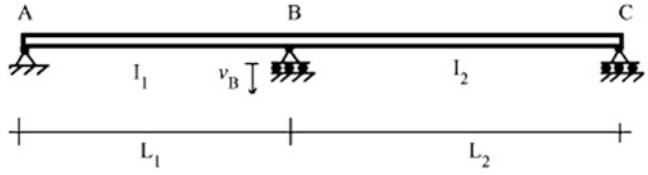

Compatibility requires the moment at B to be equal to

$$M_B = \frac{-\Delta\theta_{B,0}}{\delta\theta_{BB}} = -\frac{v_B((1/L_1)+(1/L_2))}{(1/3E)((L_1/I_1)+(L_2/I_2))}$$

The minus sign indicates that the bending moment is of opposite sense to that assumed in Fig. E9.10b.

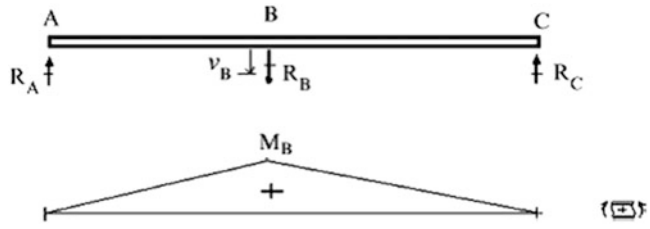

When the properties are the same for both spans ($I_1 = I_2$ and $L_1 = L_2$), M_B reduces to $M_B = \frac{3EI_1}{L_1^2} v_B$.

When the support at A moves downward an amount v_A, the behavior is reversed.

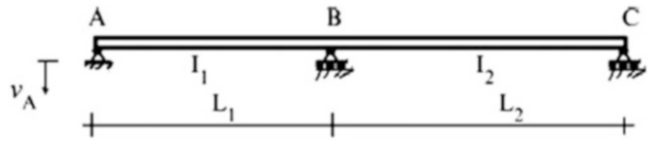

In this case, $\Delta\theta_{B,0} = -v_A/L_1$ and $M_B = \frac{v_A/L_1}{(1/3E)((L_1/I_1)+(L_2/I_2))}$

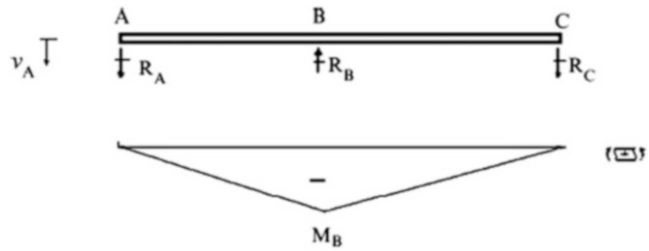

When the properties are the same for both spans ($I_1 = I_2$ and $L_1 = L_2$), M_B reduces to $M_B = \frac{3EI_1}{2L_1^2} v_A$.

9.4 Application to Arch-Type Structures

Chapter 6 introduced the topic of arch structures. The discussion was concerned with how the geometry of arch structures is defined and how to formulate the equilibrium equations for statically determinate arches. Various examples were presented to illustrate how arch structures carry

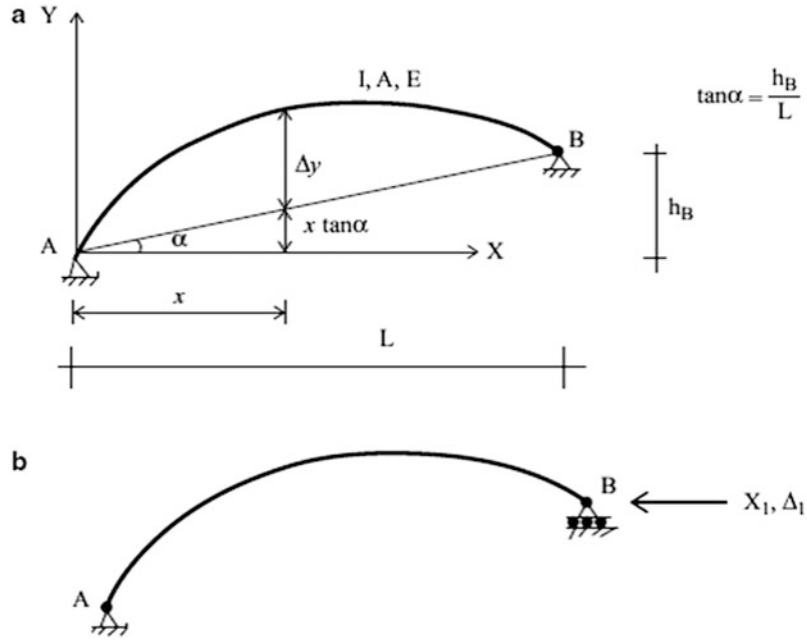

Fig. 9.27 (**a**) Actual structure—geometry. (**b**) Primary structure—redundant reaction

transverse loading by a combination of both axial and bending actions. This feature makes them more efficient than beam structures for long-span applications.

In what follows we extend the analytical formulation to statically indeterminate arches. We base our analysis procedure on the force method and use the principle of virtual forces to compute displacement measures. One of our objectives here is to develop a strategy for finding the geometry for which there is minimal bending moment in the arch due to a particular loading.

We consider the two-hinged arch shown in Fig. 9.27a. This structure is indeterminate to the first degree. We take the horizontal reaction at the right support as the force redundant and use the Principle of Virtual Forces described in Sect. 6.5 to determine $\Delta_{1,0}$, the horizontal displacement due to loading, and δ_{11}, the horizontal displacement due to a unit value of X_1.

The general expressions for these displacement measures follow from (6.9)

$$\begin{aligned}\Delta_{1,0} &= \int_s \left\{ \frac{F_0}{AE}\delta F + \frac{V_0(x)}{GA_s}\delta V + \frac{M_0(x)}{EI}\delta M \right\} \mathrm{d}s \\ \delta_{11} &= \int_s \left\{ \frac{(\delta F)^2}{AE} + \frac{(\delta V)^2}{GA_s} + \frac{(\delta M)^2}{EI} \right\} \mathrm{d}s \end{aligned} \tag{9.32}$$

We usually neglect the shear deformation term. Whether one can also neglect the axial deformation term depends on the arch geometry. For completeness, we will retain this term. The two internal force systems are summarized below. We assume the applied load is uniform per projected length (Fig. 9.28).

Substituting for the force terms leads to the following expressions for the displacement measures:

$$\begin{aligned}\Delta_{1,0} &= \int_0^L \left\{ \frac{1}{AE\cos\theta}\left(\frac{wL}{2} - wx\right)\sin\theta(\cos\theta + \tan\alpha\sin\theta) - \left(\frac{wL}{2}x - \frac{wx^2}{2}\right)\frac{\Delta y}{EI\cos\theta} \right\} \mathrm{d}x\delta_{11} \\ &= \int_0^L \left\{ \frac{(\cos\theta + \tan\alpha\sin\theta)^2}{AE\cos\theta} + \frac{(\Delta y)^2}{EI\cos\theta} \right\} \mathrm{d}x \end{aligned} \tag{9.33}$$

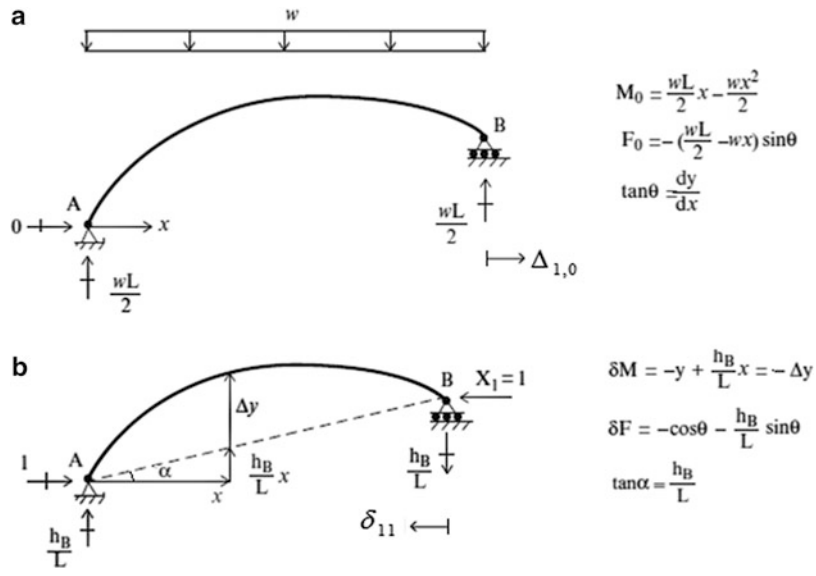

Fig. 9.28 (**a**) Force due to applied loading (F_0, M_0). (**b**) Force due to $X_1 = 1$ (δF, δM)

Geometric compatibility requires

$$X_1 = -\frac{\Delta_{1,0}}{\delta_{11}} \tag{9.34}$$

One can use either symbolic integration or numerical integration to evaluate the flexibility coefficients. We prefer to use the numerical integration scheme described in Sect. 3.6.6.

The solution simplifies considerably when axial deformation is neglected with respect to bending deformation. One sets $A = \infty$ in (9.33). This leads to

$$\begin{aligned} \Delta_{1,0} &= -\int_0^L \left(\frac{wL}{2}x - \frac{wx^2}{2}\right)\frac{\Delta y}{EI\cos\theta}\mathrm{d}x = -\int_0^L \frac{M_0 \Delta y}{EI\cos\theta}\mathrm{d}x \\ \delta_{11} &= +\int_0^L \frac{(\Delta y)^2}{EI\cos\theta}\mathrm{d}x \end{aligned} \tag{9.35}$$

Suppose Δy is chosen such that

$$\Delta y = \beta\left[\frac{wL}{2}x - \frac{wx^2}{2}\right] \equiv \beta M_0 \tag{9.36}$$

Then,

$$\Delta_{1,0} = -\frac{1}{\beta}\delta_{11}$$

and it follows that

$$\begin{aligned} X_1 &= \frac{1}{\beta} \\ M &= M_0 + X_1 \delta M = M_0 + \left(\frac{1}{\beta}\right)(-\beta M_0) = 0 \end{aligned} \tag{9.37}$$

With this choice of geometry, the arch carries the exterior load by axial action only; there is no bending. *Note that this result is based on the assumption that axial deformation is negligible*. In general, there will be a small amount of bending when h is not small with respect to L, i.e., when the arch is "shallow." *One cannot neglect* axial deformation for a shallow arch.

Example 9.11 Parabolic Arch with Uniform Vertical Loading

Given: The two-hinged parabolic arch defined in Fig. E9.11a.

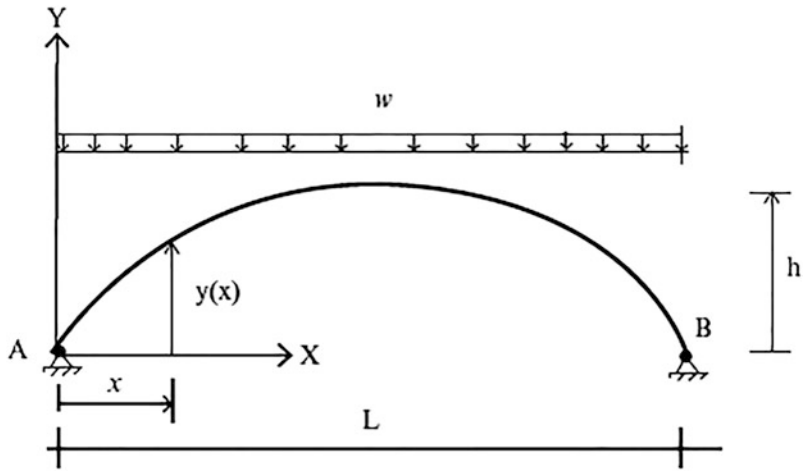

Fig. E9.11a

Determine: The bending moment distribution.

Solution: The centroidal axis for the arch is defined by

$$y = 4h\left[\frac{x}{L} - \left(\frac{x}{L}\right)^2\right]$$

The bending moment in the primary structure due to the uniform loading per unit x is

$$M_0 = \frac{wL}{2}x - \frac{wx^2}{2} = \frac{wL^2}{2}\left[\frac{x}{L} - \left(\frac{x}{L}\right)^2\right]$$

We note that the expressions for y and M_0 are similar in form. One is a scaled version of the other.

$$M_0 = \frac{wL^2}{2}\frac{1}{4h}y = \frac{wL^2}{8h}y$$

Then, noting (9.36),

$$\beta = \frac{8h}{wL^2}$$

and $X_1 = \dfrac{wL^2}{8h}$.

The total moment is the sum of M_0 and the moment due to X_1.

$$M = M_0 - yX_1 = \frac{wL^2}{8h}y - \frac{wL^2}{8h}y = 0$$

We see that there is no bending for this loading and geometry. We should have anticipated this result since a uniformly loaded cable assumes a parabolic shape. By definition, a cable has no bending rigidity and therefore no moment. We can consider an arch as an inverted cable. It follows that a two-hinged uniformly loaded parabolic arch behaves like an inverted cable.

Example 9.12 Approximate Solutions

Given: The two-hinged arch and the loading defined in Fig. E9.12a. The integral expression for X_1 is given by 9.3.4. Noting (9.35), the solution equals to

$$X_1 \approx +\frac{\int \Delta y \frac{M_0}{EI} \mathrm{d}s}{\int (\Delta y)^2 \frac{\mathrm{d}s}{EI}}$$

This result applies when there is no support movement.

Determine: An approximate expression for X_1. Assume the cross section of the arch is deeper at the abutment than at the crown, and use the following approximation to define I,

$$I = \frac{I_0}{\cos\theta}$$

where I_0 is the cross-sectional inertia at the crown.

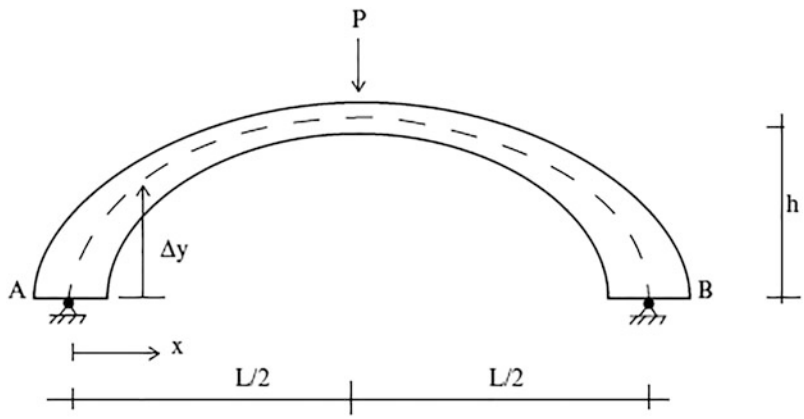

Fig. E9.12a Variable depth arch

Solution: Substituting for I and $\mathrm{d}s = \frac{\mathrm{d}x}{\cos\theta}$, the integrals simplify to

$$X_1 = \frac{+(1/EI_0)\int \Delta y M_0 \mathrm{d}x}{(1/EI_0)\int (\Delta y)^2 \mathrm{d}x}$$

and now one can easily determine analytical solutions.

Suppose a concentrated force, P, is applied at mid-span. The corresponding terms for a symmetrical parabolic arch are:

$$\Delta y = \frac{4y}{L}\left(x - \frac{x^2}{L}\right)$$
$$\frac{1}{EI_0}\int \Delta y M_0 \mathrm{d}x \Rightarrow \frac{5}{48}\frac{PhL^2}{EI_0}$$
$$\frac{1}{EI_0}\int (\Delta y)^2 \mathrm{d}x = \frac{8}{15}\frac{h^2 L}{EI_0}$$
$$X_1 = \frac{25}{128}P\left(\frac{L}{h}\right)$$

Note that the bending moment is *not* zero in this case.

Example 9.13

Given: The two-hinged arch and the loading defined in Fig. E9.13a

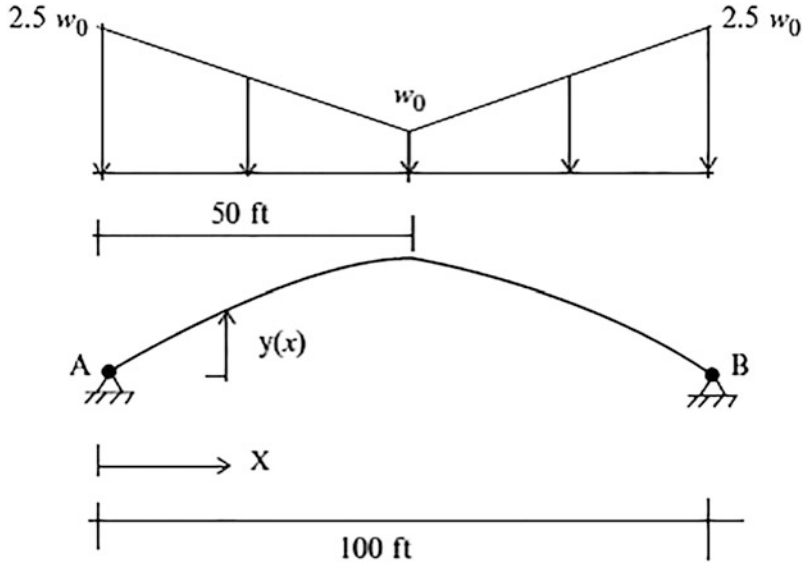

Fig. E9.13a

Determine: The particular shape of the arch which corresponds to negligible bending.
Solution: This two-hinged arch is indeterminate to the first degree. We take the horizontal reaction at the right support as the force redundant (Fig. E9.13b).

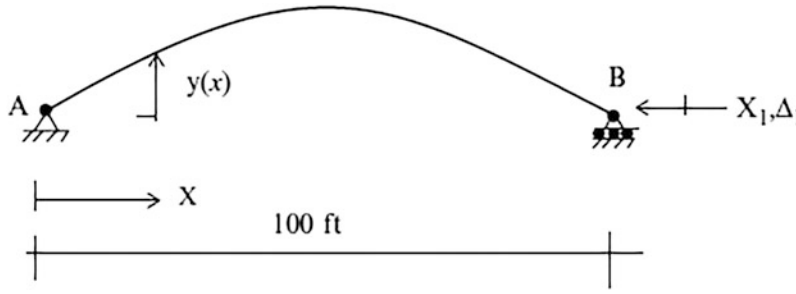

Fig. E9.13b Primary structure—redundant reaction

The applied loading is given by (Fig. E9.13c)

$$w(x) = w_0\left\{2.5 - \frac{1.5}{50}x\right\} \quad 0 < x \leq 50$$

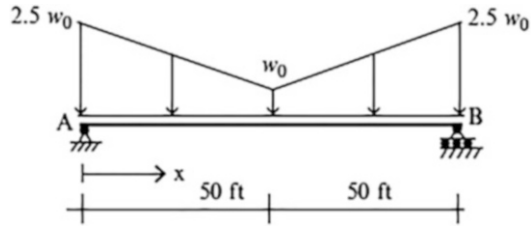

Fig. E9.13c

The corresponding shear and moment in the simply supported beam spanning AB are

$$\frac{dV}{dx} = w(x) \Rightarrow V = w_0\left\{2.5x - \frac{1.5}{100}x^2\right\} + C_1$$
$$\frac{dM}{dx} = -V \Rightarrow M = -w_0\left\{\frac{2.5}{2}x^2 - \frac{1.5}{300}x^3\right\} + C_1x + C_2$$

Enforcing the boundary conditions,

$$M(0) = 0$$
$$M(100) = 0$$

leads to

$$C_2 = 0$$
$$C_1 = w_0\left\{1.25(100) - \frac{1.5(100)^2}{300}\right\} = 75w_0$$

Finally, the expression for M reduces to

$$M = w_0\left\{75x - 1.25x^2 + 0.005x^3\right\} \quad 0 < x \leq 50$$

follows (9.36) and (9.37).

The desired shape is

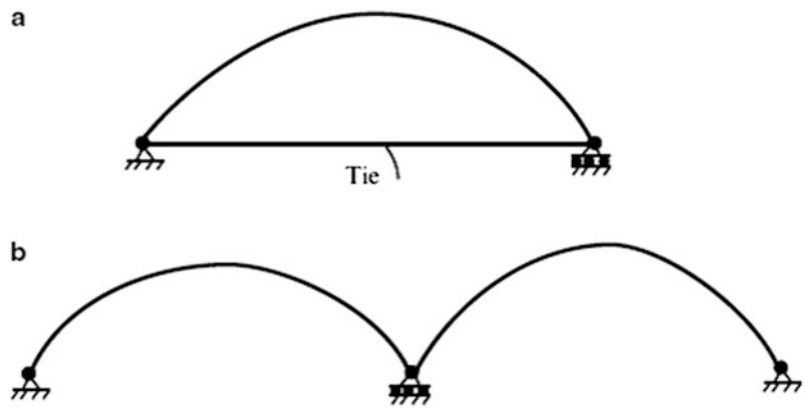

Fig. 9.29 (**a**) Single tie arch. (**b**) Multiple connected arches

$$y(x) = \frac{M(x)}{X_1} = \frac{w_0}{X_1}\left\{75x - 1.25x^2 + 0.005x^3\right\} = \frac{w_0}{X_1} f(x)$$

The function $f(x)$ is plotted below. Note that the shape is symmetrical.

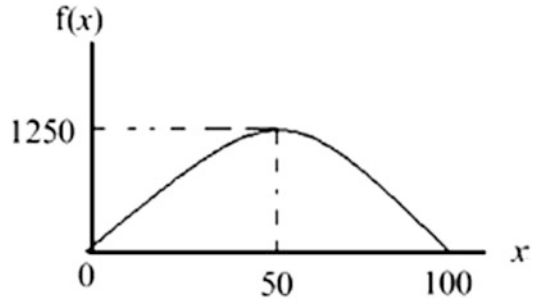

When the abutments are inadequate to resist the horizontal thrust, different strategies are employed to resist the thrust. One choice is to insert a tension tie connecting the two supports, as illustrated in Fig. 9.29a. Another choice is to connect a set of arches in series until a suitable anchorage is reached (see Fig. 9.29b). The latter scheme is commonly used for river crossings.

We take the tension in the tie as the force redundant for the tied arch. The corresponding primary structure is shown in Fig. 9.30. We just have to add the extension of the tie member to the deflection δ_{11}. The extended form for δ_{11} is

$$\rightarrow \leftarrow \quad \delta_{11} = \int y^2 \frac{\mathrm{d}s}{EI} + \frac{L}{A_t E} \tag{9.38}$$

The expression for $\Delta_{1,0}$ does not change. Then, the tension in the tie is given by:

$$X_1 = \frac{-\Delta_{1,0}}{\delta_{11}} = \frac{\int y(M_0 \mathrm{d}s/EI)}{\left(\int y^2(\mathrm{d}s/EI)\right) + (L/A_t E)} \tag{9.39}$$

Note that the horizontal reaction is reduced by inserting a tie member. However, now there is bending in the arch.

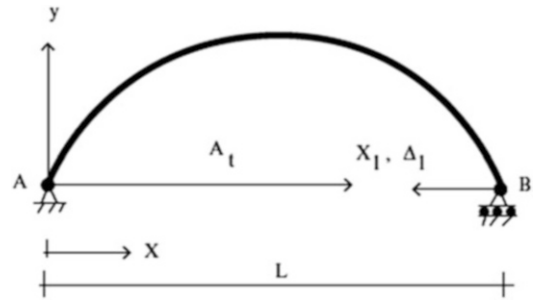

Fig. 9.30 Choice of redundant

Example 9.14

Given: A parabolic arch with a tension tie connecting the supports. The arch is loaded with a uniformly distributed load per horizontal projection. Consider I to be defined as $\frac{I_0}{\cos\theta}$.
Determine: The horizontal thrust and the bending moment at mid-span (Fig. E9.14a).

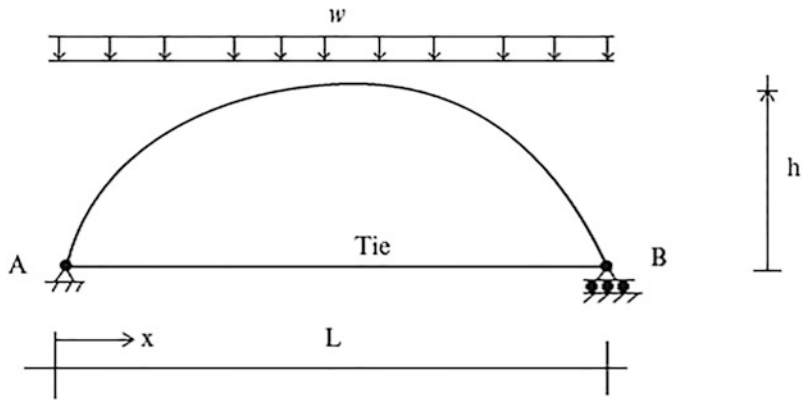

Fig. E9.14a

Solution: We note the results generated in Example 9.12 which correspond to taking $I = \frac{I_0}{\cos\theta}$.

$$\Delta_{1,0} = -\int yM_0 \frac{\mathrm{d}s}{EI} = -\frac{1}{EI_0}\int_0^L yM_0 \mathrm{d}x$$

$$= -\frac{1}{EI_0}\left(\frac{wL^2}{8h}\right)\int_0^L y^2 \mathrm{d}x$$

$$= -\frac{1}{EI_0}\left(\frac{8}{15}h^2 L\right)\left(\frac{wL^2}{8h}\right) = -\frac{whL^3}{15EI_0}$$

$$\delta_{11} = \frac{L}{AE} + \frac{8}{15}\frac{h^2 L}{EI_0}$$

The tension in the tie is

$$X_1 = \frac{-\Delta_{1,0}}{\delta_{11}} = \frac{wL^2}{8h} \frac{1}{\left(1 + (15/8)\left(I_0/Ah^2\right)\right)}$$

Using this value, we determine the moment at mid-span.

$$M\left(\frac{L}{2}\right) = M_0 - hX_1$$

$$= \frac{wL^2}{8}\left\{1 - \frac{1}{\left(1 + (15/8)\left(I_0/Ah^2\right)\right)}\right\}$$

$$M\left(\frac{L}{2}\right) = \frac{wL^2}{8}\left\{\frac{(15/8)\left(I_0/Ah^2\right)}{\left(1 + (15/8)\left(I_0/Ah^2\right)\right)}\right\} = \frac{wL^2}{8}\left\{\frac{1}{\left(1 + (8/15)\left(Ah^2/I_0\right)\right)}\right\}$$

Note that the effect of the tension tie is to introduce bending in the arch.

9.5 Application to Frame-Type Structures

Chapter 4 dealt with statically determinate frames. We focused mainly on three-hinge frames since this type of structure provides an efficient solution for enclosing a space. In this section, we analyze indeterminate frames with the force method. In the next chapter, we apply the displacement method. The analytical results generated provide the basis for comparing the structural response of determinate vs. indeterminate frames under typical loadings.

9.5.1 General Approach

We consider the arbitrary-shaped single bay frame structure shown in Fig. 9.31. The structure is indeterminate to the first degree. We select the horizontal reaction at the right support as the force redundant. The corresponding compatibility equation is

$$\Delta_{1,0} + \delta_{11} X_1 = \Delta_1$$

where Δ_1 is the horizontal support movement at D.

We compute δ_{11} and $\Delta_{1,0}$ with the Principle of the Virtual Forces described in Sect. 4.6. The corresponding form for a plane frame specialized for negligible transverse deformation is given by (4.8)

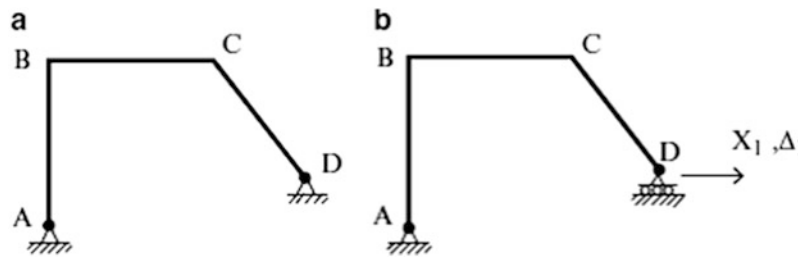

Fig. 9.31 (**a**) Actual structure. (**b**) Primary structure—redundant reaction

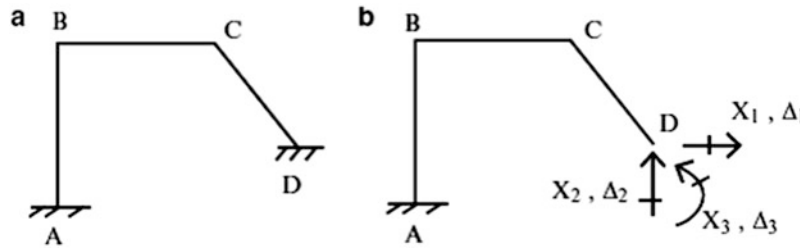

Fig. 9.32 (**a**) Actual structure. (**b**) Primary structure—redundant reactions

$$\mathrm{d}\,\delta P = \sum\nolimits_{\text{members}} \int_{s} \left\{ \left(\frac{M}{EI}\right) M + \left(\frac{F}{AE}\right) \delta F \right\} ds$$

Axial deformation is small for typical non-shallow frames and therefore is usually neglected. The δ_{11} term is the horizontal displacement due to a horizontal unit load at D. This term depends on the geometry and member properties, not on the external loads, and therefore has to be computed only once. The $\Delta_{1,0}$ term is the horizontal displacement due to the external loading and needs to be evaluated for each loading. Different loading conditions are treated by determining the corresponding values of $\Delta_{1,0}$. Given these displacement terms, one determines X_1 with

$$X_1 = -\frac{\Delta_{1,0}}{\delta_{11}}$$

Consider the frame shown in Fig. 9.32. Now there are three force redundant and three geometric compatibility conditions represented by the matrix equation (see (9.11)),

$$\underline{\boldsymbol{\Delta}}\big|_{\text{primary structure}} = \underline{\boldsymbol{\Delta}}_{\mathbf{0}} + \underline{\boldsymbol{\delta}}\,\underline{\mathbf{X}}$$

The flexibility matrix $\underline{\boldsymbol{\delta}}$ is independent of the loading, i.e., it is a property of the primary structure. Most of the computational effort is involved with computing $\underline{\boldsymbol{\delta}}$ and $\underline{\boldsymbol{\Delta}}_{\mathbf{0}}$ numerically. The integration can be tedious. Sometimes numerical integration is used. However, one still has to generate the moment and axial force diagrams numerically.

If the structure is symmetrical, one can reduce the computational effort by working with simplified structural models and decomposing the loading into symmetrical and anti-symmetrical components. It is very useful for estimating, in a qualitative sense, the structural response. We discussed this strategy in Chap. 3.

In what follows, we list results for different types of frames. Our primary objective is to show how these structures respond to typical loadings. We use moment diagrams and displacement profiles as the measure of the response.

9.5.2 Portal Frames

We consider the frame shown in Fig. 9.33a. We select the horizontal reaction at D as the force redundant.

The corresponding flexibility coefficient, δ_{11}, is determined with the Principle of Virtual Forces (see Chap. 4).

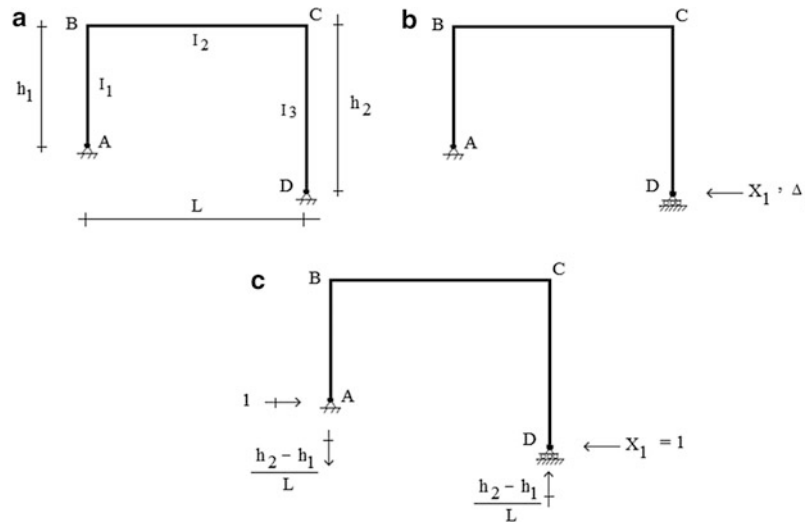

Fig. 9.33 Portal Frame. (**a**) Geometry. (**b**) Redundant. (**c**) Reactions due to $X_1 = 1$

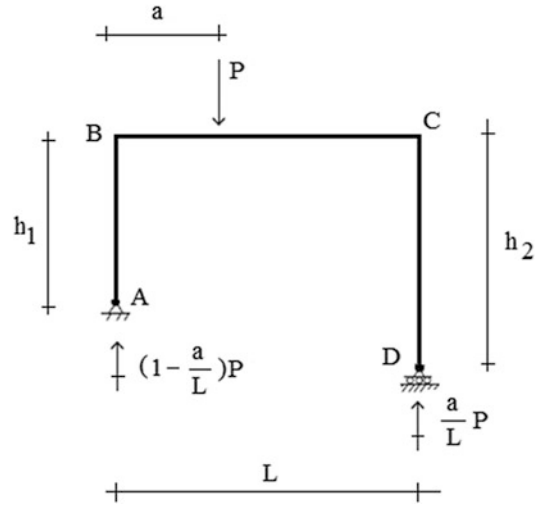

Fig. 9.34 Reactions—gravity loading

$$\delta_{11} = \frac{h_1^3}{3EI_1} + \frac{h_2^3}{3EI_3} + \frac{L}{3EI_2}\left\{h_1^2 + h_2^2 + h_1 h_2\right\} \tag{9.40}$$

This coefficient applies for all loading. Considering the arbitrary gravity loading shown in Fig. 9.34, the expression for the displacement, $\Delta_{1,0}$, is determined in a similar way.

$$\Delta_{1,0}\big|_{\text{gravity}} = -\frac{Pa(L-a)}{2EI_2L}\left\{(L-a)h_2 + a\,h_1\right\} + \frac{Pa(h_2-h_1)}{3EI_2L}\left(L^2 + 2a^2 - 3aL\right) \tag{9.41}$$

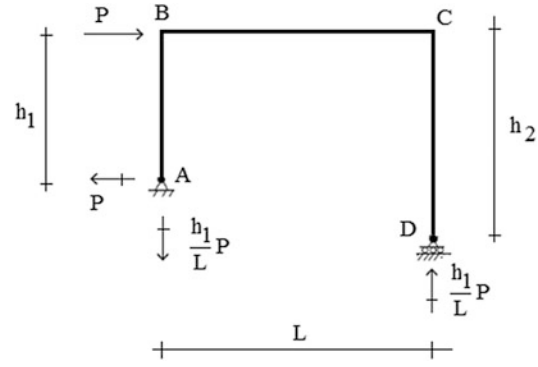

Fig. 9.35 Reactions—lateral loading

Lastly, we consider the lateral loading shown in Fig. 9.35. The displacement term due to loading is

$$\Delta_{1,0}\big|_{\text{lateral}} = -\frac{1}{EI_1}\left\{\frac{Ph_1^3}{3}\right\} + \frac{1}{EI_2}\left\{\frac{Ph_1L}{3}\left(\frac{h_2}{2}+h_1\right)\right\} \tag{9.42}$$

When $h_2 = h_1 = h$ and $I_2 = I_1 = I$, these expressions simplify to

$$\begin{aligned}
\delta_{11} &= \frac{2h^3}{3EI} + \frac{L}{EI}(h^2) \\
\Delta_{1,0}\big|_{\text{gravity}} &= -\frac{Ph}{2EI}(a)(L-a) \\
\Delta_{1,0}\big|_{\text{lateral}} &= -\frac{Ph^3}{3EI} - \frac{Ph^2L}{2EI}
\end{aligned} \tag{9.43}$$

Gravity loading:

$$\begin{aligned}
X_1\big|_{\text{gravity}} &= \left(\frac{P}{2}\frac{L}{h}\right)\frac{(a/L)(1-(a/L))}{1+(2/3)(h/L)} \\
M_1\big|_{\text{gravity}} &= hX_1\big|_{\text{gravity}} \\
M_2\big|_{\text{gravity}} &= a\left(1-\frac{a}{L}\right)P - M_1\big|_{\text{gravity}}
\end{aligned}$$

Lateral loading:

$$\begin{aligned}
X_1\big|_{\text{lateral}} &= \frac{P}{2} \\
M_1\big|_{\text{lateral}} &= hX_1\big|_{\text{lateral}}
\end{aligned}$$

The corresponding bending moment diagrams for these two loading cases are shown in Fig. 9.36.

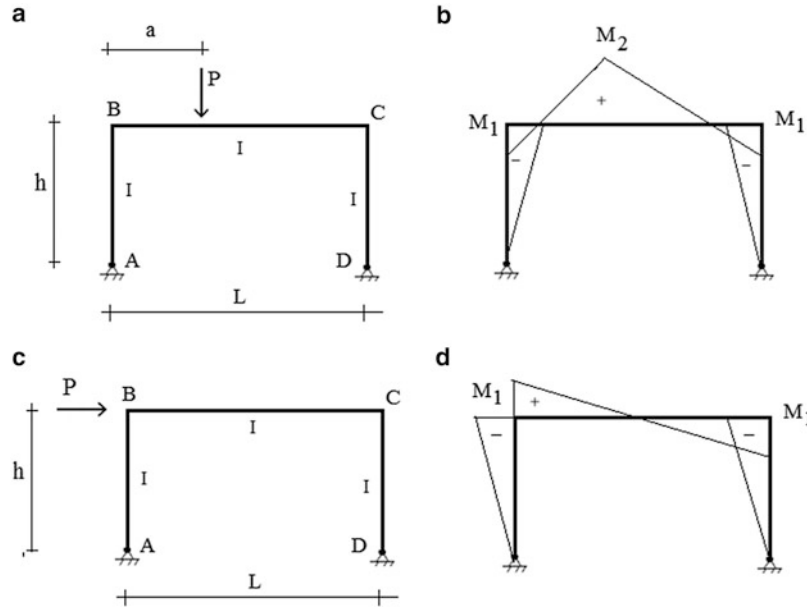

Fig. 9.36 Two-hinged frame (**a**) Gravity loading. (**b**) Moment diagram. (**c**) Lateral loading. (**d**) Moment diagram

9.5.2.1 Lateral-Loading Symmetrical Portal Frame

We consider first the two-hinged symmetrical frame shown in Fig. 9.37. This structure is indeterminate to the first degree. We decompose the loading into symmetrical and anti-symmetrical components and generate the corresponding symmetrical and anti-symmetrical structural modes using the material presented in Sect. 3.9. These results are shown in Fig. 9.38b. Point E is at mid-span. The anti-symmetrical model is statically determinate since the bending moment at mid-span must equal zero for anti-symmetrical behavior (Fig. 9.38c).

The symmetrical loading introduces no bending in the structure, only axial force in member BE. The bending moment distribution due to the anti-symmetrical component is plotted in Fig. 9.39.

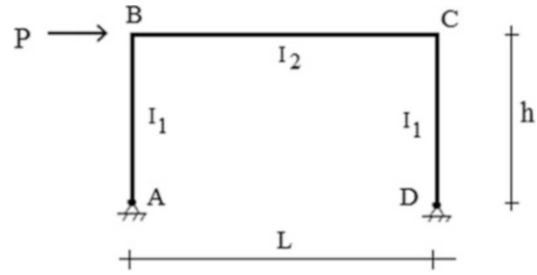

Fig. 9.37 Geometry of two-hinged portal frame

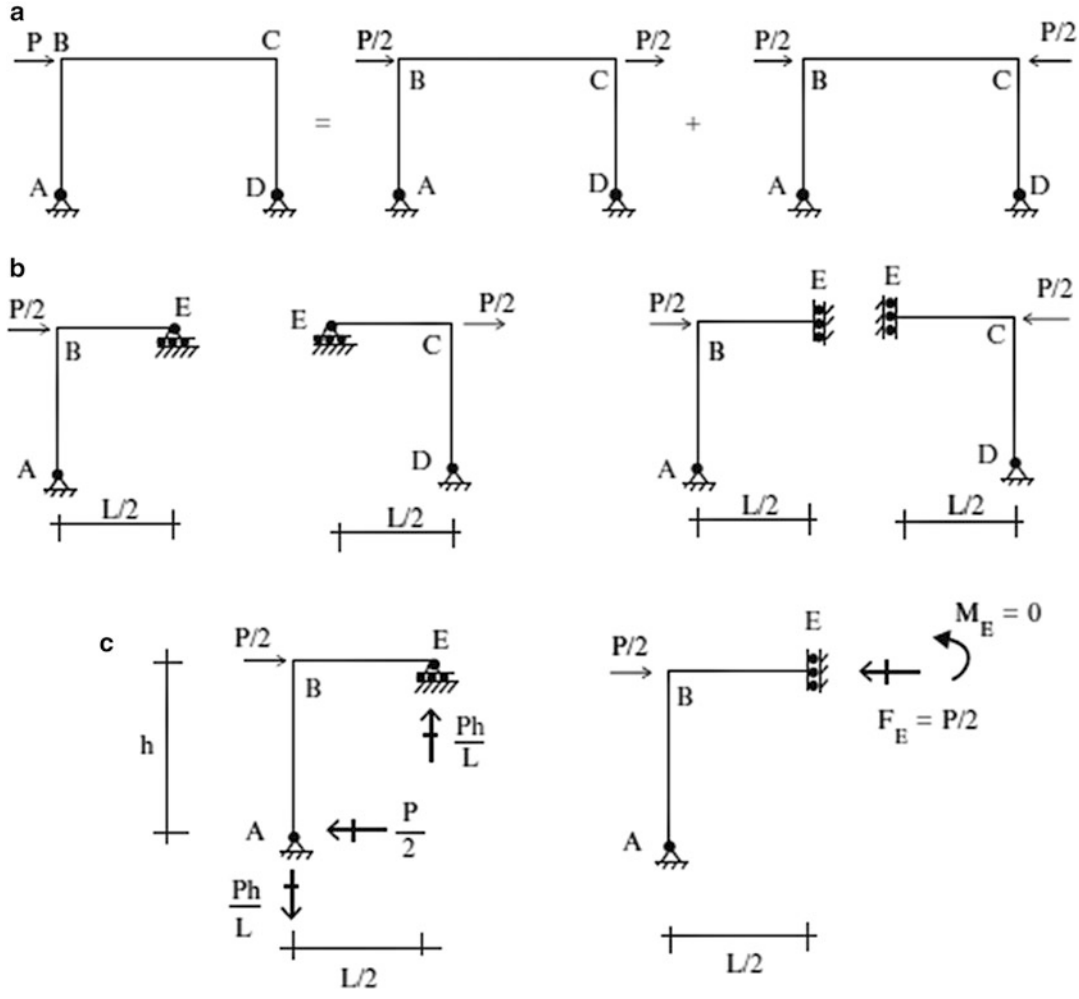

Fig. 9.38 Structural models. (**a**) Decomposition into anti-symmetrical and symmetrical loadings. (**b**) Anti-symmetric and symmetrical models. (**c**) Free body diagrams of anti-symmetric and symmetrical segments

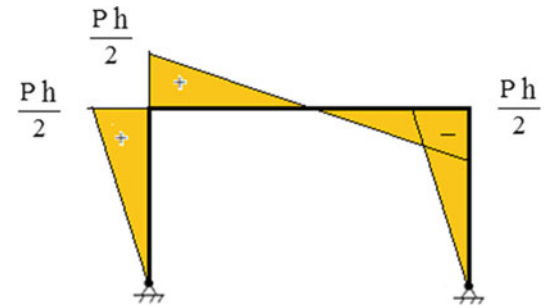

Fig. 9.39 Bending moment distribution due to the anti-symmetrical lateral loading

9.5.2.2 Gravity-Loading Symmetrical Portal Frame

We consider next the case of gravity loading applied to a two-hinged portal frame. Figure 9.40a defines the loading and geometry. Again, we decompose the loading and treat separately the two loading cases shown in Fig. 9.40b.

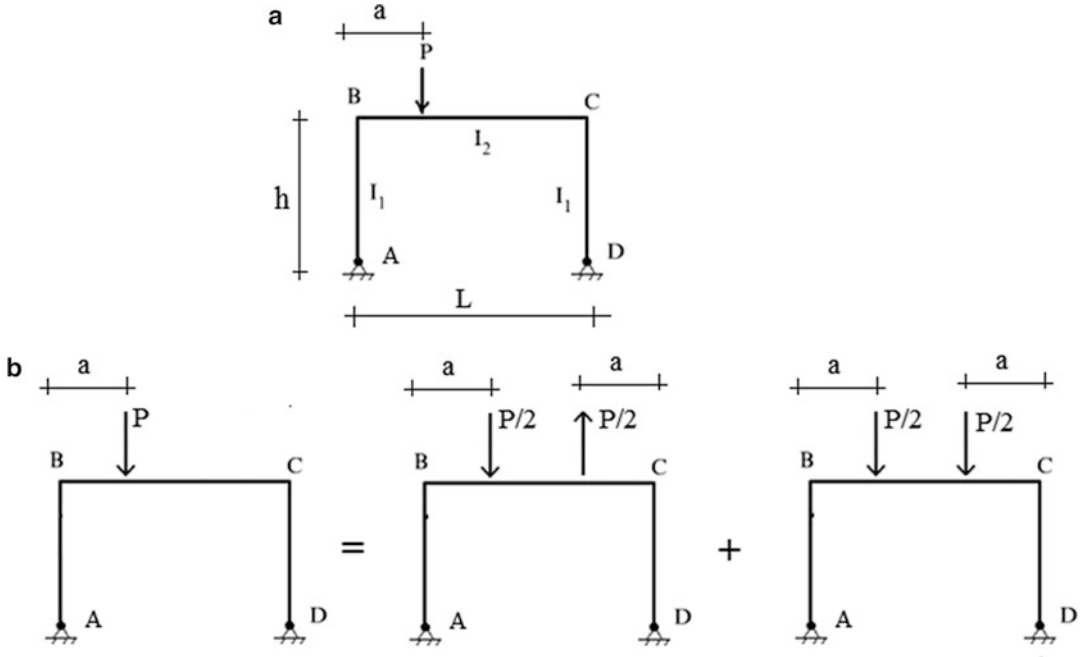

Fig. 9.40 (**a**) Two-hinged frame under gravity loading. (**b**) Decomposition of loading into symmetrical and anti-symmetrical components

Geometry and Loading

The anti-symmetrical model is statically determinate. Figure 9.41 shows the model, the corresponding free body diagram and the bending moment distribution.

The symmetrical model is statically indeterminate to one degree. We take the horizontal reaction at the right support as the force redundant and work with the primary structure shown in Fig. 9.42.

Assuming unyielding supports, the compatibility equation has the following form

$$\Delta_{\mathrm{D},0} + \delta_{\mathrm{DD}} H_{\mathrm{D}} = 0$$

where $\Delta_{\mathrm{D},0}$ and δ_{DD} are the horizontal displacements at D due to the applied loading and a unit value of H_{D}. We use the Principle of Virtual Forces specialized for only bending deformation to evaluate these terms. The corresponding expressions are

$$\begin{aligned} \Delta_{\mathrm{D},0} &= \int_S M_0 \delta M \frac{\mathrm{d}S}{EI} \\ \delta_{\mathrm{DD}} &= \int_S (\delta M)^2 \frac{\mathrm{d}S}{EI} \end{aligned} \tag{9.44}$$

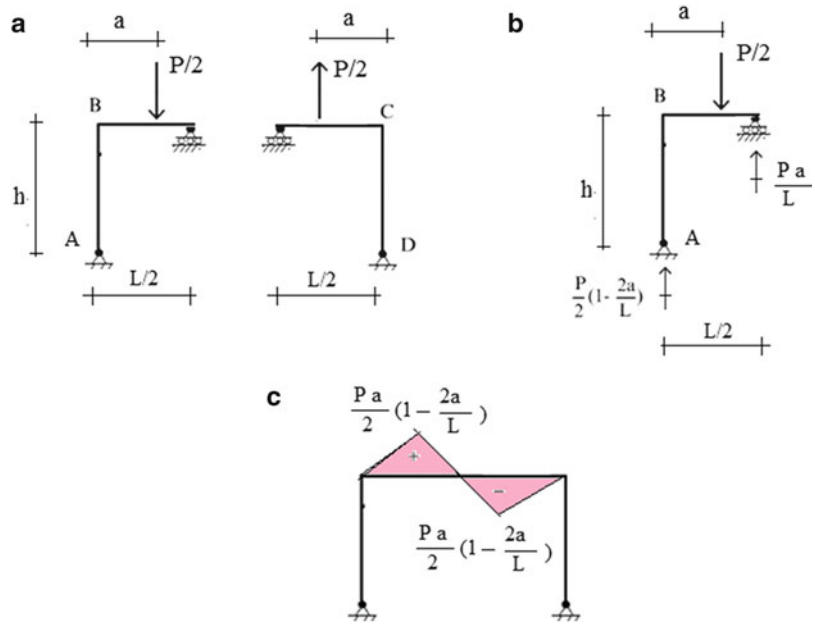

Fig. 9.41 (**a**) Anti-symmetrical model. (**b**) Free body diagram—anti-symmetrical segment. (**c**) Bending moment distribution—anti-symmetrical loading

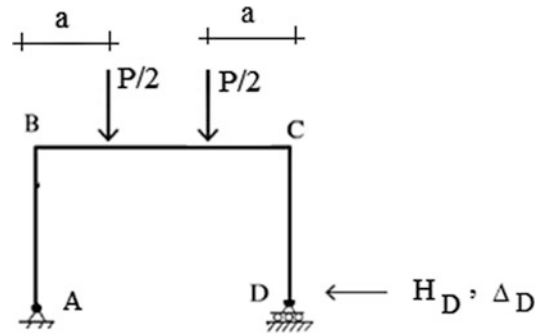

Fig. 9.42 Primary structure for two-hinged frame—symmetrical loading case

where M_0 is the moment due to the applied loading and δM is the moment due to a unit value of H_D. These moment distributions are plotted in Fig. 9.43.

Evaluating the integrals leads to:

$$\begin{aligned} \Delta_{B,0} &= -\frac{P}{2}\frac{ha}{EI_2}(L-a) \\ \delta_{BB} &= \frac{2h^3}{3EI_1} + \frac{h^2 L}{EI_2} \end{aligned} \tag{9.45}$$

Finally, the horizontal reaction at support D is

$$H_D = P\frac{a(L-a)}{2hL}\left[\frac{1}{1+(2/3)(r_g/r_c)}\right] \tag{9.46}$$

where

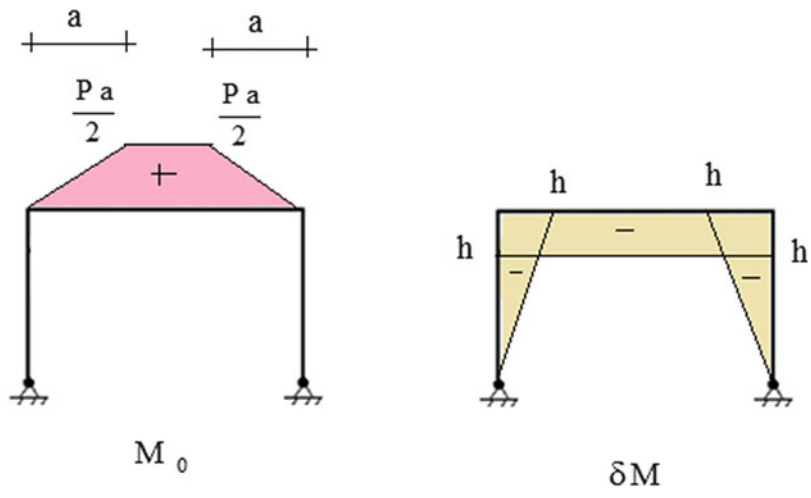

Fig. 9.43 Bending moment distributions—symmetrical loading—primary structure

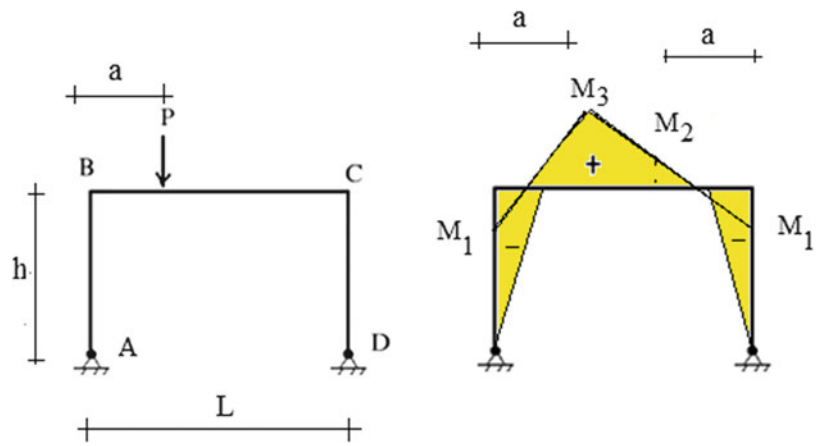

Fig. 9.44 Final bending moment distribution

$$r_c = \frac{I_1}{h} \quad r_g = \frac{I_2}{L} \tag{9.47}$$

are the relative stiffness factors for the column and girder members.

Combining the results for the symmetrical and anti-symmetrical loadings results in the net bending moment distribution plotted in Fig. 9.44. The peak moments are defined by (9.48).

$$\begin{aligned} M_1 &= -\frac{Pa}{2}\left(1-\frac{a}{L}\right)\frac{1}{1+(2/3)(r_g/r_c)} \\ M_2 &= +\frac{Pa}{2}\left[\frac{(a/L)+(2/3)(r_g/r_c)}{1+(2/3)(r_g/r_c)}\right]-\frac{Pa}{2}\left(1-\frac{2a}{L}\right) \\ M_3 &= +\frac{Pa}{2}\left[\frac{(a/L)+(2/3)(r_g/r_c)}{1+(2/3)(r_g/r_c)}\right]+\frac{Pa}{2}\left(1-\frac{2a}{L}\right) \end{aligned} \tag{9.48}$$

Example 9.15 Two-Hinged Symmetrical Frame—Uniform Gravity Load

Given: The frame and loading defined in Fig. E9.15a.

Determine: The bending moment distribution.

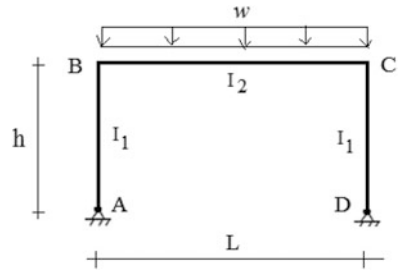

Fig. E9.15a

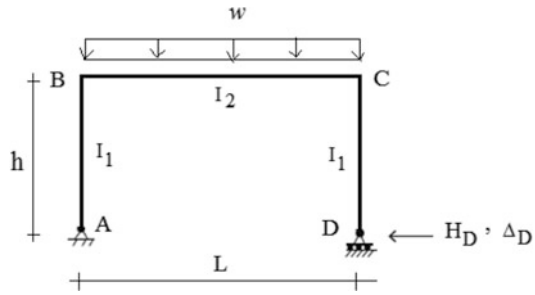

Fig. E9.15b

Solution: We work with the primary structure shown in Fig. E9.15b. We only need to determine the $\Delta_{D,0}$ term corresponding to the uniform loading since the δ_{DD} term is independent of the applied loading. The solution for H_D is

$$H_D = \frac{wL^2}{12h}\frac{1}{1+(2/3)(r_g/r_c)}$$

where

$$r_g = \frac{I_2}{L}$$
$$r_c = \frac{I_1}{h}$$

Figure E9.15c shows the bending moment distribution. The peak values are

$$M_1 = \frac{wL^2}{12}\frac{1}{1+(2/3)(r_g/r_c)}$$
$$M_2 = \frac{wL^2}{8}\left[1-\frac{2}{3}\frac{1}{1+(2/3)(r_g/r_c)}\right]$$

When members AB and CD are very stiff, $r_c \rightarrow \infty$ and $H_D \rightarrow wL^2/12h$. In this case, the moment at B approaches $wL^2/12$ which is the fixed end moment for member BC.

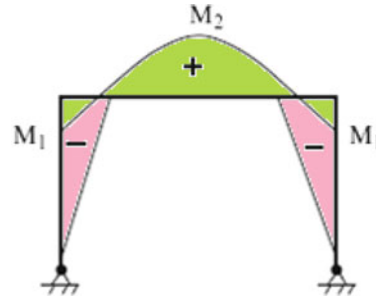

Fig. E9.15c Bending moment distribution

9.5.2.3 Symmetrical Portal Frames with Fixed Supports

We consider the symmetrical frame shown in Fig. 9.45. Because the structure is symmetrical, we consider the loading to consist of symmetrical and anti-symmetrical components. The structure is indeterminate to the second degree for symmetrical loading and to the first degree for anti-symmetrical loading (there is zero moment at mid-span which is equivalent to a hinge at that point). Figure 9.45b defines the structures corresponding to these two loading cases.

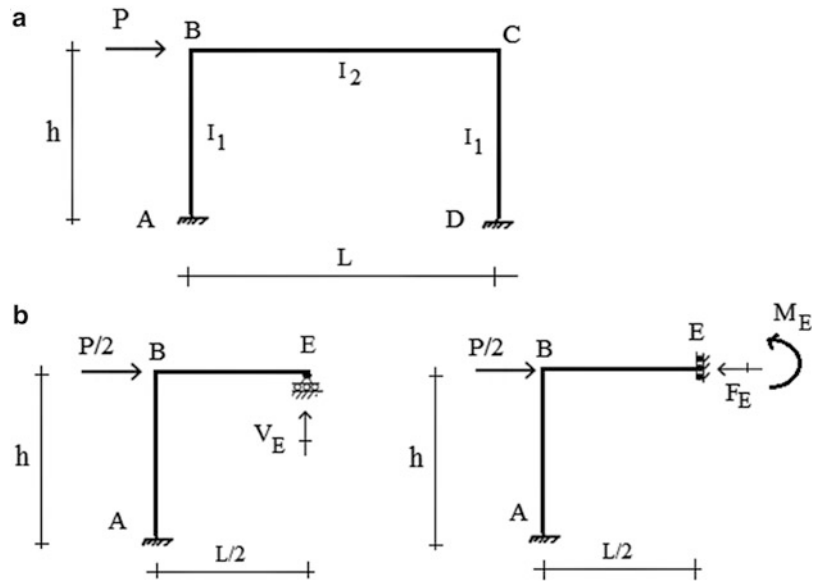

Fig. 9.45 (**a**) Geometry. (**b**) Decomposition into symmetrical and anti-symmetrical loadings

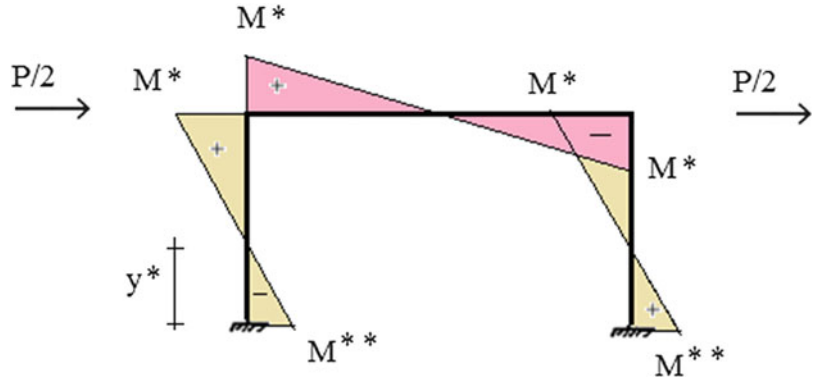

Fig. 9.46 Bending moment distribution—anti-symmetric loading

Evaluating the various displacement terms for the anti-symmetrical loading, one obtains:

$$\Delta_{\mathrm{E},0} = -\frac{PLh^2}{8EI_1}$$

$$\delta_{\mathrm{EE}} = \frac{L^3}{24EI_2} + \frac{L^2 h}{4EI_1}$$

$$V_{\mathrm{E}} = \frac{-\Delta_{\mathrm{E},0}}{\delta_{\mathrm{EE}}} = \left(\frac{Ph}{2L}\right)\frac{1}{(1+(1/6)(L/I_2)(I_1/h))}$$

The moment diagrams are plotted in Fig. 9.46. The peak values are

$$\begin{aligned} M^* &= \pm\frac{Ph}{4}\frac{1}{1+(1/6)\left(r_{\mathrm{c}}/r_{\mathrm{g}}\right)} \\ M^{**} &= \pm\frac{Ph}{2}\left[-1+\frac{1}{2\left(1+(1/6)\left(r_{\mathrm{c}}/r_{\mathrm{g}}\right)\right)}\right] \\ r_{\mathrm{c}} &= \frac{I_1}{h} \quad r_{\mathrm{g}} = \frac{I_2}{L} \end{aligned} \tag{9.49}$$

There are inflection points located in the columns at y^* units up from the base where

$$y^* = h\left[1-\frac{1}{2}\frac{1}{1+(1/6)\left(r_{\mathrm{c}}/r_{\mathrm{g}}\right)}\right] \tag{9.50}$$

When the girder is very stiff relative to the column, $r_{\mathrm{c}}/r_{\mathrm{g}} \to 0$ and $y^* \to h/2$. A reasonable approximation for y^* for typical column and girder properties is $\approx 0.6\ h$.

Figure 9.47 shows the corresponding bending moment distribution for the two-hinged portal frame. We note that the peak positive moment is reduced approximately 50 % when the supports are fixed.

We consider next the case where the girder is uniformly loaded. We skip the intermediate details and just list the end moments for member AB and the moment at mid-span (Fig. 9.48).

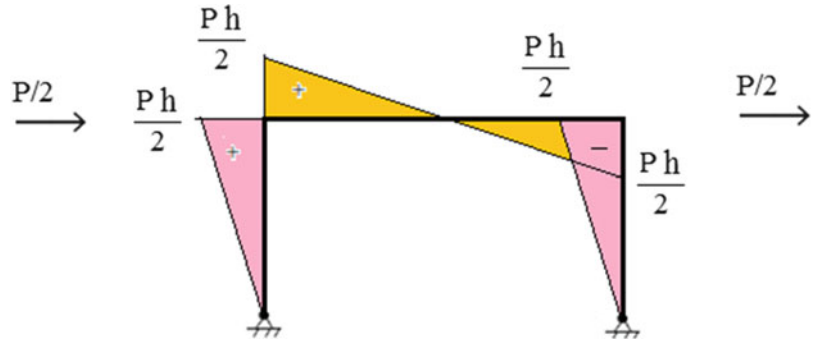

Fig. 9.47 Moment distribution for two-hinged frame

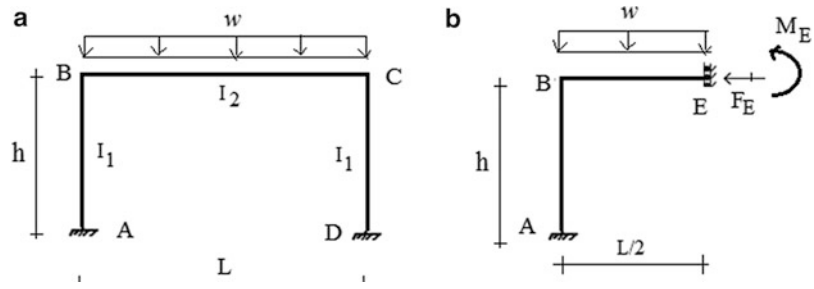

Fig. 9.48 (**a**) Portal frame with fixed supports under gravity loading. (**b**) Moment at mid-span

$$
\begin{aligned}
M_{\mathrm{BA}} &= -\frac{wL^2}{12}\frac{1}{1+(1/2)(r_{\mathrm{g}}/r_{\mathrm{c}})} \\
M_{\mathrm{AB}} &= \frac{1}{2}M_{\mathrm{BA}} \\
M_{\mathrm{E}} &= \frac{wL^2}{8}\left[1-\frac{2}{3}\frac{1}{1+(1/2)(r_{\mathrm{g}}/r_{\mathrm{c}})}\right]
\end{aligned}
\tag{9.51}
$$

The bending moment distribution is plotted in Fig. 9.49. The solution for the two-hinged case is shown in Fig. 9.50. These results show that the bending moment distribution is relatively insensitive to end fixity of the base.

$$
\begin{aligned}
M_2 &= M_{\mathrm{E}}\frac{1-\dfrac{2/3}{1+2/3(r_{\mathrm{g}}/r_{\mathrm{c}})}}{1-\dfrac{2/3}{1+1/2(r_{\mathrm{g}}/r_{\mathrm{c}})}} = \frac{wL^2}{8}\left(1-\frac{(2/3)}{1+2/3(r_{\mathrm{g}}/r_{\mathrm{c}})}\right) \\
M_1 &= M_{\mathrm{BA}}\frac{1+1/2(r_{\mathrm{g}}/r_{\mathrm{c}})}{1+2/3(r_{\mathrm{g}}/r_{\mathrm{c}})} = -\frac{wL^2}{12}\left(\frac{1}{1+2/3(r_{\mathrm{g}}/r_{\mathrm{c}})}\right)
\end{aligned}
\tag{9.52}
$$

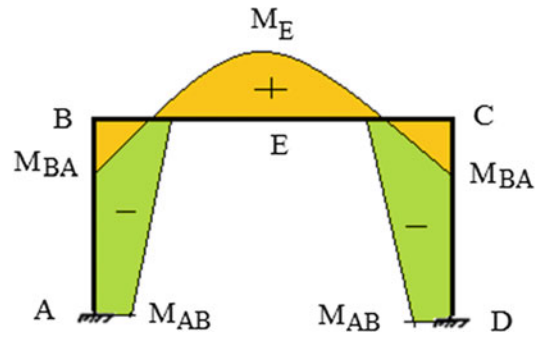

Fig. 9.49 Bending moment distribution—symmetrical loading—fixed supports

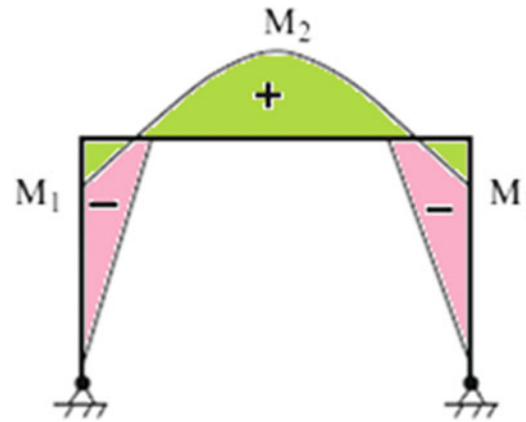

Fig. 9.50 Bending moment distribution—symmetrical loading—hinged supports

9.5.3 Pitched Roof Frames

We consider next a class of portal frames where the roof is pitched, as shown in Fig. 9.51a. We choose to work with the primary structure defined in Fig. 9.51b.

We suppose the structure is subjected to a uniform load per horizontal projection on members BC and CD. The bending moment distribution in the primary structure due to the applied loading, M_0, is parabolic with a peak value at C (Fig. 9.52). Taking $H_E = 1$ leads to the bending moment distribution shown in Fig. 9.53. It is composed of linear segments.

Assuming the supports are unyielding, the flexibility coefficients are

$$\begin{aligned} \Delta_{E,0} &= -\frac{wL^3}{12\cos\theta}\left\{h_1 + \frac{5}{8}h_2\right\}\frac{1}{EI_2} \\ \delta_{EE} &= \frac{2}{3}\frac{h_1^3}{EI_1} + \frac{L}{EI_2\cos\theta}\left\{h_1^2 + h_1h_2 + \frac{h_2^2}{3}\right\} \end{aligned} \tag{9.53}$$

We define the relative stiffness factors as

$$r_1 = \frac{I_1}{h_1} \quad r_2^* = \frac{I_2}{L^*} \tag{9.54}$$

where L^* is the length of the inclined roof members BC and CD.

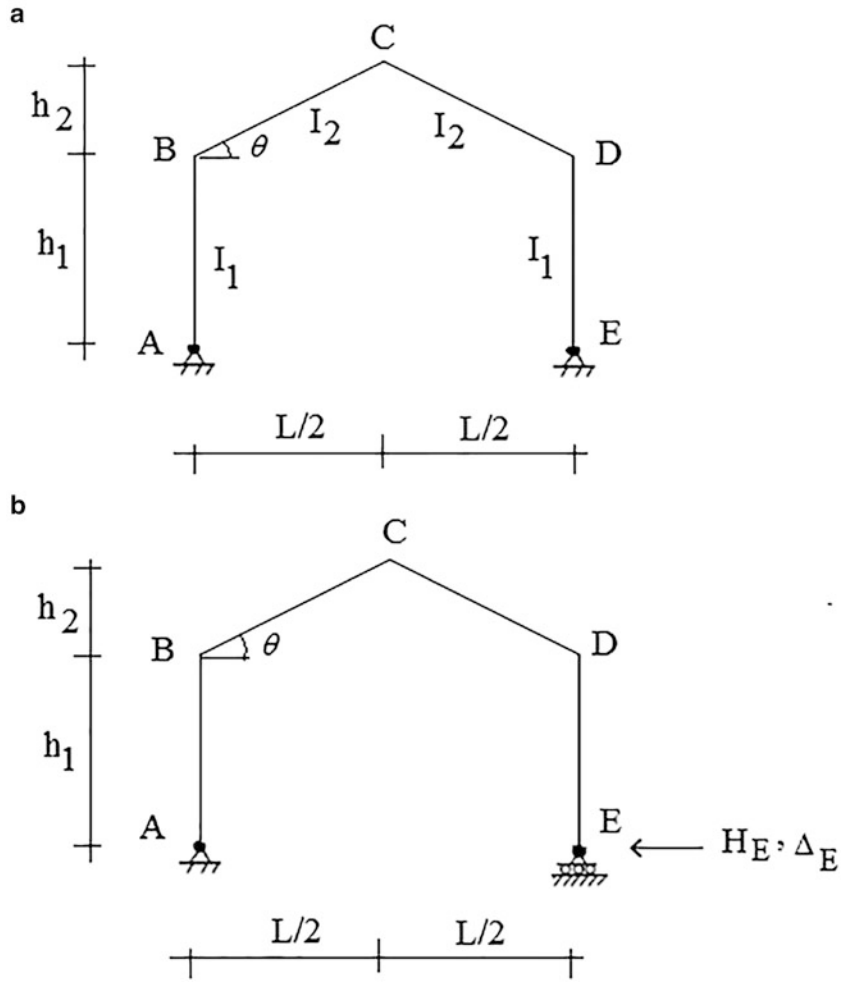

Fig. 9.51 (**a**) Pitched roof frame—definition sketch. (**b**) Primary structure—redundant reaction

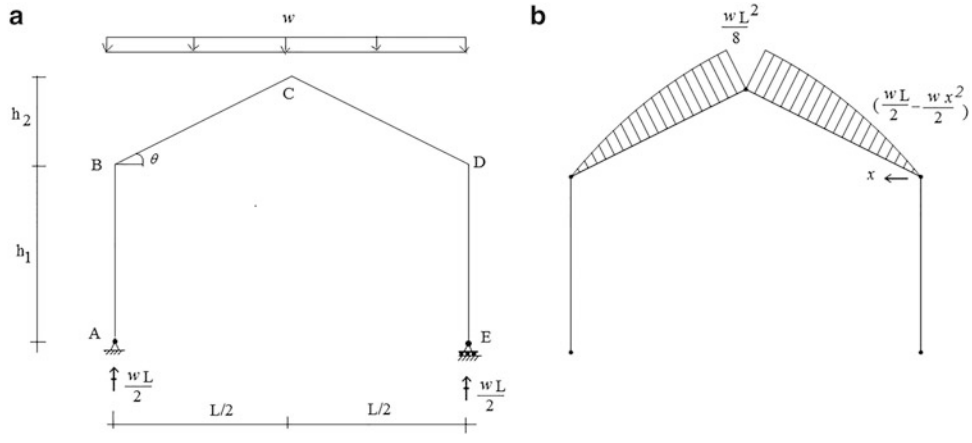

Fig. 9.52 (**a**) Primary structure-external loading. (**b**)Bending moment distribution for applied loading, M_0

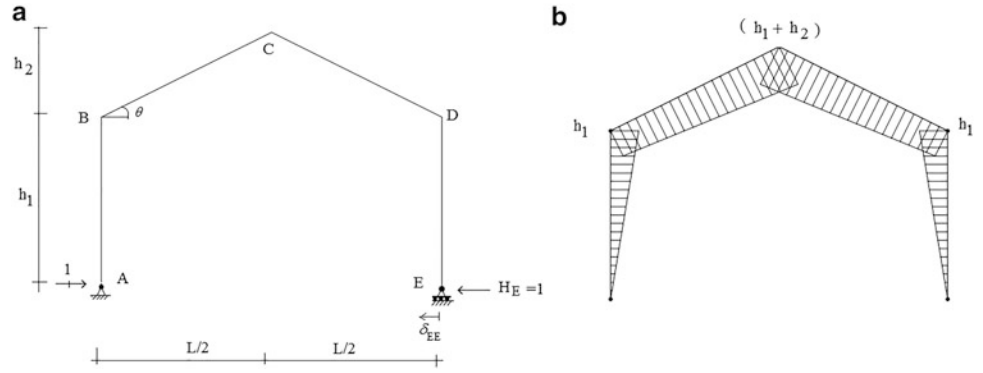

Fig. 9.53 (**a**) Primary structure-unit load. (**b**)Bending moment distribution for $H_{\mathrm{E}} = 1$

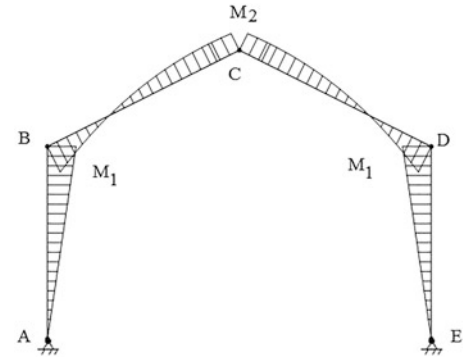

Fig. 9.54 Distribution of total bending moments

$$L^{*} = \frac{L}{2\cos\theta} \tag{9.55}$$

Using this notation, the expression for the horizontal reaction at E takes the form

$$H_{\mathrm{E}} = \frac{wL^2}{12h_1}\,\frac{1 + (5/8)(h_2/h_1)}{(1/3)\left(r_2^{*}/r_1\right) + 1 + (h_2/h_1) + (1/3)(h_2/h_1)^2} \tag{9.56}$$

The total bending moment distribution is plotted in Fig. 9.54. Equation (9.57) contains the expressions for the peak values.

$$\begin{aligned} M_1 &= -\frac{wL^2}{12}a_1 \\ M_2 &= +\frac{wL^2}{8}a_2 \end{aligned} \tag{9.57}$$

where

$$\begin{aligned} a_1 &= \frac{1 + (5/8)(h_2/h_1)}{(1/3)(r_2^{*}/r_1) + 1 + (h_2/h_1) + (1/3)(h_2/h_1)^2} \\ a_2 &= 1 - \frac{2}{3}\left(1 + \frac{h_2}{h_1}\right)a_1 \end{aligned} \tag{9.58}$$

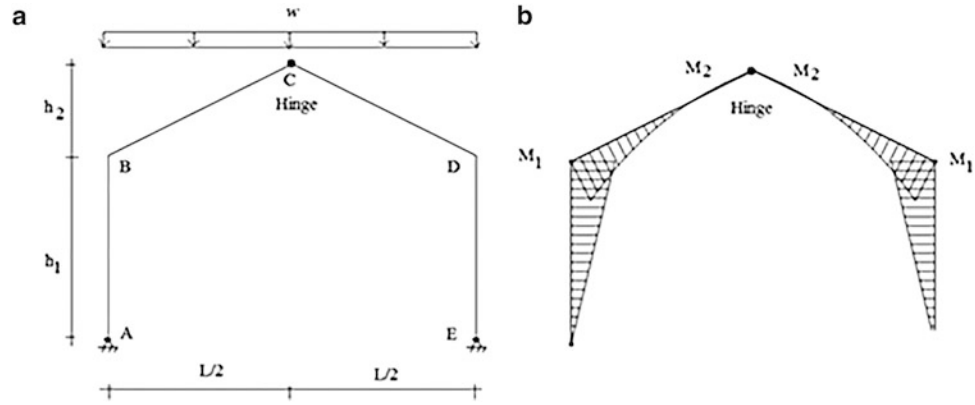

Fig. 9.55 Three-hinge solution. (**a**) Loading. (**b**) Bending moment distribution

These values depend on the ratio of heights h_2/h_1 and relative stiffness, r_2^*/r_1. One sets $h_2 = 0$ and $r_2^* = 2r_2$ to obtain the corresponding two-hinged portal frame solution. For convenience, we list here the relevant solution for the three-hinge case, with the notation modified to be consistent with the notation used in this section. The corresponding moment distributions are shown in Fig. 9.55.

The peak negative and positive moments are

$$\begin{aligned} M_1 &= \frac{wL^2}{8}\frac{h_1}{(h_1+h_2)} \\ M_2 &= \frac{wL^2}{8}\left\{\frac{1}{4} - \frac{1}{2}\frac{h_1}{h_1+h_2} + \frac{1}{4}\left(\frac{h_1}{h_1+h_2}\right)^2\right\} \end{aligned} \tag{9.59}$$

In order to compare the solutions, we assume $r_2* = r_1$, and $h_2 = h_1$ in the definition equations for the peak moments. The resulting peak values are

Three-hinge case (9.59):

$$\begin{aligned} M_1 &= -\frac{wL^2}{8}\left(\frac{1}{2}\right) \\ M_2 &= +\frac{wL^2}{8}\left(\frac{1}{16}\right) \end{aligned}$$

Two-hinge case (9.57):

$$\begin{aligned} M_1 &= -\frac{wL^2}{8}\left(\frac{13}{32}\right) = -\frac{wL^2}{8}(0.406) \\ M_2 &= +\frac{wL^2}{8}\left(\frac{3}{16}\right) \end{aligned}$$

We see that the peak negative moment is reduced by approximately 20 % when the structure is reduced to a two-hinged frame. However, the positive moment is increased by a factor of 3.

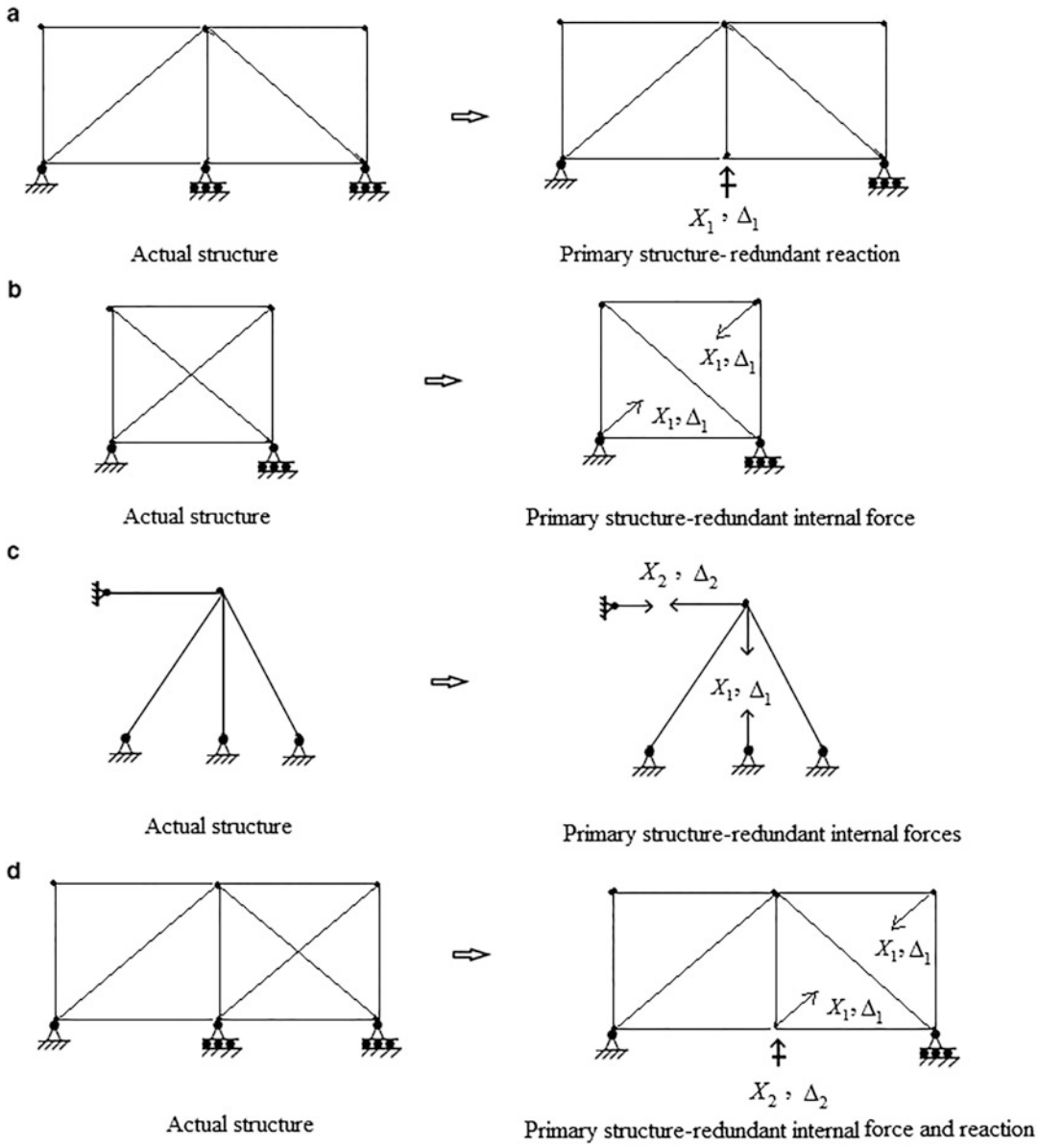

Fig. 9.56 Examples of statically indeterminate trusses

9.6 Indeterminate Trusses

Examples of indeterminate truss structures are shown in Fig. 9.56. One can choose a primary structure by taking either reactions or member forces or a combination as the force redundants. When working with member forces, one visualizes the member as being cut and works with the relative displacement of the adjacent faces. Continuity requires that the net relative displacement is zero.

We illustrate the Force Method procedure for the three-member truss shown in Fig. 9.57a. The truss is indeterminate to the first degree. The force in member BC is taken as the force redundant and

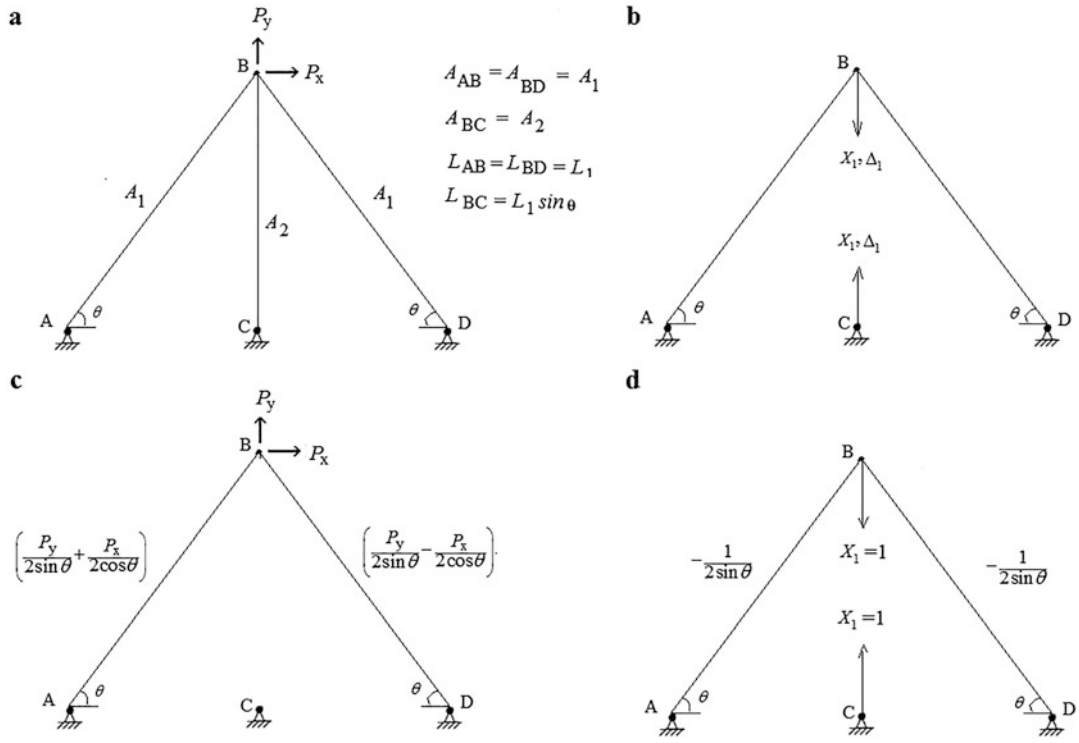

Fig. 9.57 (**a**) Three-member truss. (**b**) Primary structure—redundant internal force. (**c**) F_0. (**d**) $\delta F(X_1 = 1)$

Δ_1 is the relative displacement together at the end sections. Two deflection computations are required, one due to the external loads and the other due to $X_1 = 1$. We use the Principle of Virtual Forces discussed in Sect. 2.3.4 for these computations. Results are summarized below.

Displacement due to external loads:

$$\begin{aligned}\Delta_{1,0} &= \sum \left(\frac{F_0 L}{AE}\right)\delta F \\ &= -\frac{1}{2\sin\theta}\left(\frac{P_y}{2\sin\theta} + \frac{P_x}{2\cos\theta}\right)\frac{L_1}{A_1 E} + \left(-\frac{1}{2\sin\theta}\right)\left(\frac{P_y}{2\sin\theta} - \frac{P_x}{2\cos\theta}\right)\frac{L_1}{A_1 E} \\ &= -\frac{P_y}{2\sin^2\theta}\frac{L_1}{A_1 E}\end{aligned}$$

Displacement due to $X_1 = 1$:

$$\begin{aligned}\delta_{11} &= \sum (\delta F)^2 \frac{L}{AE} \\ &= \frac{1}{4\sin^2\theta}\frac{L_1}{A_1 E} + \frac{L_1 \sin\theta}{A_2 E} + \frac{1}{4\sin^2\theta}\frac{L_1}{A_1 E} = \frac{1}{2\sin^2\theta}\frac{L_1}{A_1 E} + \frac{L_1 \sin\theta}{A_2 E}\end{aligned}$$

Enforcing compatibility (9.3) leads to

$$\Delta_{1,0} + \delta_{11} X_1 = 0$$

$$F_{BC} = X_1 = -\frac{\Delta_{1,0}}{\delta_{11}} = \frac{\left(P_y/2\sin^2\theta\right)(L_1/A_1E)}{(1/2\sin^2\theta)(L_1/A_1E) + (L_1\sin\theta/A_2E)}$$
$$= P_y\frac{(A_2/\sin\theta)}{(A_2/\sin\theta) + 2A_1\sin^2\theta} \tag{9.60}$$

Lastly, the remaining forces are determined by superimposing the individual solutions.

$$F = F_0 + \delta F X_1$$
$$F_{AB} = \frac{P_x}{2\cos\theta} + P_y\left\{\frac{A_1\sin\theta}{(A_2/\sin\theta) + 2A_1\sin^2\theta}\right\} \tag{9.61}$$
$$F_{DB} = -\frac{P_x}{2\cos\theta} + P_y\left\{\frac{A_1\sin\theta}{(A_2/\sin\theta) + 2A_1\sin^2\theta}\right\}$$

As expected for indeterminate structures, the internal force distribution depends on the relative stiffness of the members. When A_2 is very large in comparison to A_1, P_y is essentially carried by member BC. Conversely, if A_2 is small in comparison to A_1, member BC carries essentially none of P_y.

Example 9.16

Given: The indeterminate truss shown in Fig. E9.16a. Assume AE is constant, $A = 2$ in.^{2}, and $E = 29{,}000$ ksi.

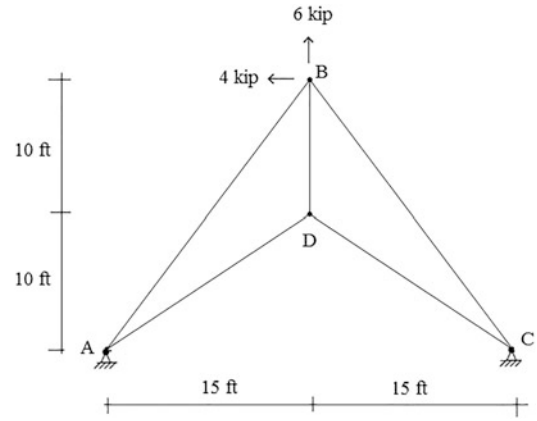

Fig. E9.16a

Determine: The member forces.

Solution: The truss is externally indeterminate to the first degree. The horizontal component of the reaction at C is taken as the force redundant (Fig. E9.16b).

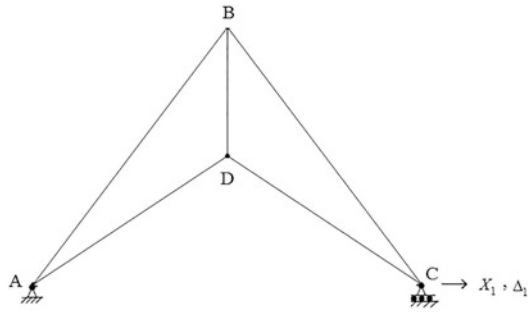

Fig. E9.16b Primary structure—redundant reaction

We apply the geometric compatibility equation to this truss,

$$\Delta_{1,0} + \delta_{11} X_1 = 0$$

where

$$\Delta_{1,0} = \sum F_0 \delta F \frac{L}{AE}$$

$$\delta_{11} = \sum (\delta F)^2 \frac{L}{AE}$$

The corresponding forces are listed in Figs. E9.16c and E9.16d.

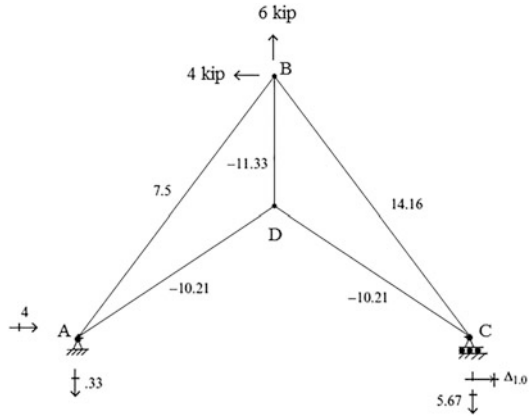

Fig. E9.16c F_0

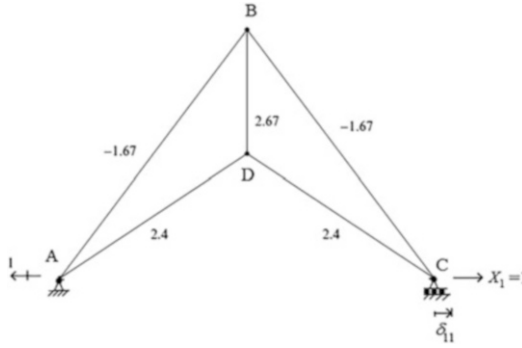

Fig. E9.16d $\delta F(X_1 = 1)$

Member	L (in.)	A (in.^{2})	$\frac{L}{A}$	F_0	δF	$(\delta F)^2 \frac{L}{AE}$	$F_0 \delta F \frac{L}{AE}$
AB	300	2	150	7.5	−1.67	418.3/E	−1878.7/E
BC	300	2	150	14.16	−1.67	418.3/E	−3547/E
CD	216.3	2	108.2	−10.21	2.4	625.1/E	2656/E
DA	216.3	2	108.2	−10.21	2.4	625.1/E	2656/E
BD	120	2	60	−11.33	2.67	422.7/E	−1815/E
Σ						2509.5/E	−12,552.7/E

Inserting this data in the compatibility equation leads to

$$X_1 = -\frac{\Delta_{1,0}}{\delta_{11}} = \frac{12552.7}{2509.5} = 5$$

Then, the forces are determined by superimposing the individual solutions

$$F = F_0 + \delta F X_1$$

The final member forces and the reactions are listed below:

Member	F_0	$\delta F X_1$	F
AB	7.5	−8.35	−0.85
BC	14.16	−8.35	5.81
CD	−10.21	12.0	1.8
DA	−10.21	12.0	1.8
BD	−11.33	13.35	2
R_{ax}	4.0	−5.0	−1.0
R_{ay}	−0.33	0	−0.33
R_{ex}	0.0	+5.0	+5.0
R_{ey}	−5.67	0	−5.67

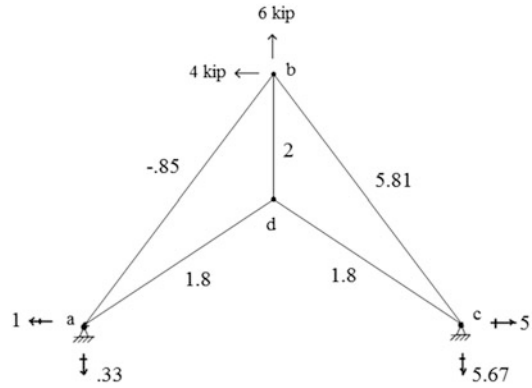

Example 9.17

Given: The indeterminate truss shown in Fig. E9.17a.

Determine: The member forces. Assume AE is constant, $A = 200\ \text{mm}^2$, and $E = 200$ GPa.

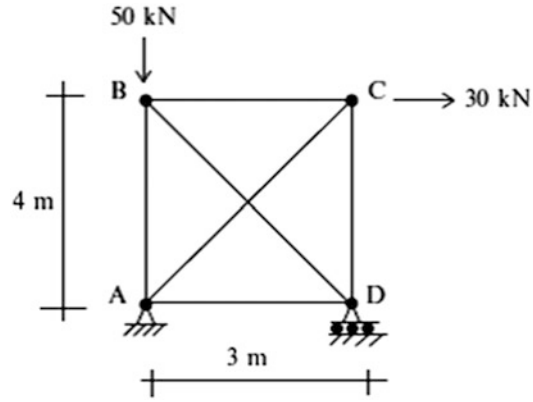

Fig. E9.17a

Solution: The truss is internally indeterminate to the first degree. The force in member BD is taken as the force redundant (Fig. E9.17b).

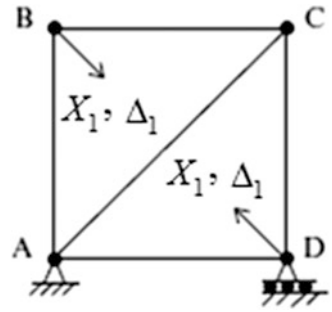

Fig. E9.17b Primary structure—internal force redundant

We apply the geometric compatibility equation to this truss,

$$\Delta_{1,0} + \delta_{11} X_1 = 0$$

where

$$\Delta_{1,0} = \sum F_0 \delta F \frac{L}{AE}$$

$$\delta_{11} = \sum (\delta F)^2 \frac{L}{AE}$$

The corresponding forces are listed in Figs. E9.17c and E9.17d.

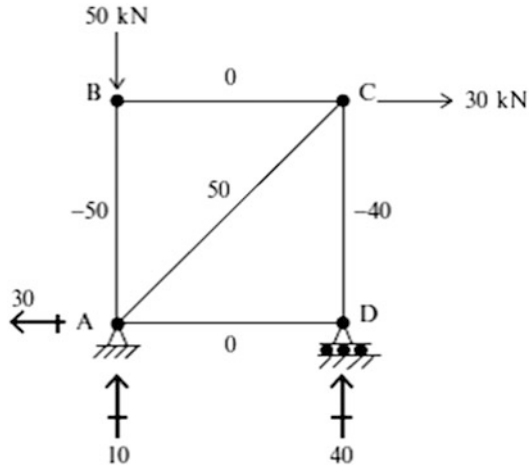

Fig. E9.17c F_0

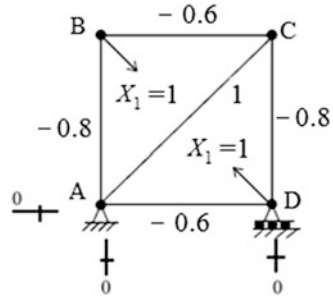

Fig. E9.17d $\delta F(X_1 = 1)$

Member	L (mm)	A (mm^2)	$\frac{L}{A}$	F_0	δF	$(\delta F)^2(L/AE)$	$F_0\delta F(L/AE)$
AB	4000	200	20	−50	−0.8	12.8	800
BC	3000	200	15	0	−0.6	5.4	0
CD	4000	200	20	−40	−0.8	12.8	640
DA	3000	200	15	0	−0.6	5.4	0
BD	5000	200	25	0	1	25	0
AC	5000	200	25	50	1	25	1250
Σ						86.4/E	2690/E

Enforcing comparability leads to

$$X_1 = F_{BD} = -\frac{\Delta_{1,0}}{\delta_{11}} = -\frac{2690}{86.4} = -31.13$$

$$\therefore F_{BD} = 31.13\,\text{kN} \quad \text{compression}$$

Then, the forces are determined by superimposing the individual solutions.

$$F = F_0 + \delta F X_1$$

The final member forces and the reactions are listed below.

Member	F_0	$\delta F X_1$	F
AB	−50	24.9	−25.1
BC	0	18.68	18.68
CD	−40	24.9	−15.1
DA	0	18.68	18.68
BD	0	−31.13	−31.13
AC	50	−31.13	18.87
R_{Ax}	−30	0	−30
R_{Ay}	10	0	10
R_{Dy}	40	0	40

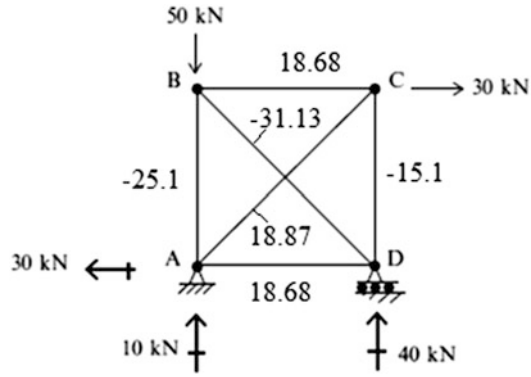

9.7 Summary

9.7.1 Objectives

- The primary objective of this chapter is to present the force method, a procedure for analyzing statically indeterminate structures that work with force quantities as the unknown variables.
- Another objective is to use the force method to develop analytical solutions which are useful for identifying the key parameters that control the response and for conducting parameter sensitivity studies.

9.7.2 Key Factors and Concepts

- The force method is restricted to linear elastic behavior.
- The first step is to reduce the structure to a statically determinate structure by either removing a sufficient number of redundant restraints or inserting force releases at internal points. The resulting determinate structure is called the primary structure.
- Next one applies the external loading to the primary structure and determines the resulting displacements at the points where the restraints were removed.
- For each redundant force, the displacements produced by a unit force acting on the primary structure are evaluated.
- Lastly, the redundant forces are scaled such that the total displacement at each constraint point is equal to the actual displacement. This requirement is expressed as

$$\Delta\big|_{\text{actual}} = \Delta\big|_{\text{loading}} + \sum_{\text{redundant forces}} (\delta_{\text{unit force}})X$$

where the various terms are displacements at the constraint points. One establishes a separate equation for each constraint point. Note that all calculations are carried out on the primary structure.

9.8 Problems

Problem 9.1 Determine the vertical reaction at B. Take $E = 29{,}000$ ksi and $I = 200$ in.^{4}

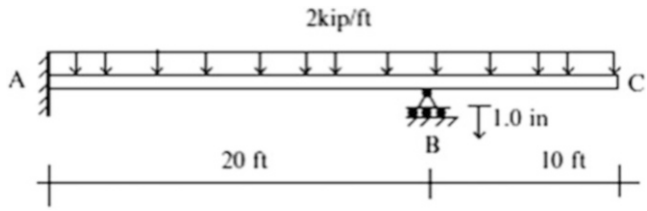

Problem 9.2 Determine the vertical reaction at B. Take $E = 200$ GPa and $I = 80(10)^6$ mm^4.

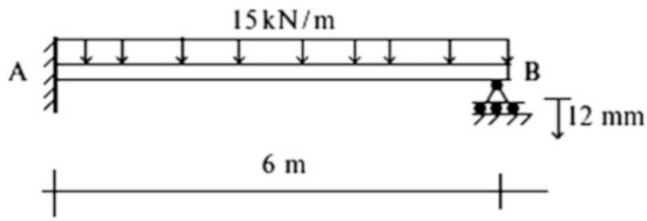

Problem 9.3 Determine the force in spring CD.

$k_v = 60$ kip/in.
$E = 29{,}000$ ksi
$I = 200$ in.^{4}

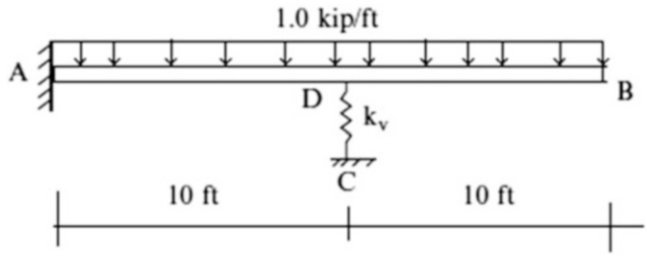

Problem 9.4 Given the following properties and loadings, determine the reactions.

$P = 40$ kN
$w = 20$ kN/m
$L = 10$ m
$E = 200$ GPa
$I = 170(10)^6$ mm^4
$k_v = 40$ kN/mm
$\delta = 20$ mm

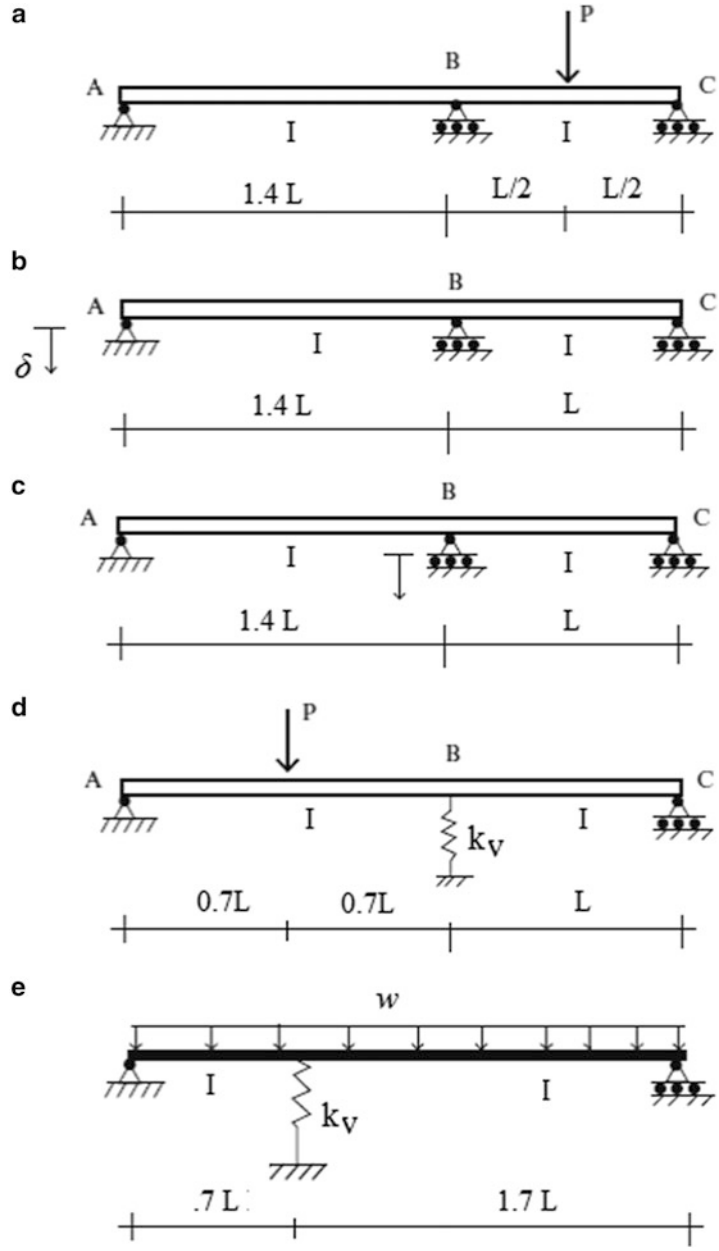

Problem 9.5 Use the force method to determine the reaction at B caused by:

1. The distributed load shown
2. The support settlement at B

$$
\begin{aligned}
I &= 400\,\text{in.}^4 \\
L &= 54\,\text{ft} \\
w &= 2.1\,\text{kip/ft} \\
\delta_B &= 1.2\,\text{in.}\downarrow \\
E &= 29,000\,\text{ksi}
\end{aligned}
$$

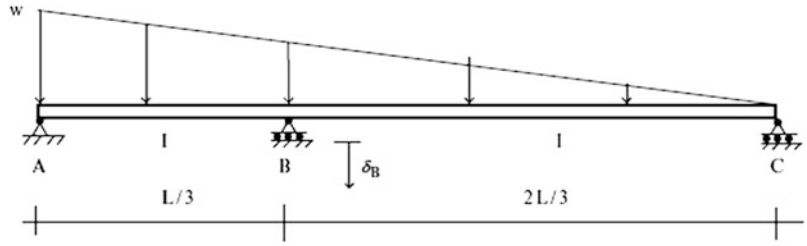

Problem 9.6 Use the force method to determine the forces in the cables. Assume beam is rigid. $A_C = 1200\ \text{mm}^2$, $L = 9$ m, $P = 40$ kN, and $E = 200$ GPa.

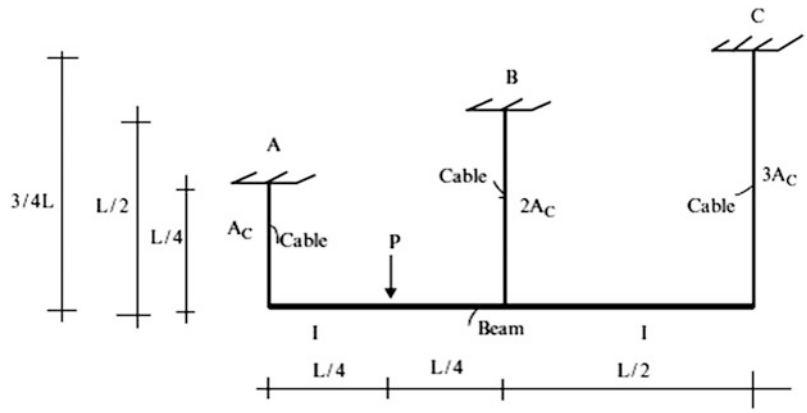

Problem 9.7 Consider the parabolic arch shown below. Assume the arch is non-shallow, i.e., *h*/*L* is order of (1/2).

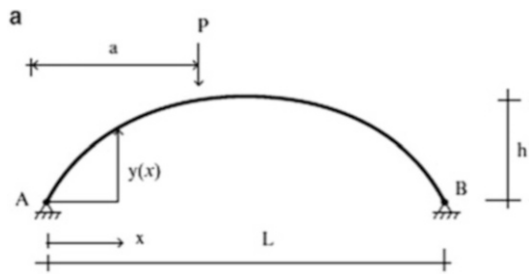

$$y = 4h\left(\frac{x}{L} - \left(\frac{x}{L}\right)^2\right)$$

$$I = \frac{I_o}{\cos\theta}$$

(a) Determine the horizontal reaction at B due to the concentrated load.
(b) Utilize the results of part (a) to obtain an analytical expression for the horizontal reaction due to a distributed loading, $w(x)$.
(c) Specialize (b) for a uniform loading, $w(x) = w_0$.
(d) Suppose the horizontal support at B is replaced by a member extending from A to B. Repeat part (a).

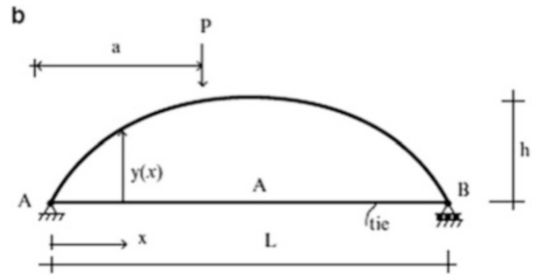

Problem 9.8 Consider the semicircular arch shown below. Determine the distribution of the axial and shear forces and the bending moment. The cross-section properties are constant.

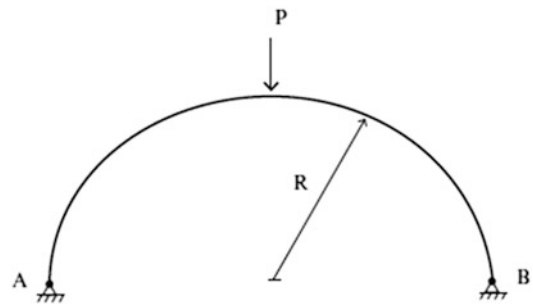

Problem 9.9

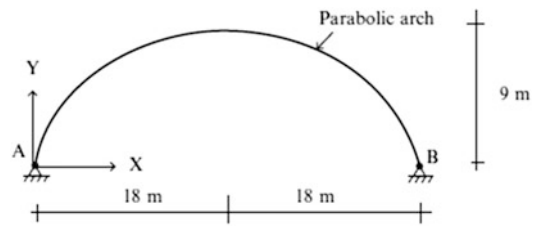

Use a computer software system to determine the bending moment distribution and deflected shape produced by the following loadings.

$$\text{Take } A = 20,000\,\text{mm}^2, \quad I = 400(10)^6\,\text{mm}^4 \text{ and } E = 200\,\text{GPa}$$

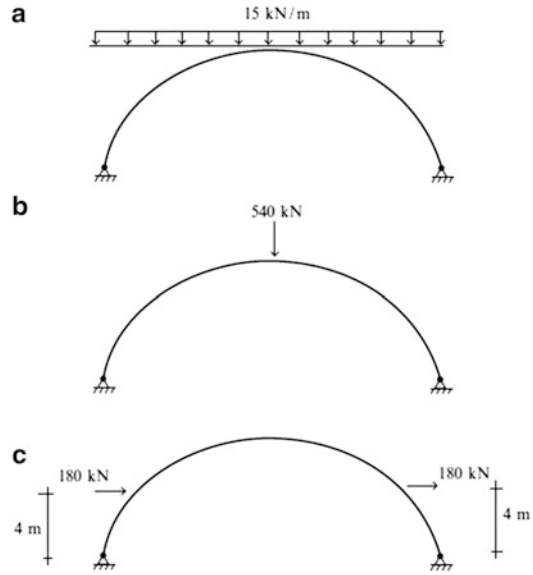

Problem 9.10

$$A = 30\,\text{in.}^2 \quad I = 1000\,\text{in}^4 \quad E = 29,000\,\text{ksi}$$

Use a computer software system to determine the maximum bending moment and the axial force in member ABC. Consider the following values for the area of the tension rod AC: 4, 8, and 16 in.^{2}

Problem 9.11

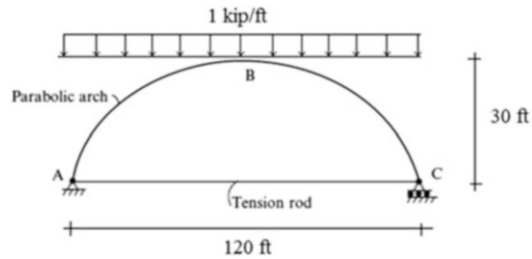

$$A = 40\,\text{in.}^2 \quad I = 1200\,\text{in.}^4 \quad E = 29,000\,\text{ksi}$$

Use a computer software system to compare the bending moment distributions generated by the following loadings:

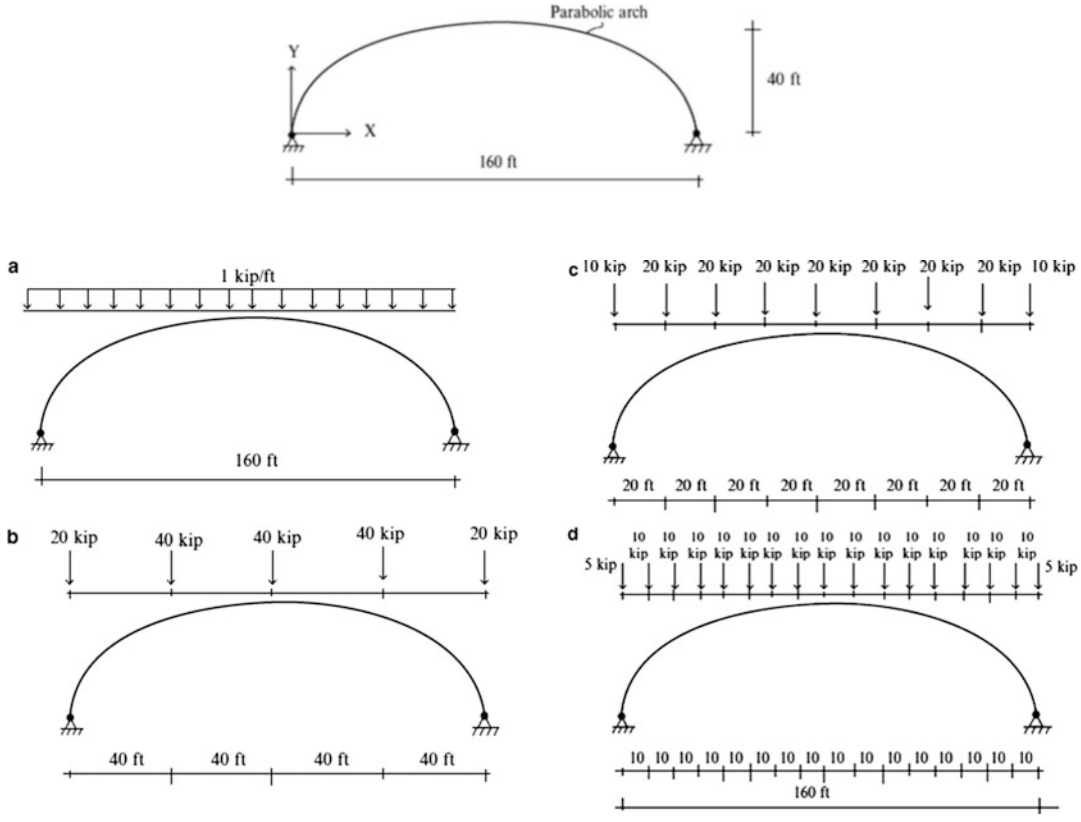

Problem 9.12 Determine the horizontal reaction at support D.

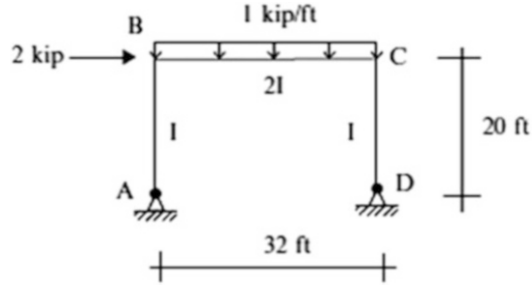

Problem 9.13 Determine the peak positive and negative moments as a function of h. Consider $h = 2, 4, 6$ m.

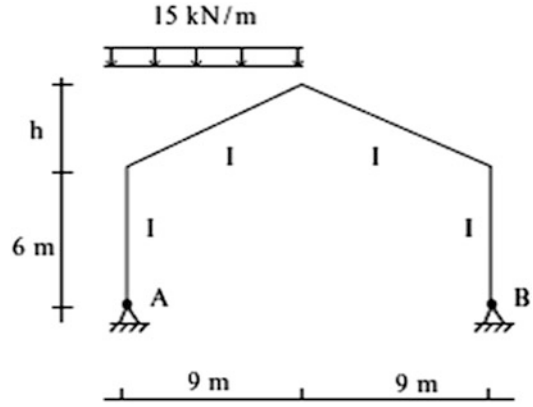

Problem 9.14 Determine the peak positive and negative moments as a function of h. Consider $h = 10, 20, 30$ ft.

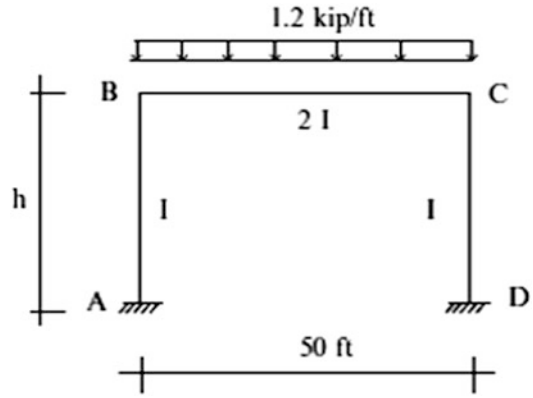

Problem 9.15 Using a computer software system, determine the bending moment distribution and deflected shape due to the loading shown.

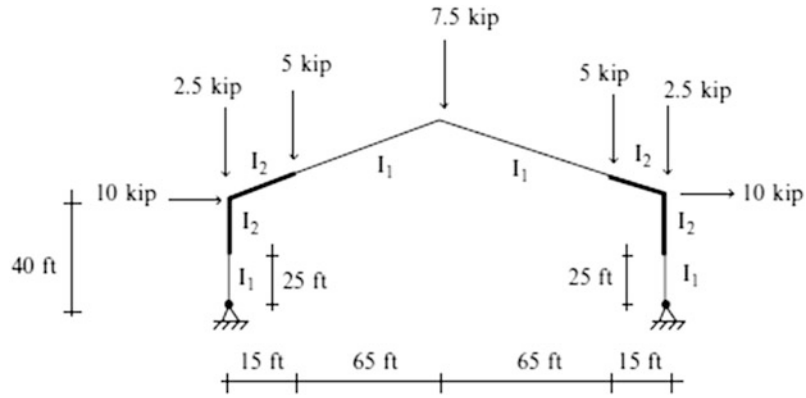

Take $I_1 = 1000$ in.^{4}, $I_2 = 2000$ in.^{4}, $E = 29{,}000$ ksi, and $A = 20$ in.^{2} all members.

Problem 9.16 Compare the bending moment distributions and the vertical displacement at B for the structures defined below. Take $E = 200$ GPa, $I = 400(10)^6$ mm^4, $A = 100{,}000$ mm^2, and $A_c = 1200, 2400, 4800$ mm^2. Use a computer software system.

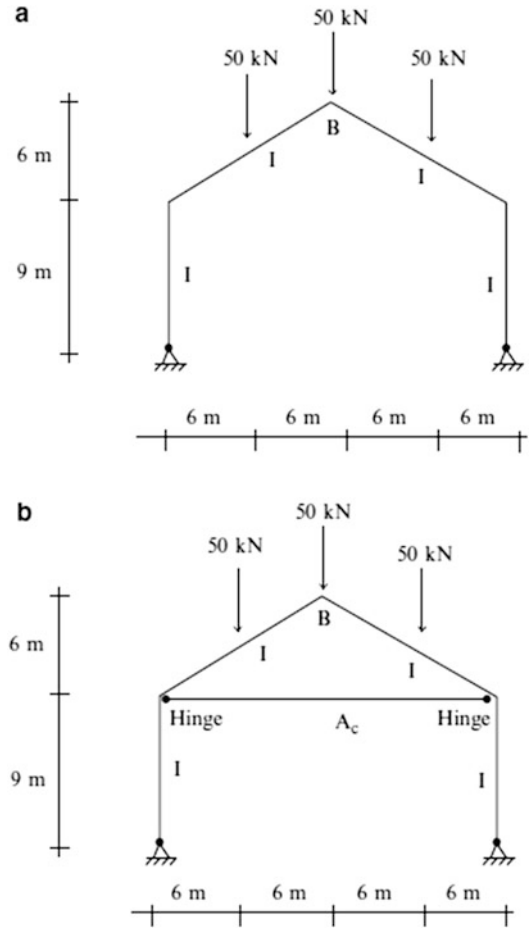

Problem 9.17 Is there any difference in behavior for the structures shown below? Answer the question without resorting to calculations.

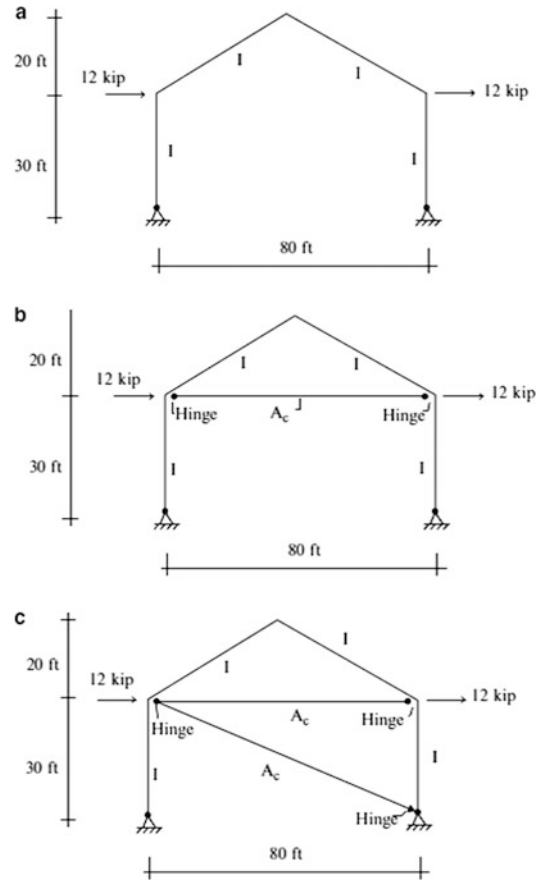

Problem 9.18 Determine the reactions and the member forces for the truss shown. Assume the vertical reaction at d as the force redundant.

$E = 200$ GPa
$A = 660$ mm^2 all members
$\alpha = 12 \times 10^{-6}$/°C
$\Delta T = 10$ °C

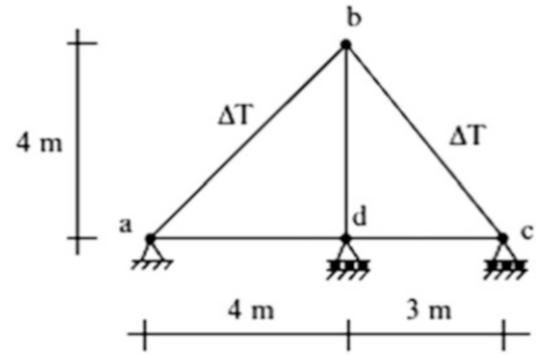

Problem 9.19 Determine the forces in the members. $E = 29{,}000$ ksi and $A = 1$ in.^{2} all members.

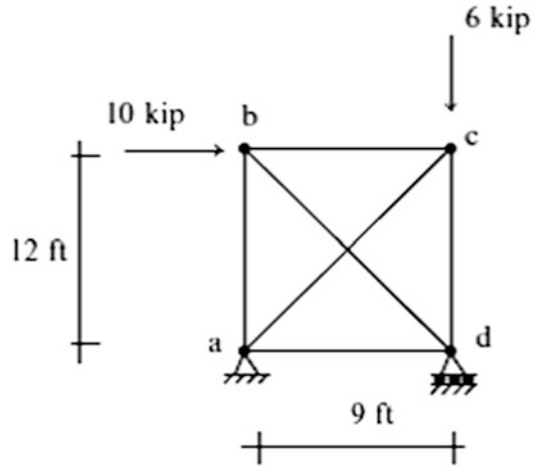

Problem 9.20 Determine the member forces of the truss shown. Assume the horizontal reaction at c as the force redundant.

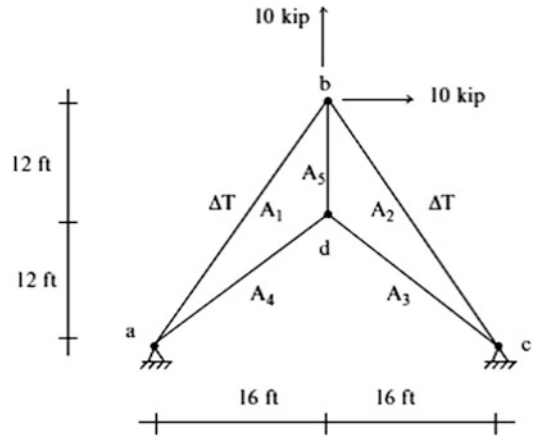

$A_1 = A_2 = A_3 = A_4 = 10$ in.^{2}
$A_5 = 5$ in.^{2}
$\alpha = 6.5 \times 10^{-6}$/°F
$\Delta T = 60$ F
$E = 29{,}000$ ksi

Problem 9.21 Determine the member forces for the truss shown. Assume $A = 1000\ \text{mm}^2$ and $E = 200$ GPa for all the members. Take the force in member ac and the reaction at support f as the force redundants.

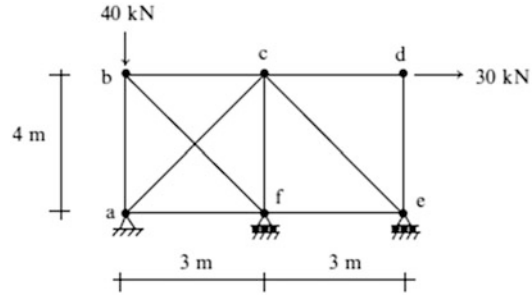

Reference

1. Tauchert TR. Energy principles in structural mechanics. New York: McGraw-Hill; 1974.